Dissertation zur Erlangung des Doktorgrades

der Fakultät für Chemie und Pharmazie

der Ludwig-Maximilians-Universität München

Overexpression and purification of membrane proteins in yeast:

The GPCR α-factor receptor and a methanococcal transporter

Anna Le Bris

aus

Quimper (Frankreich)

2007

Erklärung

Diese Dissertation wurde im Sinne von §13 Abs.3 bzw. 4 der Promotionsordnung vom 29. Januar 1998 von Herrn Prof. Dr. Dieter Oesterhelt betreut.

Ehrenwörtliche Versicherung

Diese Dissertation wurde selbständig, ohne unerlaubte Hilfe erarbeitet.

München, am 27. April 2007

Dissertation eingereicht am 27te April 2007

1. Gutachter   Prof. Dr. D.Oesterhelt
2. Gutachter   Prof. Dr. R. Beckmann

Mündliche Prüfung am   19. Oktober 2007

Communications

Publication in preparation:

Anna Le Bris, Birgit Wiltschi, Douglas D. Griffith, Dieter Oesterhelt.

Expression and purification of a homogeneous functional *Saccharomyces cerevisiae* α-factor receptor variant

Poster presentation:

Anna Le Bris, Douglas D. Griffith, Dieter Oesterhelt

Heterologous overexpression and purification of a putative amino-acid transporter from *Methanococcus jannaschii*

3rd international conference on structure, dynamics and function of proteins in biological membranes, Switzerland, Ascona, 14 -19 May 2006

Contents

Summary

Structural and functional studies of integral membrane proteins currently represent a most challenging research area. Since many integral membrane proteins are involved in disease, understanding their structure/function relationship could greatly improve the efficiency of drug discovery. This requires the acquisition of detailed structural data, however, these are tedious to obtain due to the several limitations encountered in the expression, purification and crystallisation of integral membrane proteins. To date, the 3D structures of only 93 membrane proteins are known in molecular detail, though several thousand structures of soluble proteins have already been solved.

This work was directed towards the elucidation of the structure of a G-protein-coupled receptor (GPCR), the *Saccharomyces cerevisiae* alpha-factor receptor Ste2p, and a putative amino-acid transporter of *Methanococcus jannaschii*, designated Aatp.

GPCRs comprise one of the largest superfamily of membrane proteins, and from the viewpoint of pharmacology, the most interesting one. They act as cell surface receptors responsible for the transduction of a remarkable diversity of exogenous signals (hormones, neurotransmitters, photons, ions, growth factors, odorants) into a cellular response by activating intracellular heterotrimeric G-protein complexes. Only one 3D structure of a GPCR, namely of bovine rhodopsin, has been resolved so far.

In the present work, Ste2p was modified to remove post-translational modifications, so as to obtain a homogenously yet functionally expressed protein product. It additionally carries both a FLAG- and His$_6$-tag to facilitate immunodetection and affinity purification. The modified receptor was cloned, and homologously overexpressed in *S.cerevisiae*. It could be rapidly and efficiently purified, and the final purification protocol yielded about 5 mg of 90% pure protein from 10 litres of culture. Finally, purified receptor was subjected to 3D crystallisation trials in an attempt to obtain high quality crystals for X-ray crystallography.

Hyperthermophilic proteins are of high interest for the biotechnological industry because of their stability at high temperatures (>60°C). In that sense, they are expected to be more stable crystallisation targets than mesophilic proteins. A special challenge is to understand the molecular mechanisms that confer thermostability. Until now, crystal structures of only a few proteins from thermophilic organisms have been determined, thus limiting the understanding of these features.

The present study aimed at different hyperthermophilic transporters, in particular the amino acid transporter Aatp. Although all proteins were cloned in *S.cerevisiae* only Aatp was overexpressed. Aatp carries a hexahistidine tag at its C-terminus. A fast and efficient purification protocol was developed that yielded 6 mg of Aatp from 10 litres of culture. Aatp purified in this way was homogenous, monodisperse and 90% pure, which allowed 3D- and 2D-crystallisation trials for the production of high quality crystals for X-ray crystallography.

Introduction

1. Structure and function of membrane proteins: challenges of the study

1.1. Importance of membrane proteins

The genome sequencing projects reveal that integral membrane proteins represent up to one third of the predicted proteins of all organisms examined so far. Furthermore, membrane proteins are the target of the large majority of drugs currently in use. About 80% of all cellular responses are thought to occur through proteins linked to the cell membrane. An ultimate understanding of their function depends on detailed structural data for each class of membrane proteins, such as transporters, receptors, channels and pumps. The structural information could also greatly improve the efficiency of drug discovery (Sachs and Engelman, 2006; Loll, 2003; Kuhn *et al.*, 2002; Werten *et al.*, 2002). To date, the 3D structures of only a tiny fraction of polytopic helical-type membrane proteins, 58 in total (in addition to 35 polytopic β-stranded and monotopic membrane proteins), are known in molecular details, though several thousand structures of soluble proteins have already been solved (source: http://www.mpibp-frankfurt.mpg.de/michel/public/memprotstruct.html).

1.2. The difficulties in studying membrane proteins

The lack of structural data on integral membrane proteins is mainly due to the difficulty to determine their 3D structure. This difficulty is most notably related to their hydrophobic nature and to their low natural abundance. They are usually expressed at comparably low levels and constitute less than 0,1% of the total cellular proteins (McPherson, 2004).

This requires to find an accurate and efficient overexpression system to produce sufficient amounts of protein for crystallisation experiments. In general, the term "overexpression" is used to describe the production of proteins at a level that exceeds the endogenous one, e.g., 10–100 mg of protein per litre of culture. Indeed, for systematic 3D crystallisation experiments, several tens of milligrams or more of highly pure protein are needed, however, few membrane proteins are abundant enough in natural sources. An expression level of 0,2 mg per 1 l of culture will rapidly be limiting, particularly when considering that the overall yield of the purification procedure is generally very low.

Many membrane proteins are post-translationally modified. Since the modification is not always uniform, this is a source of inhomogeneity that interferes with successful protein crystallisation. Overexpression systems usually allow genetic engineering of the target protein in order to prevent the modification, that can, as long as the protein function is preserved, yield more homogeneous protein.

Other limitations for the study of membrane proteins are their transmembrane domains which result in sometimes extreme hydrophobicity. This makes them refractory to direct manipulation in aqueous solutions and necessitates the use of detergents for their functional solubilisation from the membrane and maintenance of their solubility throughout the purification process.

The choice of the expression system is critical in order to obtain a functional protein product. An overexpression system can be either homologous or heterologous. Both systems have their specific advantages and limitations, like how promising successful overexpression of a given target membrane protein appears, the genetic characterisation, the amenability to manipulation, the costs, and so on. The organisms commonly used for protein overexpression are bacteria (*Escherichia coli*), yeasts (*Saccharomyces cerevisiae*, *Schizosaccharomyces pombe*, *Pichia pastoris*), bacculovirus/ insect cells, and mammalian cells.

The advantages offered by *E.coli* are numerous, e.g., the homogeneity of recombinant proteins, no post-translational modifications, its short generation time (20 min), or its short delay of expression. However, *E.coli* is not the first choice organism for the overexpression of integral membrane proteins. Most importantly, *E.coli* cells simply do not contain enough membranes for the overproduction of membrane proteins. Moreover, the reductive environment of the bacterial cytoplasm can considerably slow down the production of functional integral membrane proteins, particularly if the correct folding of the protein requires formation of disulfide bridges (Sarramegna *et al.*, 2003).

Yeast is an excellent alternative to *E.coli* for the production of recombinant proteins. It is more easily amenable to rapid genetic manipulation than other eukaryotic cell systems (Bill, 2001). Yeast can perform post-translational modifications which are often required for the proper function of a (heterologous) protein. This feature is exploited when foreign proteins are expressed in yeast in order to study their function *in vivo*. However, it plays a minor role for the overproduction of a protein for crystallisation where monodisperse preparations are required, and post-translational modifications can be a source of inhomogeneity.

In particular, *S.cerevisiae* is a very attractive expression system, because of its capacity for high level protein production (including integral membrane proteins), its easy and usually inexpensive manipulation, its well-characterized genetics (the complete genome sequence is now available) as well as the availability of a large number of cloning vectors for the expression of foreign genes, and the short generation time (2 h) on very simple, low cost media.

The recent successful structure determination of the oligomeric mitochondrial cytochrome bc1 membrane protein complex from *S.cerevisiae* (Hunte *et al.*, 2000) shows that the large-scale purification of membrane proteins from *S.cerevisiae* is feasible in a suitable form for crystallisation.

Other yeasts, like *S.pombe* and *P.pastoris* were also tested for production of membrane proteins. In particular, *P.pastoris* is a very efficient system for protein overproduction, however only few membrane proteins have been successfully expressed in *P.pastoris* so far (Lin-Cereghino and Cregg, 2000). Moreover, certain disadvantages, e.g., a comparatively sparse palette of methods for genetic manipulation and limited knowledge of the biochemistry of that organism have still to be overcome .

For this study, the yeast *Saccharomyces cerevisiae* was then chosen as the expression system.

These features taken together make the development of methods for the study of membrane proteins lag far behind those of soluble proteins. Finally, one has to point out that large amounts of pure and homogeneous protein are absolute prerequisites to begin with crystallisation experiments. However, growing crystals with which to obtain high quality structural data is yet another story.

2.   Membrane protein families of interest

Up to now, 58 polytopic membrane proteins from bacteria and eukaryotic cells have been solved. Among them are plant photosystems and bacterial reaction centres (7), bacterial rhodopsins (5), light harvesting complexes (14), potassium channels (5), aquaporins and glycerofacilitators (5) and diverse transporters (7). The structure of only one GPCR has as yet been solved (source: http://www.mpibp-frankfurt.mpg.de/michel/public/memprotstruct.html).

2.1.   G-Protein Coupled Receptors

GPCRs represent a superfamily of integral membrane proteins. They are highly conserved through evolution and expressed in nearly all organisms ranging from yeast to humans. Almost 1% of all human genes code for this receptor family. They are involved in a wide spectrum of hereditary and somatic disorders and diseases, and are, thus, of enormous importance for the pharmaceutical industry (Pausch, 1997). GPCRs are the targets of more than 50% of the drugs currently used in therapeutics (Sautel and Milligan, 2000; Gudermann *et al.*, 1997), e.g., medicines such as beta blockers and anti-histamines, or drugs like opium and cannabis.

GPCRs are located in the plasma membrane. Their highly conserved three-dimensional structure is characterised by a common hydrophobic core composed of seven transmembrane α-helices, linked with three extracellular and three cytosolic loops. The N-terminal domain is extracellular, the C-terminal domain is cytosolic. The extracellular loops and the N-terminal domain are often glycosylated. All receptors cloned to date have at least one consensus sequence for N-linked glycosylation (Asn-X-Ser/Thr) in the extracellular domain. There are two highly conserved Cys residues in the second and third extracellular loops. The C-terminal domain usually contains a cystein residue attached to a lipid group. This group, often a myristoyl residue, is embedded in the membrane (Strader *et al.*, 1994).

Fig. 1 presents the classification of the different sub-families of GPCRs, with their main features (Bockaert and Pin, 1999)
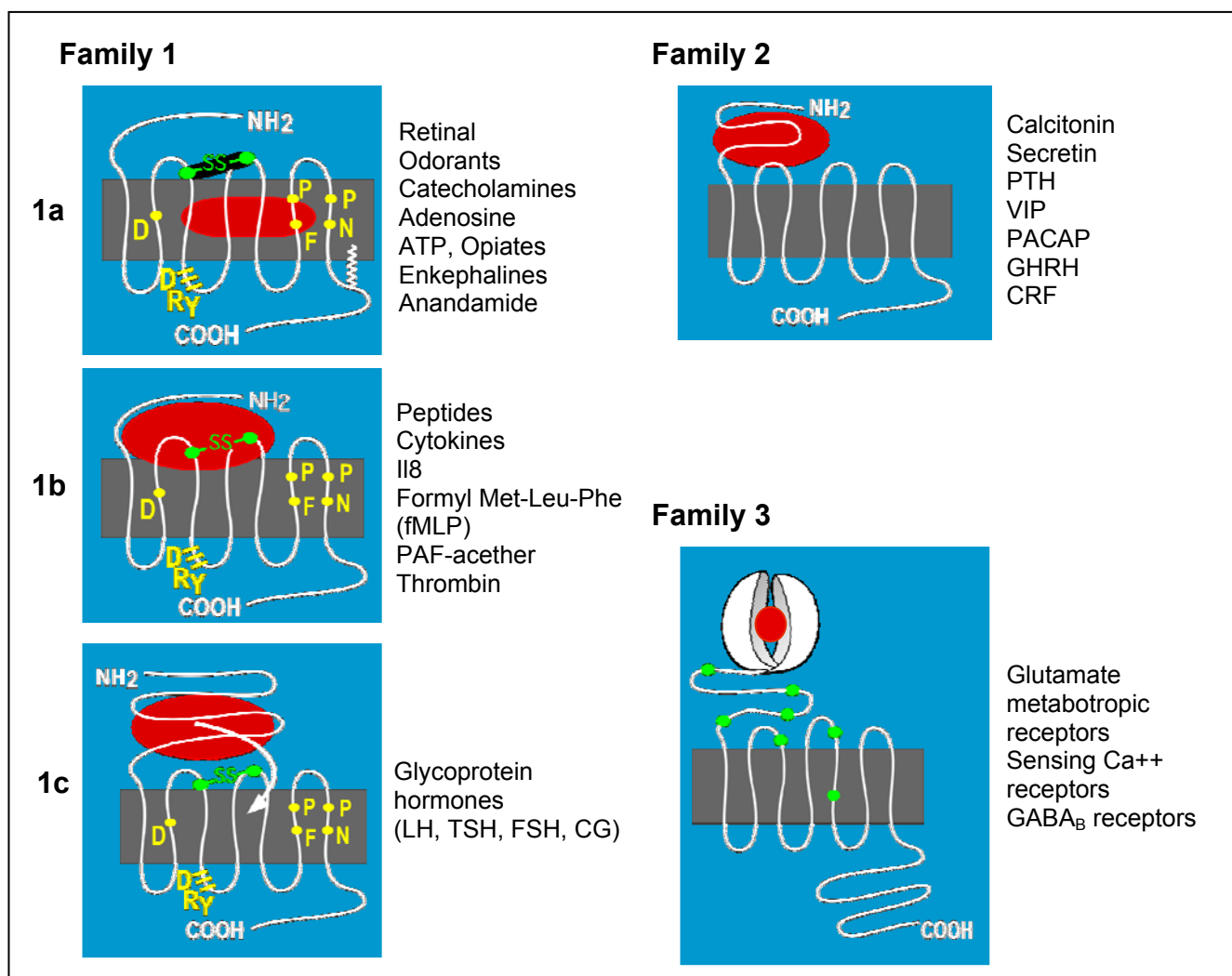
Fig. 1: **Classification of the G-protein coupled receptors, according to Bockaert and Pin (1999) (coloured schematic representation: courtesy of J. Bockaert)**. Family 1: Rhodopsin receptors and similar. Family 1a: receptors binding small ligands and with a binding site located between the membrane domains constituting the GPCRs "central region". Family 1b: Receptors binding peptides, with a binding site located in the N-terminus and the upper part of the transmembrane domains. Family 1c: glycoproteic hormone receptors, binding site in the external N-terminus. Family 2: Peptidic hormone receptors (secretin and similar). The family 2 present a similar morphology to the family 1 but no sequence similarity. Family 3: mGluRs and Ca^{2+}-detecting receptors, like the G_0 coupled $GABA_B$ (metabotropic GABA receptor pheromone-receptors. LH: luteneizing hormone, TSH: thyroid stimulating hormone, FSH: follicle stimulating hormone, CG: chorionic gonadotropin, PTH: parathyroid hormone, VIP: vasoactive intestinal peptide, PACAP: pituitary adeny/y/ cyclase activating peptide, GHRH: growth hormone releasing hormone, CRF: corticotropin releasing hormone, Il8: interleukine 8, PAF-acether: platelet-activating-factor-acether, GABA: gamma-amino-butyric acid. Green points in the family 3 are very well conserved cysteines in the metabotropic glutamate receptors.

GPCRs are responsible for the direct communication between the surroundings and the cell. They relay various extracellular signals and stimuli from the periplasmic side into the interior of the cell by activation of intracellular, heterotrimeric G-protein complexes (guanine nucleotide-binding regulatory protein) (Schoneberg *et al.*, 1999).

The cues for these signals are as diverse as hormones, pheromones, growth factors, neurotransmitters, odorants, photons and ions ((Watson and Arkinstall, 1994).

The signal is transmitted through the transmembrane helices to the cytosolic side where the G protein becomes activated and leads, usually through a cascade of kinase activations, to the initiation of gene transcription (Galvez and Pin, 2003; Gudermann *et al.*, 2000; Bockaert and Pin, 1999; Bockaert and Pin, 1998; Gudermann *et al.*, 1997; Strader *et al.*, 1994; Strader *et al.*, 1989) Dysfunction of GPCRs results in diseases as diverse as Alzheimer's, Parkinson's, diabetes, dwarfism, colour blindness, retina pigmentosa and asthma. GPCRs are also involved in depression, schizophrenia, sleeplessness, hypertension, impotence, anxiety, stress, renal failure, several cardiovascular disorders and inflammations (Schoneberg *et al.*, 2002; Young *et al.*, 2002; Spiegel, 2000; Schoneberg *et al.*, 1999; Spiegel, 1996).

About 1000 GPCR protein sequences are currently available in the publicly accessible databases, and about a dozen new sequences become available every month (e.g. the Swiss-Prot database). However, in contrast with this wealth of sequence data and in spite of their widespread occurrence in humans and other eukaryotes and tremendous importance to the pharmaceutical industry, only one structure of a GPCR is available, that was solved at sufficient resolution to reveal mechanistic details of ligand binding and signal transmission. This is the structure of bovine rhodopsin, determined by X-ray crystallography at 2,8 Å resolution (Fig. 2) (Palczewski, 2006; Palczewski *et al.*, 2000). Light activated bovine rhodopsin is the representative of a number of GPCRs in which the activating extracellular chemical stimulus is bound to a binding pocket within the bundle of the seven α-helices, in the plane of the lipid bilayer.
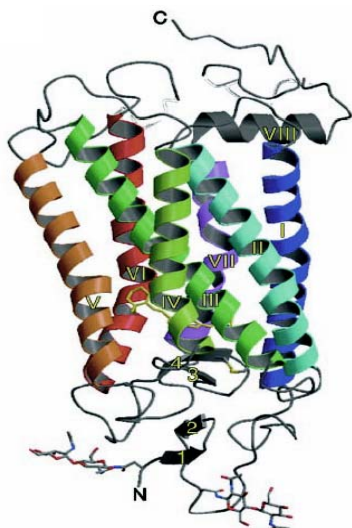
Fig. 2 **Representation of the 3D-structure of bovine rhodopsin**. (Palczewski, 2006; Palczewski *et al.*, 2000). View parallel to the plane of the membrane. The transmembrane domains are designated with roman numbers I to VII.

Because of their central role in biological systems, detailed understanding of the process that controls the interaction of GPCRs with their ligands and associated G proteins is very challenging. This understanding would be greatly improved by high-resolution 3D structures of these receptors.

2.2. Hyperthermophilic transporters from *Methanococcus jannaschii*

2.2.1. The archeon *Methanococcus jannaschii* (*Methanocaldococcus jannaschii*)

Archaea, although they are prokaryotic organisms, share specific features with Eukarya, and they have now been recognized as their closest ancestors. Their unique phylogenetic position, and the fact that in many cases they actually bridge the gap between Eukarya and Bacteria, renders them an ideal system for genomic comparisons.

Methanococcus jannaschii is the first archaeal organism whose genome has been completely sequenced (Bult *et al.*, 1996).

Discovered in 1983, strain JAL-1 was originally isolated from a sediment sample collected from the sea floor surface of a 2600 m-depth "white smoker" chimney, in the East Pacific Rise near the western coast of Mexico (Jones *et al.*, 1983). Two similar strains were isolated from hydrothermally active sediments in the Guaymas Basin at a depth of 2000 meters (Jones *et al.*, 1983). *M.jannaschii* is able to grow at high temperatures, ranging from 48 to 94 °C, with an optimum growth temperature at 85 °C. It also grows in habitats with pressures up to more than 200 Atm (Mombelli *et al.*, 2002), and is adapted to moderate salinity as well. *M.jannaschii* is a hyperthermophilic methanogenic archaeon, and a typical autotroph. Though it has not yet been demonstrated that *M.jannaschii* can fix nitrogen like a number of other methanogens, the sequencing of its genome revealed the presence of all the genes necessary for this pathway. It is a strict anaerobe organism, and, thus, it performs anaerobic respiration and obtains its energy by the reduction of CO_2 with H_2 to generate methane. Cells of *M.jannaschii* are irregular cocci (Jones *et al.*, 1983). The cell envelope is composed of a cytoplasmic membrane and a protein surface layer. Polar bundles of flagella are also present. This morphology is common among methanococci.

2.2.2. Hyperthermophilic proteins from *M.jannaschii*

Proteins from hyperthermophilic organisms are of major interest for the biotechnological industry because of their enormous stability, especially against thermal denaturation (Perl, 2002 ; Jaenicke, 1996; Gross and Jaenicke, 1994).

Hyperthermophilic proteins are expressed and function optimally at high temperature, (60°C and higher), and they are in general thermodynamically more stable than mesophilic proteins, that are expressed at a temperature between 20 and 40°C.

Understanding the molecular principles that furnish the proteins of extremophiles with stability at high temperatures, under high pressure or at extreme pH values would be very useful for future biotechnology.

Crystal structures of only a few proteins from thermophilic organisms have, until now, been determined. Due to limited 3D structural analysis data of hyperthermophilic proteins, it is difficult to determine the critical factors for protein thermostability. No general rules or definitive explanations for thermal stabilisation have been deduced so far from sequence (Bohm and Jaenicke, 1994) and/or structural data (Jaenicke and Bohm, 1998). Nevertheless, reasons for high thermostability that have been suggested are hydrogen-bonds (Vogt and Argos, 1997; Vogt *et al.*, 1997), hydrophobic interactions (Spassov *et al.*, 1995), internal packing (Thompson and Eisenberg, 1999), salt-bridges (Chan *et al.*, 1995; Yip *et al.*, 1995; Kelly *et al.*, 1993) and secondary structural features (e.g. intra-loop, rop-loop, (Nagi and Regan, 1997)) .

Comparison between thermophilic and mesophilic protein sequences shows that amino acid residues capable of forming hydrophobic, hydrogen or ionic bonds occur more frequently in hyperthermophilic proteins (Shiraki *et al.*, 2001; Vieille and Zeikus, 2001; Thompson and Eisenberg, 1999; Vetriani *et al.*, 1998; Rice *et al.*, 1996; Chan *et al.*, 1995; Spassov *et al.*, 1995; Szilagyi and Zavodszky, 1995). In integral membrane proteins, the bonds result in strong interactions between pairs of transmembrane domains (TM), and they are expected to add extra-stability to transmembrane domain interactions at higher temperatures (Schneider *et al.*, 2002).

Comparisons of the structure and of the conformational stability (by comparison of thermodynamics and unfolding profiles) between thermophilic and mesophilic proteins revealed that clusters of salt bridges may be an important factor contributing to high thermostability. Evidently, packing density enhanced by van der Waals interactions and additional networks of ion pairs and hydrogen bonds seem to play a major role in the thermal adaptation strategies. Indeed, owing to a tighter helical packing, thermophilic proteins are thought to be better able to resist denaturation due to the decrease of lateral pressure (Schneider *et al.*, 2002; Shiraki *et al.*, 2001).

The glutamate transporter (GltT) from *Bacillus stearothermophilus* is an example of a highly stable thermophilic membrane protein (Wang *et al.*, 2003). GltT constitutes an extremely stable protein in comparison to similar transporters from mesophiles. It remains dimeric from pH 4-9 in different detergents. When incubated at 37°C for 2h, GltT shows no aggregation or change in oligomeric state.

As membrane proteins from thermophilic organisms are expected to be more stable in the detergent-solubilised state than their mesophilic counterparts (Schneider *et al.*, 2002; Shiraki *et al.*, 2001), they are thought to represent ideal crystallisation targets.

For this reason, we chose to study different membrane proteins from *M.jannaschii*.

3.   Characteristics of the proteins of interest

Considering the difficulties inherent to studies on membrane proteins and the small number of 3D-structures of membrane proteins that are currently solved, a GPCR of *S.cerevisiae*, and several transporters of *M.jannaschii* were chosen for expression in yeast in order to select among them the best candidates for subsequent crystallisation experiments.

3.1. Ste2p, a G-Protein Coupled Receptor of *Saccharomyces cerevisiae*

We chose to study the alpha-factor pheromone receptor of *Saccharomyces cerevisiae*, Ste2p. We presumed it would be a good candidate for structural analysis, since Ste2p belongs to the class D pheromone family of G-protein coupled receptors. Ste2p has been frequently used as a model for studying the structure and function of GPCRs (Lee and Altenberg, 2003; Dohlman and Thorner, 2001; Leberer *et al.*, 1997).

3.1.1. Function of Ste2p

S.cerevisiae haploid cells of either a- or α- mating-type, secrete peptide pheromones, the a- and α-factors, which bind to their GPCRs, Ste3p or Ste2p, respectively that are located in the plasma membrane. Binding leads to activation of the mating signal-transduction pathway, which results in cell-cycle arrest in G1, morphological changes and transcriptional activation of genes involved in the pheromone response and mating process. Upon binding of the α-factor, a tridecapeptide pheromone (Trp-His-Trp-Leu-Gln-Leu-Lys-Pro-Gly-Gln-Pro-Met-Tyr), Ste2p initiates a cascade of intracellular events that lead to mating of haploid yeast cells.

The molecular details of this pathway have been extensively investigated (Dohlman and Thorner, 2001; Versele *et al.*, 2001; Pausch, 1997) (Fig. 3). After binding of their ligands, the pheromone receptors interact with a heterotrimeric G protein, (whose α-, β- and γ-subunits are encoded by GPA1, STE4 and STE18, respectively), that catalyses the exchange of GDP for GTP bound to the α-subunit. Subsequently, the β/γ-subunit complex dissociates from the α-subunit, and initiates a MAP kinase cascade by activation of the protein kinase Ste20p and the scaffold protein Ste5p. Ste5p forms the core of a signaling complex that contains the Ste11p MAPKKK, the Ste7p MAPKK and the Fus3p/Kss1p MAPK. Activated Fus3p/Kss1p then induces the transcription of several specific mating factor-inducible genes by activating the transcription factor Ste12p. The activation of Fus3p/Kss1p also leads to the cell cycle arrest at the G1/S transition by activating the inhibitor of the Cdc28-Cln kinase, Far1p (Posas *et al.*, 1998).
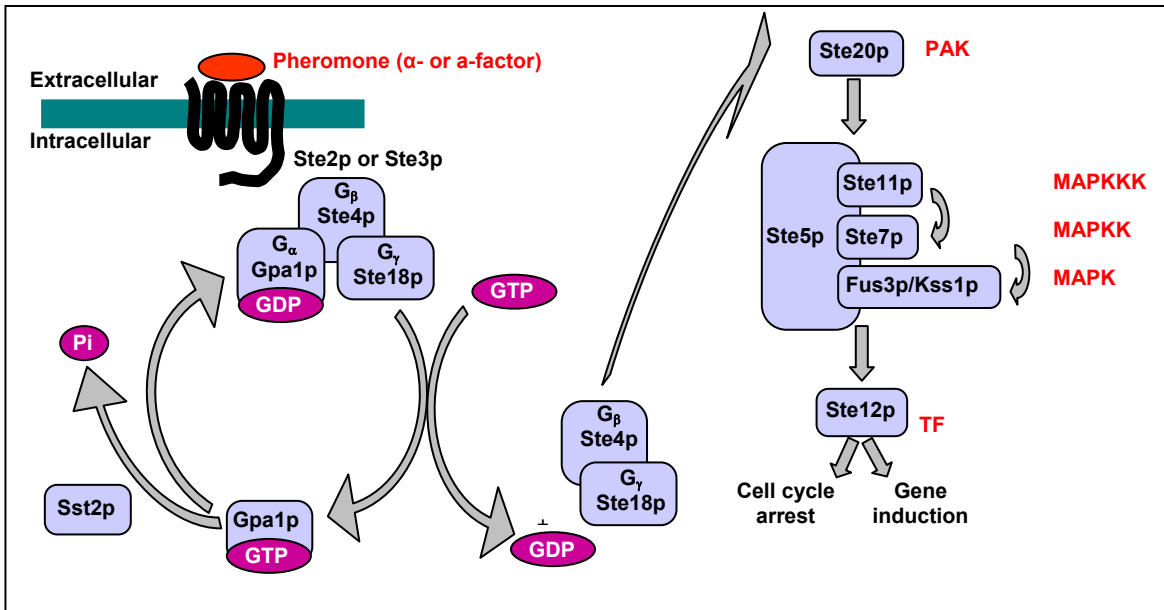
Fig. 3: *Saccharomyces cerevisiae* **pheromone response pathway.** Involved proteins are represented in coloured blocks. Gα, Gβ and Gγ represent respectively the α, β and γ subunits of the heterotrimeric G-protein. PAK: Protein Activated Kinase, MPAK: Mitogen Activated Protein Kinase MAPKK: MPAK Kinase, MAPKKK: MPAK Kinase Kinase, TF: Transcription Factor.

3.1.2. Secondary structure of Ste2p

Ste2p features 5 possible glycosylation sites, among which only the Asn^{32} and the Asn^{25} are used. It presents an endocytosis signal in the C-terminus (Fig. 4).
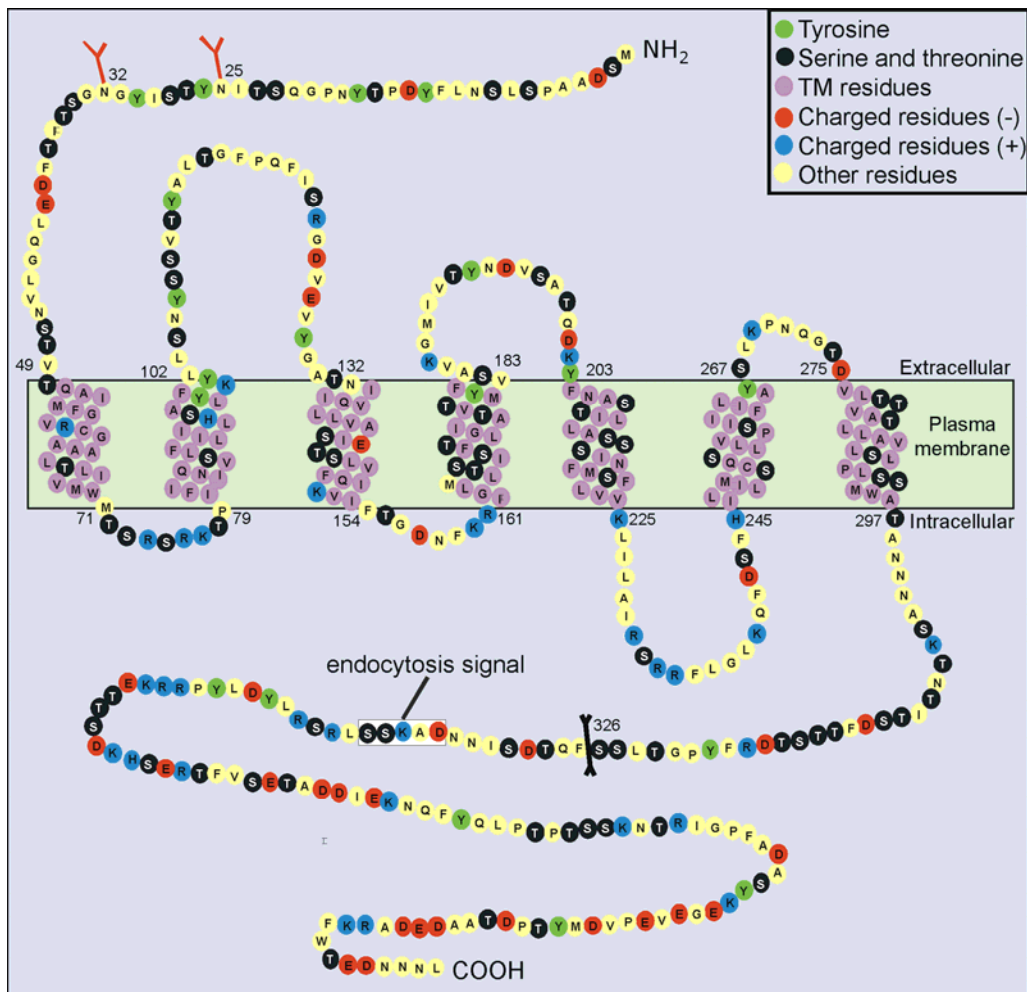
Fig. 4: **Topology model of Ste2p secondary structure.** The model was established manually, based on the topology prediction of the software TMHMM. Ste2p features 471 amino-acids and a molecular weight of 47848,7 kDa. Ste2p presents 7 transmembrane domains, between the amino-acids #49-#71, #79-#102, #132-#154, #161-#183, #203-#225, #245-#267 and #275-#297. The N-terminal part NH_2 is periplasmic, and the C-terminal part COOH is cytosolic. The residues Asn^{25} and Asn^{32} are glycosylation sites. The mutant receptor used in this work was truncated after the residue Ser^{326}.

In fact, Ste2p shows no significant sequence similarity to human receptors of clinical interest. Nevertheless, previous biochemical studies on this receptor (mutational and homology modeling) revealed characteristics of GPCRs that highlight the underlying structural and functional similarities between the yeast and mammalian homologues (Eilers *et al.*, 2005). An activation of mammalian G-protein by Ste2p and a reciprocal activation of the yeast pheromone responsive pathway by mammalian GPCRs were demonstrated (Ladds *et al.*, 2005; Yin *et al.*, 2005; Ladds *et al.*, 2003). These observations taken together made Ste2p a very attractive candidate for experimental structure determination and the study of GPCR signal transduction mechanisms. The elucidation of its structure should provide fundamental insights into the structure-function relationships of ligand-binding and activation of peptide-responsive human GPCRs.

3.2. Hyperthermophilic transporters from *M.jannaschii*

We chose to overexpress five different types of putative membrane transporters from *Methanococcus jannaschii*: an amino-acid transporter (AAT), a sodium-dicarboxylate transporter (DASS), a sodium transporter (NSS), a potassium uptake protein (TRK) and a putative phosphate permease (PHOP). Their secondary structure pattern and selected biophysical parameters of the different membrane proteins, such as size, numbers of transmembrane helices and isoelectric point are outlined in Fig. 5.
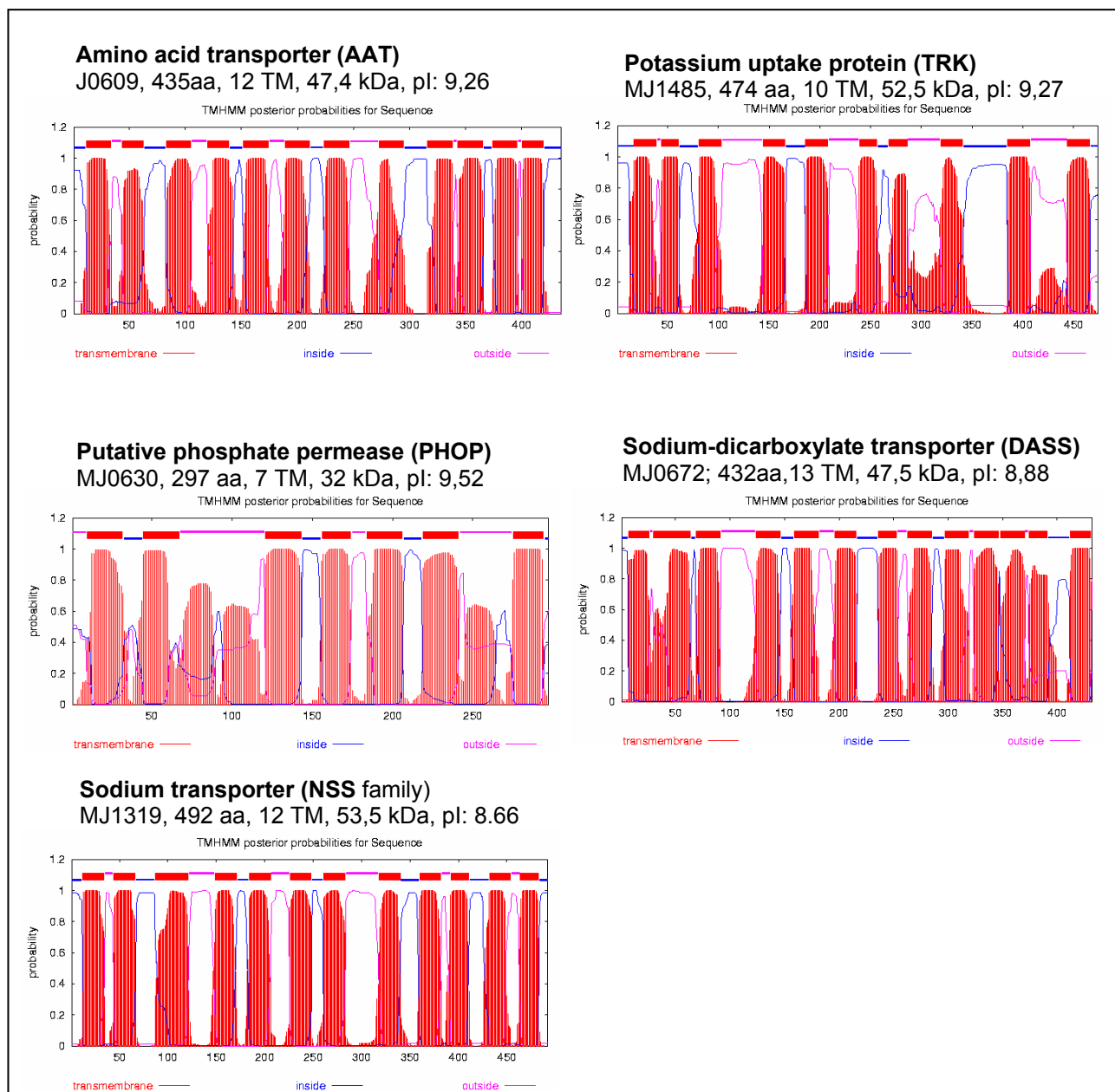
Fig. 5: **Secondary structure pattern of the proteins of interest**. Prediction by the TMHMM software.

4. Reasons for the overexpression of Ste2p and hyperthermophilic transporters in *S.cerevisiae*

4.1. Expression of the GPCR Ste2p in *S.cerevisiae*

The majority of heterologously expressed GPCRs are from murine and human origin and, therefore, require a specific lipid environment. Indeed, the activity of certain receptors such as the oxytocin (Gimpl et al., 1995), the transferrin (Nunez and Glass, 1982) and human *μ*-opioid receptors (Lagane *et al.*, 2000; Hasegawa *et al.*, 1987) strongly depends on the lipid environment. Obviously, mammalian cells represent the most appropriate expression system for these GPCRs, more so as they can provide the G proteins necessary for a functionality test of the expressed GPCR. However, these advantages are opposed by problems like relatively long generation times, the need for stable cell lines, that are expensive and time-consuming to generate, and the requirement of complex and costly culture media (Sarramegna *et al.*, 2003).

The expression level of a given GPCR can significantly vary in different expression systems. For instance, the human β2-adrenergic receptor is very efficiently expressed in almost every system, (Sarramegna *et al.*, 2006; Opekarova and Tanner, 2003; Sarramegna *et al.*, 2003; Sizmann *et al.*, 1996), whereas the human μ-opioid receptor is expressed at low levels in whatever system used (eukaryotic or prokaryotic, (Sarramegna *et al.*, 2003)).

Of the 25 GPCRs expressed in yeast, 14 were expressed at a level above the minimal expression yield of 5 pmol/mg of total membrane protein. In *E.coli*, out of 25 expressed GPCRs, only 4 exceeded the minimal expression level as compared to 13 out of 60 in insect cells and 10 out of 55 GPCRs in mammalian cells (Shi *et al.*, 2005; Yin *et al.*, 2005). This survey which is far from being complete argues strongly for GPCR expression in yeast as it is the system in which the minimal expression yield was most frequently obtained. Yeasts are an attractive expression system also with regard to lipid environment since their membranes are composed of lipids similar to those of mammalian cells.Nevertheless, the optimal expression system has to be individually chosen for each single GPCR (Sarramegna *et al.*, 2003; Chapot *et al.*, 1990).

The functional expression of a number of G-protein coupled receptors was demonstrated in yeast (Ladds *et al.*, 2005; Reilander and Weiss, 1998; Grisshammer and Tate, 1995). Some of these receptors were expressed at good levels, like the human α2-adrenergic receptor subtype C2 (70 to 350 pmol/mg membrane protein) (Sizmann *et al.*, 1996; King *et al.*, 1990) and the human β2-adrenergic receptor (Sizmann *et al.*, 1996; King *et al.*, 1990). For other GPCRs the expression in *S.cerevisiae* was the only possible way.

The *S.cerevisiae* α-factor receptor, Ste2p, was homologously expressed in *S.cerevisiae* for *in vivo* functional studies (Caponigro *et al.*, 2003; Lee and Altenberg, 2003; Lin *et al.*, 2003; Overton and Blumer, 2002; Parrish *et al.*, 2002; Mentesana and Konopka, 2001; Konopka *et al.*, 1988).

Homologously overexpressed Ste2p was purified and used in reconstitution and ligand binding experiments that demonstrated that the detergent-solubilised receptor retained its native structure (David *et al.*, 1997). Although expression levels were the highest ever obtained for a GPCR (350 pmol/mg membrane protein*,* (Sarramegna *et al.*, 2003)), the yields of purified protein (1 mg of receptor at 95% purity from 20 litres of cell culture) were lower than expected, suggesting that the efficiency of solubilisation and/or purification can still be improved. Ste2p was also expressed in mammalian cells (Shi *et al.*, 2005; Yin *et al.*, 2005), however, even if the expressed proteins were functional, their expression levels were very low. This example clearly illustrates the importance of a native receptor environment.

For protein crystallisation experiments, high amounts of pure and monodisperse protein are required, although automated crystallisation experiments by robots need only few nanoliters amounts of proteins. In order to obtain the required quantity, we decided to overexpress Ste2p in its native environment, the plasma membrane of *S.cerevisiae.* Furthermore, we modified the amino acid sequence of Ste2p in a way that excluded post-translational modifications but did not adversely affect the receptor activity. For facilitated purification, we fused the receptor to two affinity tags.

4.2. Expression of the hyperthermophilic membrane proteins in *S.cerevisiae*

The heterologous expression of thermophilic proteins in mesophilic hosts greatly facilitates the purification of the desired thermostable product. Non heat-stable proteins can be denatured and precipitated by a heat treatment step whereas the desired protein remains soluble and functional due to its inherent thermostability. Thermophilic archea use rare codons for translation. Thus, if *E. coli* is chosen as the expression host, it has to carry plasmids encoding tRNAs that recognise rare codons, whereas the same codons are frequently used by eucaryotic organisms. Some hyperthermophilic membrane proteins from *Thermotoga maritima* were expressed in *E.coli*, but a low levels (Columbus *et al.*, 2006).

The functional expression of hyperthermophilic membrane proteins has been demonstrated in *S.cerevisiae*, at good levels, like a H^+-PPase and a V-PPase from *Thermotoga maritima* (López-Marqués *et al.*, 2005; Perez-Castineira *et al.*, 2001) and the Ca^{2+}-ATPase from *M.jannaschii* (Morsomme *et al.*, 2002), and eight other membrane proteins from *T.maritima* (Columbus *et al.*, 2006)). It was also previously shown that the H+-PPase from *T.maritima*, overexpressed in *S.cerevisiae*, was resistant to yeast proteases (Perez-Castineira *et al.*, 2001) and that hyperthermophilic proteins proved to be resistant to proteolyse (triosephosphate isomerase from *Pyrococcus furiosus*, (Mukherjee and Guptasarma, 2005). *S.cerevisiae* also proved to be efficient for the functional expression of Ca^{2+}-signaling and Ca^{2+}-transporting ATPases (Ton and Rao, 2004). A vacuolar-type H^+-PPase from *T.maritima* and a plant H+-ATPase were as well functionally expressed and characterised in *S.cerevisiae* (Perez-Castineira *et al.*, 2001; Lanfermeijer *et al.*, 1998; Lanfermeijer *et al.*, 1997).

For these reasons and because eukaryotic cells are generally better suitable for the expression of integral membrane proteins, *S.cerevisiae* was chosen for the expression of the *M.jannashii* membrane transporters.

The general aim of this study was therefore the overexpression and isolation of membrane proteins in general, and Ste2p and Aatp specifically, in *S.cerevisiae* in order to initiate the approach for 3D-structural elucidation by crystallisation.

Results

In this study, the GPCR Ste2p was cloned, modified and homologously overexpressed in *Saccharomyces cerevisiae*. The receptor was purified by affinity chromatography, and crystallisation experiments were finally undertaken. We worked with a mutant form of the α-factor receptor Ste2p, designated Ste2^{m}p. Ste2p was truncated at the C-terminus and site-specific amino acid mutations were introduced in order to avoid post-translational modification. Two-affinity-tags, a His$_6$-tag and a FLAG-tag, were added to the C-terminal part of the truncated protein, to facilitate purification by affinity chromatography procedures. Activity assays were conducted to rule out a possible interference of the modifications with protein function. Three different plasmid constructs and several different culture conditions were tested in order to optimise Ste2^{m}p expression. Once suitable overexpression conditions were implemented, several detergents were tested for Ste2^{m}p solubilisation and affinity chromatography was customised for the purification of detergent-solubilised Ste2^{m}p. After a final characterisation of the purified integral membrane protein it was subjected to preliminary crystallisation experiments.

5. Homologous overexpression and isolation of the *Saccharomyces cerevisiae* α-factor receptor Ste2p in *Saccharomyces cerevisiae*

5.1. Cloning strategy

5.1.1. Ste2p amino-acid sequence alterations: mutations of N-glycosylations sites and truncation of the C-terminal part

Eukaryotic cells are able to perform post-translational modifications, such as N-glycosylation, that, e.g., can influence protein folding and/or stability, or phosphorylation that is involved in signal transduction. Post-translational modifications, despite their biochemical importance can, however, lead to protein structure heterogeneities and subsequently problems during crystallisation. Previously, it had been shown that purified wild-type Ste2p displayed heterogeneity on SDS gels, which in part originated from N-glyclosylation of the receptor (Mentesana and Konopka, 2001). Ste2p is glycosylated at two consensus N-glycosylation sequences present at the extracellular N-terminal domain of the protein (Mentesana and Konopka, 2001).

In order to obtain a homogenous protein preparation for crystallisation, all known post-translational modification sites were removed from Ste2p. Thus, the cytoplasmic C-terminal part of Ste2p was truncated at position Ser^{326} to remove endocytosis signals as well as residues that are phosphorylated in the receptor´s basal state (Konopka *et al.*, 1988; Reneke *et al.*, 1988).

Out of the five potential N-glycosylation sites, Asn^{25}, Asn^{32}, Asn^{46}, Asn^{105} and Asn^{205}, only Asn^{25} and Asn^{32} are actually glycosylated (Mentesana and Konopka, 2001).

Thus, only these two were inactivated to prevent carbohydrate attachment by substituting the asparagine residues for glutamines. This modified Ste2p was designated Ste2p$^{N25,32Q-T326-FT.HT}$, Ste2^{m}p for short.

5.1.2. Construction of the Ste2^{m}p expression vector pT326 and the expression strain YpT326

A vector was generated to express a C-terminally FLAG-His$_6$ double-tagged variant of Ste2^{m}p.

The modified receptor gene was designated *STE2*$^{N25,32Q-T326-FT.HT}$, *ste2*^{m} for short, and inserted into the multi-copy *E.coli* / yeast shuttle vector pYES2 to yield expression vector pT326. The vector pT326 carries the ampR and *URA3* markers for selection in *E.coli* and *S.cerevisiae*, respectively. The 2 µ origin of replication allows multi-copy autonomous replication of the plasmid in yeast, and the strong galactose-inducible *GAL1* promoter drives expression of the cloned *ste2*^{m} gene. Successive in-frame C-terminal FLAG- and His$_6$-tags facilitate purification by affinity chromatography.

Transformation of the yeast uracil auxotrophic strain BJ5464 with vector pT326 yielded strain YpT326 for the expression of the modified Ste2^{m}p receptor.

5.1.3. Alternative expression strains

In order to push the expression level of Ste2^{m}p, two additional expression strains were constructed.

For the first alternative, the strain BJ5464 was transformed with a version of the expression vector pT326 that carries the *ura3d* selection marker instead of *URA3* (pT326-*ura3d*). The resulting expression strain was designated YpT326-*ura3d*. Since *ura3d* is a promoterless selection marker, uracil auxotrophic yeast cells carrying pT326-*ura3d* can only grow on medium without uracil if they maintain the plasmid at high copy numbers (Loison *et al.*, 1989). This is achieved in combination with the 2 µ origin of replication on pT326-*ura3d*, leading to very high copy numbers, and, expectedly, to increased Ste2^{m}p expression.

The second alternative expression strain, YpMEGA/pT326-*ura3d*, was generated by co-transforming BJ5464 with pT326-*ura3d* and the pMEGA vector (Sil *et al.*, 2000). The pMEGA vector allows overexpression of the Gal3p, Gal80p and Gal4p switch proteins for enhanced transcription from the *GAL1* promoter. Co-expression of these switch proteins in a strain already sustaining high copy numbers of pT326-*ura3d* was expected to boost Ste2^{m}p expression even further.

The features of the three expression strains are summarised in the Table 1.

Strain	Plasmid	Important features
YpT326	pT326	- 2 µ origin of replication
		- *URA3* selection marker
YpT326-*ura3d*	pT326-*ura3d*	- 2 µ origin of replication
		- promoterless *ura3d* selection marker
YpMEGA/T326-*ura3d*	pT326-*ura3d*	- 2 µ origin of replication
		- promoterless *ura3d* selection marker
	pMEGA	- enhanced transcription from the *GAL1* promoter

Table 1: **Denominations and important features of each construction.**

5.2. Selection of a suitable Ste2^{m}p expression strain

5.2.1. Selection by Ste2^{m}p expression level

The expression levels of Ste2^{m}p were compared in the three different strains (see Table 1). The aim of this experiment was to test whether enhanced transcription of the *ste2^m* gene by overexpression of the Gal transcription factors from the pMEGA vector leads to increased levels of Ste2^{m}p expression.

Expression strains YpT326, YpT326-*ura3d* and YpMEGA/T326-*ura3d* were inoculated to OD$_{600}$ 0,02 and the cultures grew overnight at 30°C in non-inducing selective complete medium lacking uracil and leucine, and containing raffinose as the sole carbon source (Sc∅Uracil∅Leucine-4% raffinose pH 6; selective raffinose medium; see material and methods section, chapter 13.2.1). Cells were induced by the addition of 2% galactose at an OD$_{600}$ of 1 to 2. Representative growth curves of the three different strains in selective raffinose medium are shown in Fig.6.
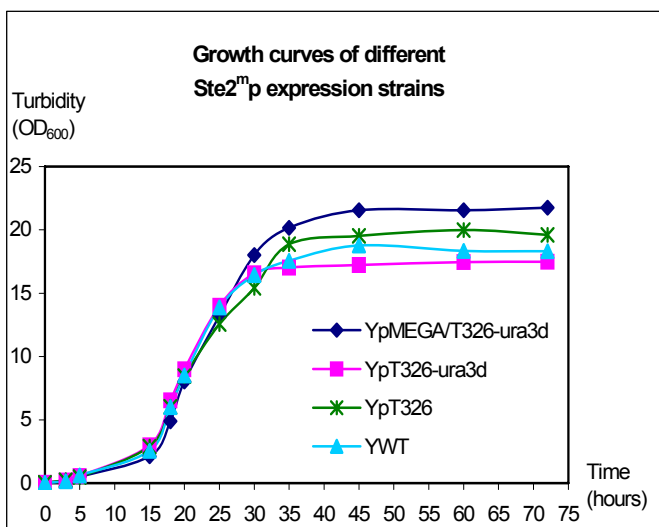
Fig. 6: **Growth curves of different Ste2^{m}p expression strains**. Ste2^{m}p is a mutant Ste2p as explained in chapter 5.1.1. YpMEGA/T326-*ura3d*, YpT326-*ura3d* and YpT326 are detailed in Table 1; YWT, strain expresses the wild-type Ste2p.

The different Ste2^{m}p expression strains grew indiscernibly which indicates that growth was not affected by overexpression.

The expression levels of Ste2^{m}p from isolated total membranes were analysed in three independent transformants (#1, #2, #3) of each strain by Western-blotting with a specific anti-His$_6$ antibody. As is clearly evident from Fig. 7, Ste2^{m}p expression varied noticeably in the different strains.
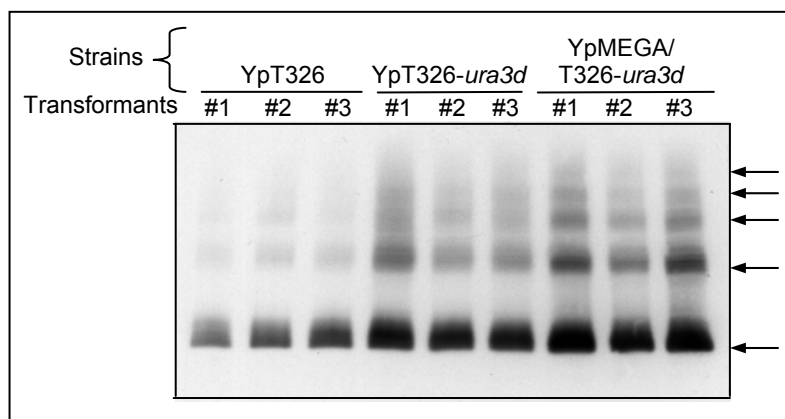
Fig. 7: **Comparison of the Ste2^{m}p expression level in different yeast strains**. Three independent transformants each were examined. 5 µg of isolated total membranes from the strains YpT326, YpT326-*ura3d* and YpMEGA/T326-*ura3d* were analysed for Ste2^{m}p by immuno-blotting.
Arrows indicate oligomeric Ste2^{m}p.

As expected, the strain YpMEGA/T326-*ura3d* yielded the most prominent Ste2^{m}p signal on the immunoblot as compared to YpT326-*ura3d* and YpT326.

Obviously, the combination of a strong inducible promoter (*GAL1*) and consitutive overexpression of the GAL transcription factors with very high plasmid copy number (2 µ origin of replication plus promoterless *ura3d* selection marker) considerably improves Ste2^{m}p expression.

Consequently, the expression strain YpMEGA/T326-*ura3d* was chosen to express Ste2^{m}p in all subsequent experiments.

5.2.2. Alpha-factor functionality test I: the halo assay

It was previously shown by others that the structural modifications (mutations of the N-glycosylation sites and truncation after Ser^{326}) generated in Ste2^{m}p do not alter receptor function or its subcellular localisation (Mentesana and Konopka, 2001; Konopka *et al.*, 1988).

A halo-assay was performed in order to determine whether the modified receptor Ste2^{m}p was still functional *in vivo*. We exploited the fact that binding of α-factor ligand to a functional Ste2p receptor leads to the arrest of cell growth (see introduction section, chapter 3.1.1).

Yeast cells were mixed with agar, as described in the Materials and Methods section (chapter 13.1.4), and poured into petri dishes. Various quantities of α-factor were spotted onto sterile filter paper disks that were positioned on the agar plates. After incubation at 30°C, the plates were inspected for halos around the α-factor filter disks. If halos were present, they would indicate areas where yeast cells had not grown due to diffusion of the α-factor into the agar; that means, halos indicate growth arrest of yeast cells. Growth arrests only if the α-factor receptor expressed by the yeast cells is functional and can bind its ligand, the α-factor, and relay the external signal to the cell interior.

We intended to ensure that possible growth effects were dependent on the Ste2p mutants expressed and not on the endogenous wild-type Ste2p. Therefore, we transformed a Δste2 null mutant, a knock-out strain that does not express Ste2p, with the plasmid constructs for expression of the desired Ste2p mutants (see Material and methods section, chapter 9.1.1.1). An untransformed Δste2 null mutant was used as negative control. In this case, no halos were observed (ΔSte2p, Fig. 8, lower right plate), confirming that Ste2p is implicated in and necessary for the growth arrest. On the petri dish inoculated with a yeast strain that expressed the unmodified Ste2p receptor (Ste2p, Fig. 8, lower left plate), halos were observed whose size was directly related in a proportional manner to the amount of α-factor peptide loaded onto the filter disk. A similar halo pattern was observed with a yeast strain expressing the unmodified receptor carrying His$_6$- and FLAG affinity tags (Ste2p$^{FT.HT}$, Fig. 8, upper right plate). The same halo pattern was observed in the case of yeast cells expressing Ste2^{m}p, Fig. 8, upper left plate. In all cases, the modified Ste2p receptors could recognise and bind the α-factor ligand with the same sensitivity as the wild-type, and were able to mediate growth arrest in response to it.

Obviously, the modifications in Ste2^{m}p, i.e. the amino acid exchanges N25Q and N32Q, the truncation at Ser^{326} and the C-terminal attachment of the FLAG- and His$_6$-tags, did neither alter nor compromise the *in vivo* functionality of the receptor.
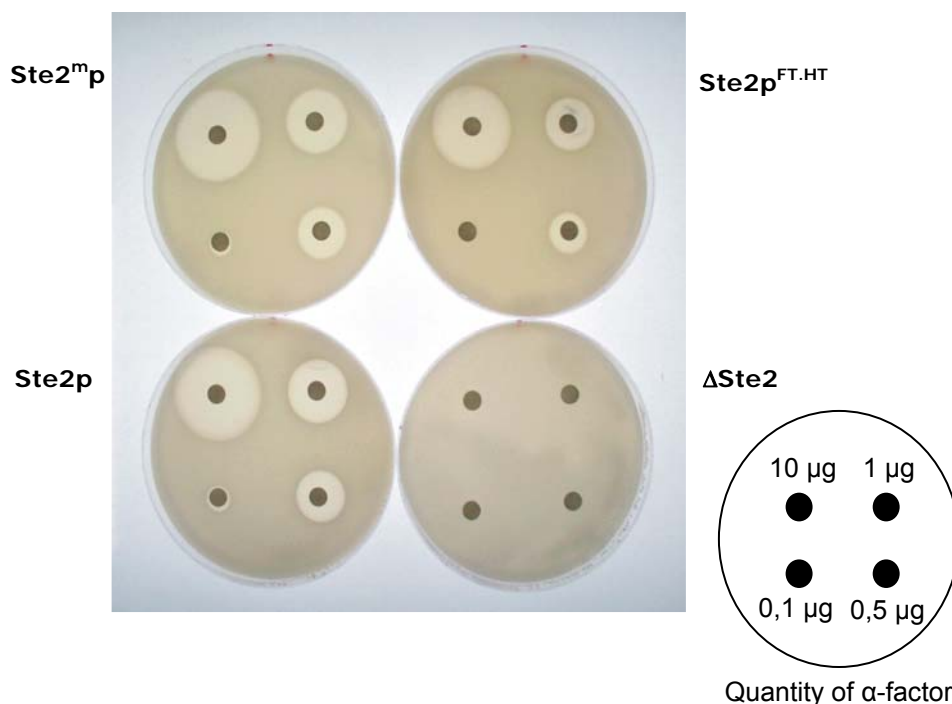
Fig. 8**: Halo-assay for assessment of the *in vivo* functionality of Ste2p and its mutant derivatives.** Paper disks on each plate contain 0,1 µg, 0,5 µg, 1 µg and 10 µg of α-factor as shown in the cartoon on the lower right. Halo-assays were performed with BY4741, a strain expressing wild-type **Ste2p**; a strain unable to express functional Ste2p (**ΔSte2**); a strain carrying the vector for expression of Ste2p with the FLAG- and His$_6$-tags (**Ste2p$^{FT.HT}$**); and a strain expressing the modified Ste2^{m}p (for vector construction details see above).

5.2.3. Alpha-factor functionality test II: the binding-assay, characterisation of binding properties K_d/B_{max}

In the halo assay, we had shown that Ste2^{m}p is active. In a subsequent binding assay which employed radioactive [^{3}H]α-factor we intended to assess the substrate binding constants and compare them to those of the wild-type Ste2p. [^{3}H]α-factor binding was assessed by incubating 2 µg of stripped membranes from transformants of the strain YpMEGA/T326-*ura3d* with a saturating concentration of [^{3}H]α-factor (300 nM final concentration), in the presence or absence of an excess of unlabelled peptide (Fig. 9). Specific binding was calculated by substracting the unspecific binding from the total binding in the presence of unlabelled peptide. We obtained a maximum binding capacity B_{max} value of 91 ± 7 pmol/mg protein and a K_d of 87 ± 16 nM.. The K_d is 4-5-fold higher than reported for the wild-type (David *et al.*, 1997).
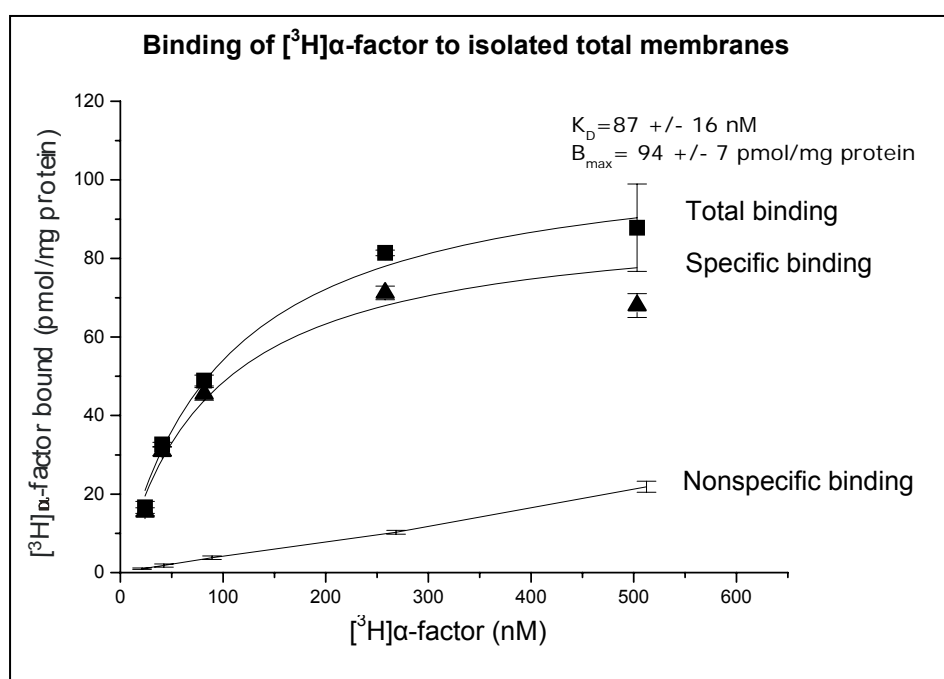
Fig. 9**: Binding of [^{3}H]α-factor to isolated total membranes (stripped).** Total binding was determined with six samples in the presence of a 1000-fold molar excess of non-radioactive α-factor. Specific binding (▲) was obtained by subtracting nonspecific binding (I) from total binding (■).

5.2.4. Alpha-factor functionality test III: competitive inhibition assays, stereospecificity

Having determined that the Ste2^{m}p expression was effective and yielded active α-factor receptor function, it was necessary to demonstrate that the mutant receptor still retained its ability to discriminate between atomically identical (but stereochemically distinct) α-factor analogues (Fig. 10), as the unmodified receptor does in its native membrane environment.

Competition studies were conducted with two different stereoisomers of the α-factor peptide, the [L-Ala^9]α-factor and the [D-Ala^9]α-factor.

These stereoisomers were chosen because of their identical atomic compositions and, thus, identical hydrophobicity. They were compared for their ability to displace the bound [³H]α-factor. Equilibrium curves for [³H]α-factor binding and its inhibition by the stereoisomers were determined (Fig. 10). These inhibition assays, carried out on stripped total membranes, showed that the modified Ste2^{m}p has a 16-fold greater affinity for [L-Ala^9]α-factor than for [D-Ala^9]α-factor (IC$_{50}$ of ~1600 and ~100 nM, respectively). These stereoisomers are reported to vary at least 400-fold in their affinities for the wild-type Ste2p (IC$_{50}$ of ~4000 and ~10 nM respectively, for the L- and D-isomers (David *et al.*, 1997)).
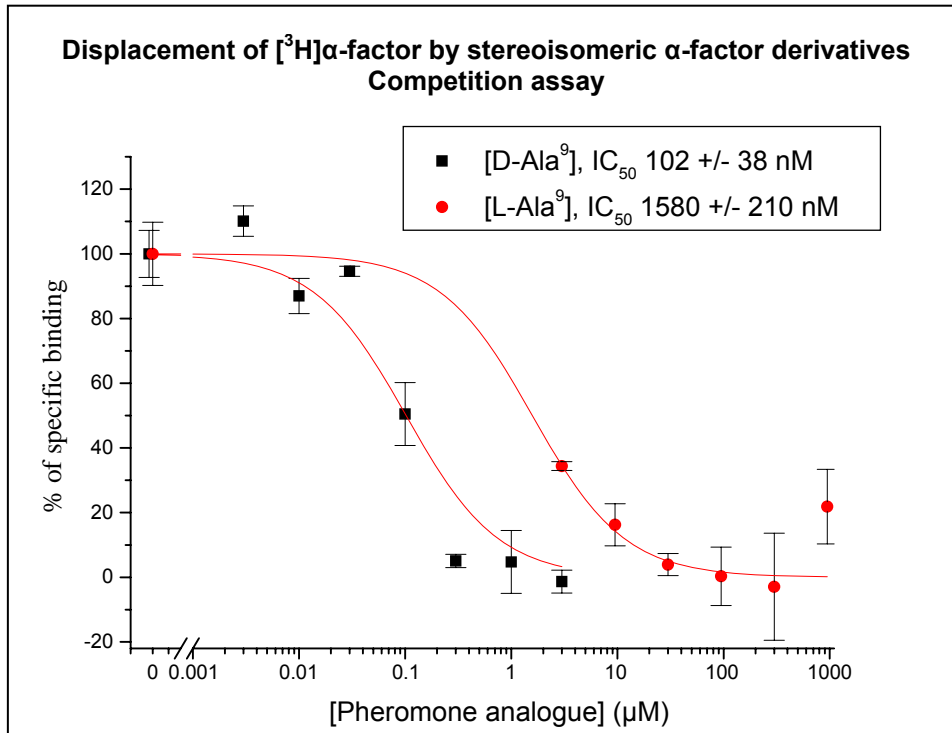
Fig. 10: Competition assay: Displacement of [³H]α-factor bound to isolated membranes by stereoisomeric α-factor derivatives. Membranes were incubated with [³H]α-factor and increasing amounts of non-radioactive [L-Ala^9]α-factor or [D-Ala^9]α-factor as the competitor peptides. For the generation of the competitive curves, relative percentage occupancies for binding were determined for each competitor at each concentration relative to the specific binding.

5.3. Culture and overexpression

The first successful production of a GPCR in *S.cerevisiae* was reported in 1990. Here, *S.cerevisiae* was examined for the production of the human β$_2$-adrenergic receptor and the Human M1 muscarinic acetylcholine receptor (King *et al.*, 1990; Payette *et al.*, 1990).

We determined optimal growth conditions for Ste2^{m}p overexpression in the YpMEGA/T326-*ura3d* strain (summarised in the Fig. 11). A starter culture of YpMEGA/T326-*ura3d* was grown for 48h until an OD$_{600}$ around 11 was reached.

The strain was then inoculated to an OD$_{600}$ of 0,02 into 150 ml of selective complete medium containing raffinose as the sole carbon source or rich medium (for description of the media, see the Material and Methods section, chapter 13.2.1), and shaken at 30°C.
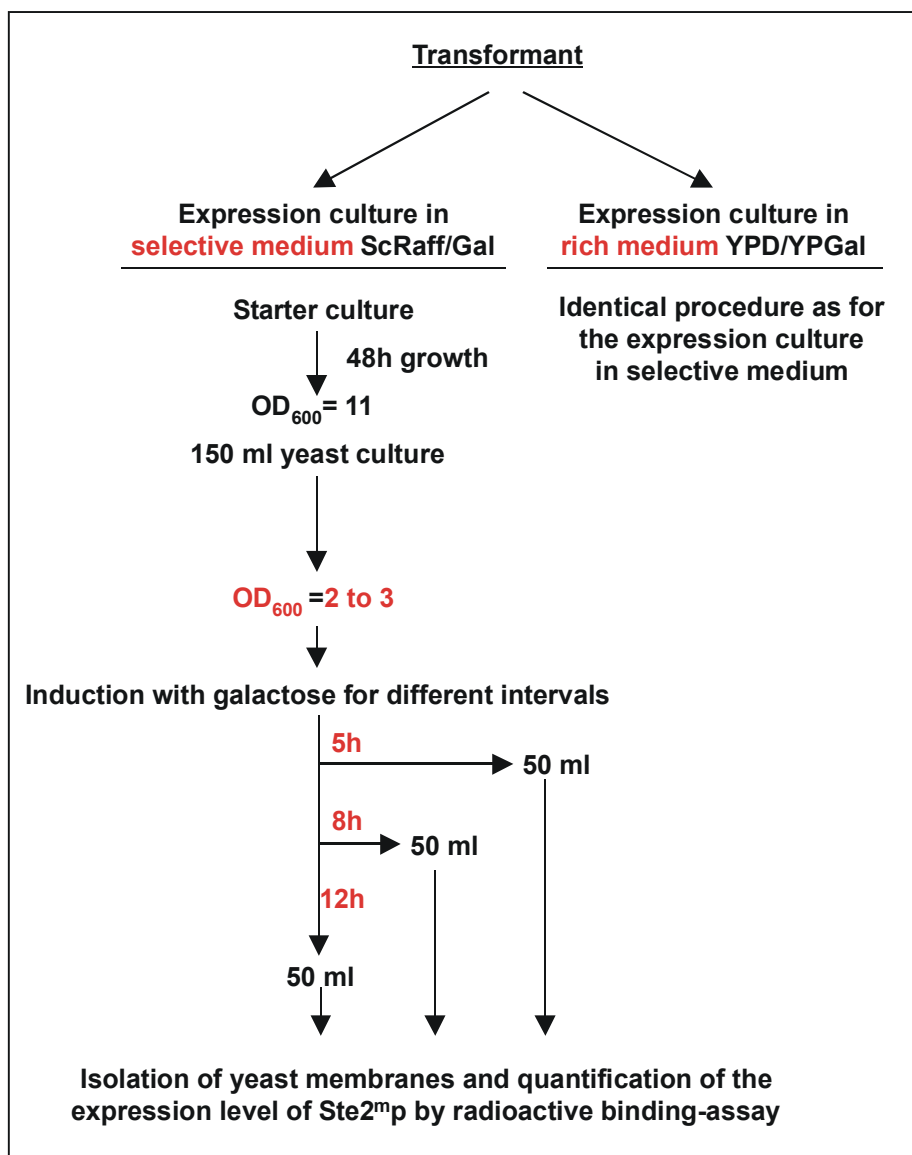
Fig. 11: **Protocol for the determination of optimal growth conditions and concurrent high level Ste2^{m}p expression**

From the 150 ml culture, 50 ml aliquots were withdawn at different timepoints during non-inducing growth, and transferred to fresh sterile flasks.

The cultures were then supplemented with 2% galactose to induce gene expression for 5h, 8h or 12h. After the induction, yeast membranes were prepared, and the expression level of Ste2^{m}p was analysed by radioactive α-factor binding assay.

During the isolation of the membranes, a stripping step with 400 mM NaCl in the homogeneisation buffer was included in order to remove extrinsic membrane proteins and to enrich the sample in Ste2^{m}p.

A control immunoblot and its corresponding silver-stained SDS gel (Fig. 12) show that membrane stripping did not remove Ste2^{m}p, as the same amount of protein was retained in the membranes after the stripping step, and almost none was present in the wash fraction.
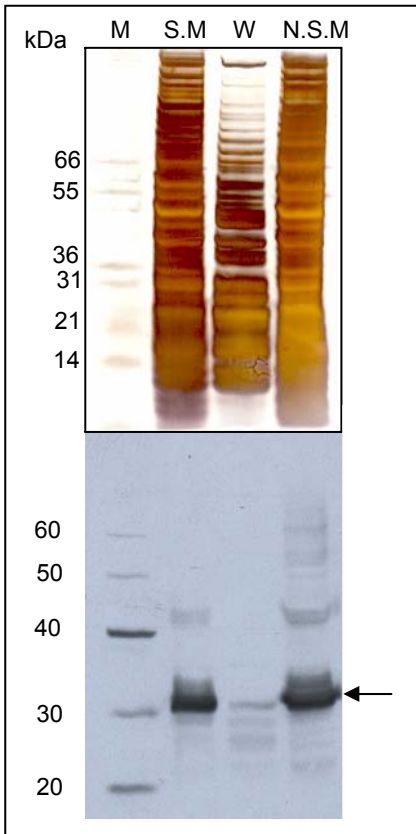
Fig. 12**: Efficiency of the membrane stripping step and enrichment of Ste2[m]p.** Silver-stained SDS gel and corresponding immunoblot of isolated membranes with or without a stripping-step during the isolation procedure: 5 µg of membranes were loaded. M: Size marker, S.M: stripped membranes, W: wash after stripping, N.S.M: Non-stripped membranes. The arrow indicates monomeric Ste2[m]p with a calculated molecular weight of ~38 kDa.

Isolated membranes from cells grown under different conditions were incubated with [^{3}H]α-factor whose binding was assessed (pmol of [^{3}H]α-factor/ mg of membranes). The quantification graph (Fig. 13) shows that the best expression level was obtained either after growth in selective complete medium ScRaff/ScGal, followed by 5h of induction with 2% galactose, or in complete medium YPD/YPGal and 8h induction.with 2% galactose.
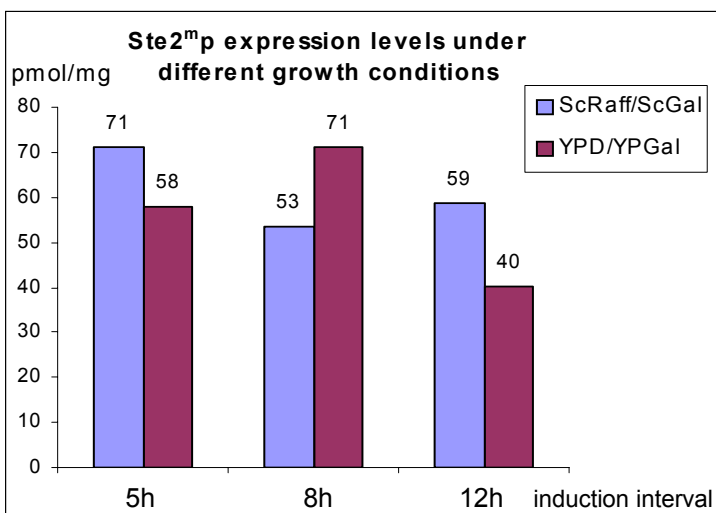
Fig. 13**: Comparison of the Ste2[m]p expression levels under different growth conditions.** A [^{3}H]α-factor binding-assay was performed with isolated stripped membranes from YpMEGA/T326-*ura3d* transformants that grew in selective (ScRaff/ScGal) or rich (YPD/YPGal) medium. Gene expression was induced with 2% galactose for 5h, 8h or 12h. Two µg of isolated membranes were incubated with [^{3}H]α-factor, the bound radioactivity mesured, and the concentration of Ste2[m]p in total membranes calculated (pmol of Ste2[m]p /mg of membranes).

5.4. Solubilisation of Ste2^{m}p

5.4.1. Solubilisation

Once overexpression of the desired protein is achieved, the protein must be extracted from the membrane and purified. Binding experiments with detergent solubilised wild-type Ste2p demonstrated that the receptor solubilised in DDM (N-Dodecyl-β-D-maltoside) retained its native structure (David et al., 1997). For this reason, we preferentially chose DDM to solubilise the Ste2^{m}p mutant receptor, although we also tested other non-ionic detergents: TX100 (Triton X-100), LDAO (N,N-Dimethyldodecylamine-N-oxide), C$_{12}$E$_9$ (Polyoxyethylene-9-laurylether), OG (N-Octyl-β-D-Glucopyranoside), NG (N-Nonyl-β-D-Glucopyranoside), FOS12 (N-Dodecyl-phosphocholine).

For each detergent, solubilisation experiments were performed under identical conditions: Isolated stripped membranes were mixed with detergent at a protein/detergent ratio of 1:4, and incubated at 4°C for 30 minutes. Subsequently, soluble material was separated from insoluble debris by a high speed spin (200 000 x g). The amount of Ste2^{m}p present in the supernatant was compared to that in the pellet after ultra-centrifugation by immunoblotting with an anti-His antibody.

Densitometric analysis on the Western-blot (Fig.14A) and its corresponding quantification graph (Fig.14B) show that among these detergents, DDM and LDAO most efficiently solubilised Ste2^{m}p at 50% and 38% respectively. FOS12 and TX100 were efficient (35% and 37% solubilisation, respectively (Fig.14B) and are far less expensive than DDM. However, they were not used in subsequent purification experiments since DDM solubilised the protein even more efficiently and had proved to keep the wild-type Ste2p in a native state (David *et al.*, 1997). We therefore decided to go on with DDM and LDAO.
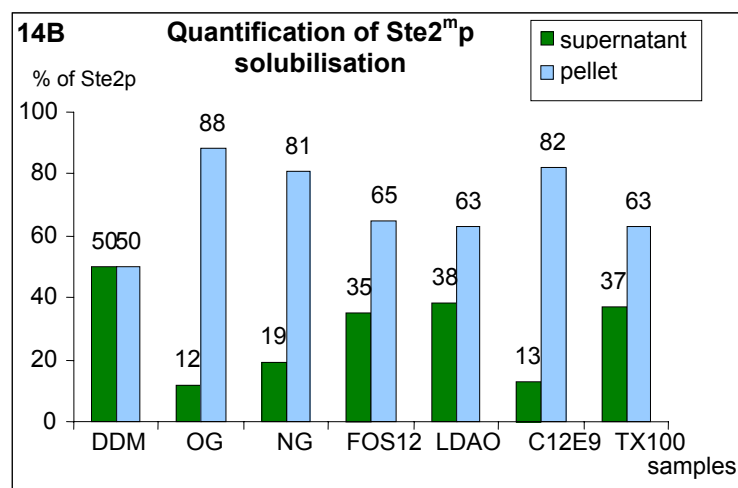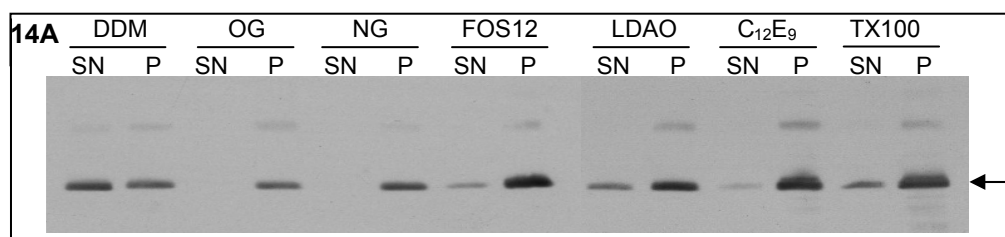
Fig. 14: **Solubilisation of Ste2^{m}p with different detergents. 14A:** Immunoblot showing the amount of Ste2^{m}p in soluble or membrane fractions. Solubilisation from 2 mg of total membranes (final concentration: 5mg/ml). Pellets (P) were resuspended in the same volume as supernatants (SN) and equal volumes (15 μl) were loaded onto the gel. The anti-His$_6$ antibody used to probe the blot specifically labeled Ste2^{m}p. **14B:** quantification graph of solubilised Ste2^{m}p with the different detergents. DDM: N-Dodecyl-β-D-maltoside, OG: N-Octyl-β-D-Glucopyranoside, NG: N-Nonyl-β-D-Glucopyranoside,FOS12:N-Dodecyl-phosphocholine,LDAO:N,N-Dimethyldodecyl-amine-N-oxide,C$_{12}$E$_9$:Polyoxyethylene-9-lauryl-ether,TX100: Triton X-100

The solubilisation was optimised with LDAO (Fig. 15), which included a protein/detergent ratio of 1/2 to 1/4 and a final concentration of 1% to 2,5%, after a 30 minutes incubation at 4 °C.
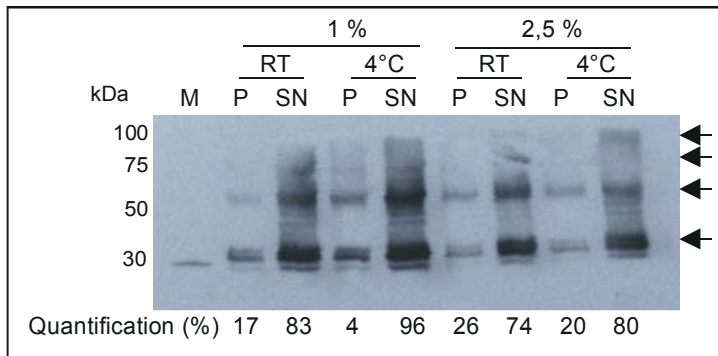
Fig. 15: **Solubilisation in LDAO.** Immunoblot showing the amount of Ste2^{m}p in soluble or membrane fractions. Solubilisation from 10 mg of total membranes after a 30 min incubation in different final concentrations of LDAO (1% and 2,5%), at different temperatures (RT, 4°C). M: Size marker, P: Pellet, SN: Supernatant. Pellets were resuspended in a volume corresponding to that of the supernatants and equal volumes (15 µl) were loaded onto the gel. The anti-His$_6$ antibody used to probe the blot specifically labeled Ste2^{m}p. Arrows indicate oligomeric Ste2^{m}p.

In order to optimise solubilisation with DDM we tested different concentrations of DDM (membrane protein/detergent ratios of 1/1, 1/2, 1/6, corresponding to final concentrations of 0,5%, 1% and 3% respectively) at 4°C (Fig. 16A) and room temperature (RT, Fig. 16B)) and for incubation times of 30 minutes and longer. At 4°C, more proteins were found solubilised in the supernatant with 3% DDM (89%) than with 1% (73%) and with 0,5% (58%). The solubilisation was less efficient at RT than at 4°C: with 3% and 1% of DDM, only 56% of proteins were solubilised at RT as compared to 89% and 73% at 4 °C, respecitvely. Only with 0,5% DDM more protein was solubilised at RT (64%) than at 4 °C (58%). Thus, the solubilisation was more efficient at 4°C than at RT.
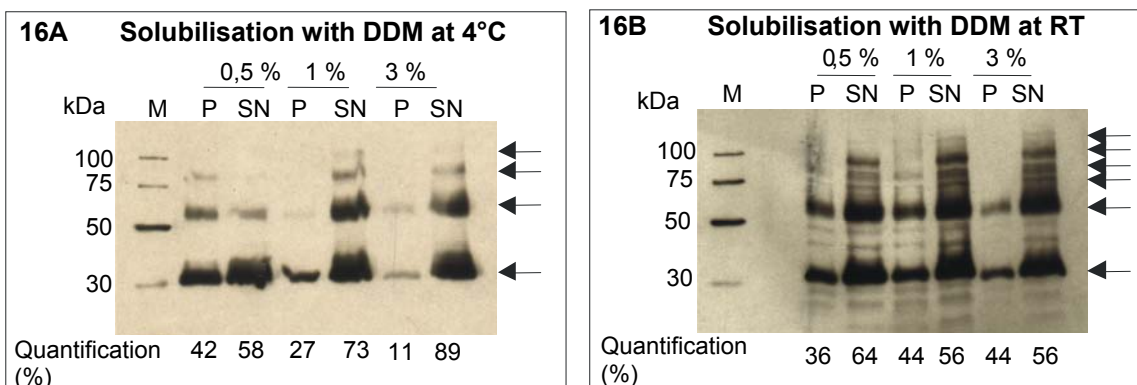
Fig. 16: **Solubilisation of Ste2^{m}p by dodecylmaltoside (DDM).** Immunoblot showing the amount of Ste2^{m}p in soluble or membrane fractions. Solubilisation from 10 mg of total stripped membranes after a 30 min incubation in different final concentrations of DDM (0,5%, 1% and 3%). M: Size marker, P: Pellet, SN: Supernatant. Pellets were resuspended in a volume corresponding to that of the supernatants and equal volumes (15 µl) were loaded onto the gel. The anti-His$_6$ antibody used to probe the blot specifically labeled Ste2^{m}p, whose monomer migrates with an apparent molecular weight of ~30 kDa, plus multiple bands of higher molecular weight (indicated by the arrows).**16A**: solubilisation performed at 4°C. **16B**: solubilisation performed at room temperature (RT).

The best solubilisation conditions with DDM were obtained with a protein/detergent ratio between 1/2 and 1/6, for 30 minutes at 4°C. Solubilisation was not improved with longer incubation times. We finally chose an intermediate protein/detergent ratio of 1/4, given the fact that the amount of detergent should not be in surplus for the further crystallisation trials, and that DDM is relatively expensive.

Under these conditions, we could routinely solubilise around 60% of Ste2^{m}p. The protein was solubilised in a heterogenous oligomeric state, as attested on the immunoblot by the several distinct bands of oligomeric Ste2^{m}p.

5.4.2. Presolubilisation

Different detergents solubilise membrane proteins with varying efficiency. This can be exploited in a presolubilisation step where membrane proteins other than Ste2^{m}p are removed from the membrane, and Ste2^{m}p, is selectively enriched. A second solubilisation step is then performed to extract Ste2^{m}p from the membrane.

The presolubilisation test was performed with different detergents such as DDM, OG, NG, FOS12, LDAO and C$_{12}$E$_9$.

Fig. 17 presents the results of the presolubilisation.

The Coomassie-stained SDS gel in Fig. 17A shows the amount of total membrane proteins that were present in the supernatant (lanes designated SN) and the pellet (lanes designated P) after presolubilisation with these different detergents. The relative amounts of membrane proteins in the soluble and membrane fractions were quantified by densitometric analysis and are shown in the graph in Fig. 17D. The immunoblot in Fig. 17B shows the amount of Ste2^{m}p present in the supernatant (SN) or the pellet (P) after presolubilisation and the according relative quantification is presented in Fig. 17C. The graphs in Fig. 17C and D show that all tested detergents were able to solubilise roughly 50% of the total membrane proteins. However, only NG and C$_{12}$E$_9$ solubilised also only minimal amounts, 12% and 28% respectively, of Ste2^{m}p. On the contrary, DDM and LDAO specifically solubilised Ste2^{m}p (around 50%) which corroborates the results of the solubilisation trials described above.
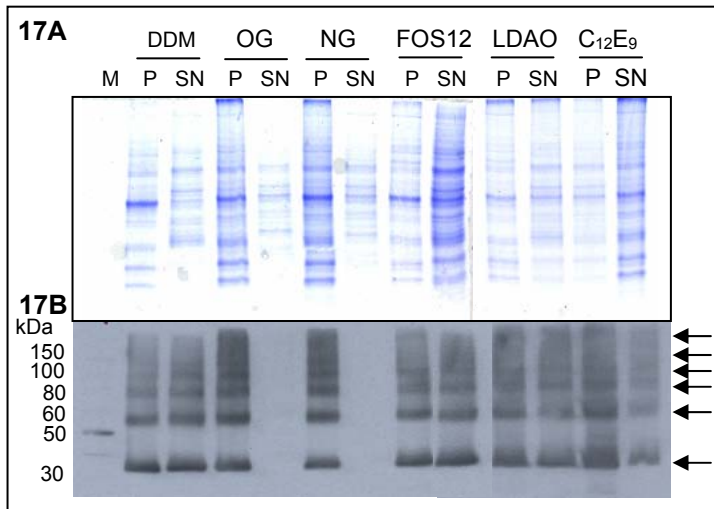
Fig. 17**: Presolubilisation with different detergents.** Presolubilisation from 2 mg of total stripped membranes after a 30 min incubation at 4 °C, at a final concentration of 5 mg/ml and a protein/detergent ratio of 1/4. P: Pellets, SN: Supernatants. Pellets were resuspended in the same volume as supernatants and equal volumes (15 µl) loaded onto gels. The anti-His$_6$ antibody used to probe the blot labeled specifically Ste2^{m}p. **17A** and **17C** Coomassie-stained SDS gel and corresponding quantification graph showing the amount of total membrane proteins in soluble or membrane fractions. **17B** and **17D**: Western-blot and corresponding quantification graph showing the amount of Ste2^{m}p in soluble or membrane fractions.
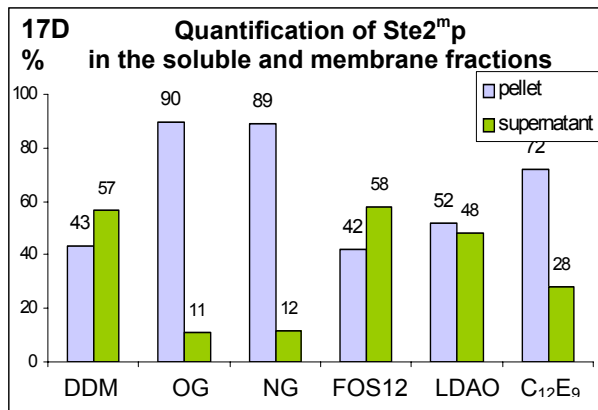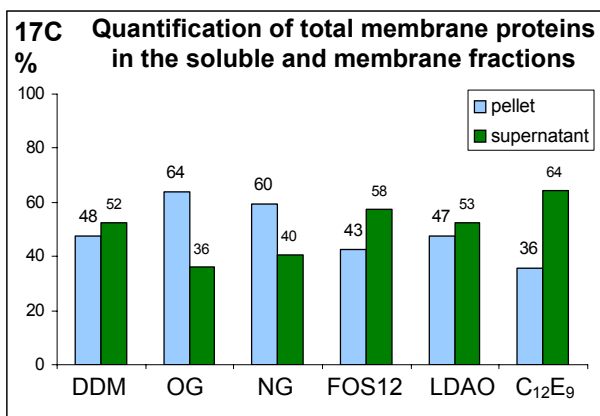
Seizing the results of the presolubilisation trials, stripped membranes were treated with 2% NG or 2% C$_{12}$E$_9$, to remove contaminating total membrane proteins. After presolubilisation, remaining Ste2^{m}p was solubilised from these membranes with DDM or LDAO.

The analysis of these 2 consecutive solubilisation steps is shown on a Western-blot (Fig. 18) and the corresponding quantification graph (Fig. 18B). Briefly, after the presolubilisation in NG or C$_{12}$E$_9$ DDM and LDAO solubilised Ste2^{m}p very inefficiently. Only between 7 and 21% of Ste2^{m}p were extracted in the supernatant.
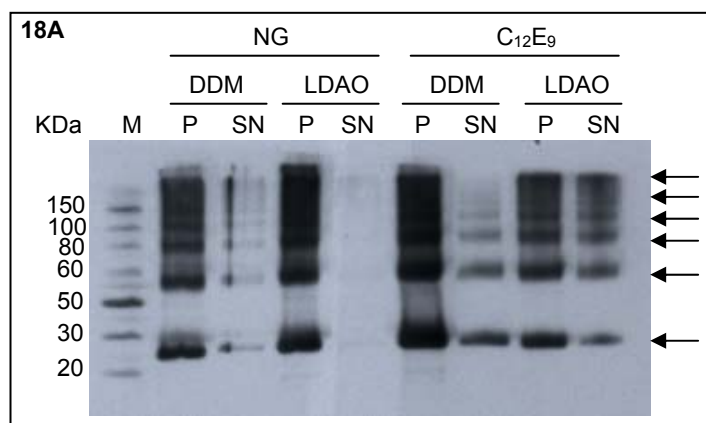
Fig. 18: **Presolubilisation of total membrane proteins and subsequent solubilisation of Ste2^{m}p with different detergents.** Presolublisation from 2 mg of total membrane protein with NG or C$_{12}$E$_9$, after a 30 min incubation at 4$^°$C, at a final concentration of 5mg/ml and a protein/detergent ratio of 1/4. P: Pellet, SN: Supernatant. Pellets were resuspended in the same volume as supernatants and equal volumes (15 µl) were loaded onto the gel. After the presolubilisation, proteins still present in the pellet were solubilised with DDM or LDAO **18A**: Immunoblot using anti-His$_6$ antibody that specifically shows the amount of Ste2^{m}p in the soluble and membrane fractions after the two solubilisation steps. Arrows indicate oligomeric Ste2^{m}p. **18B**: Corresponding quantification graph.
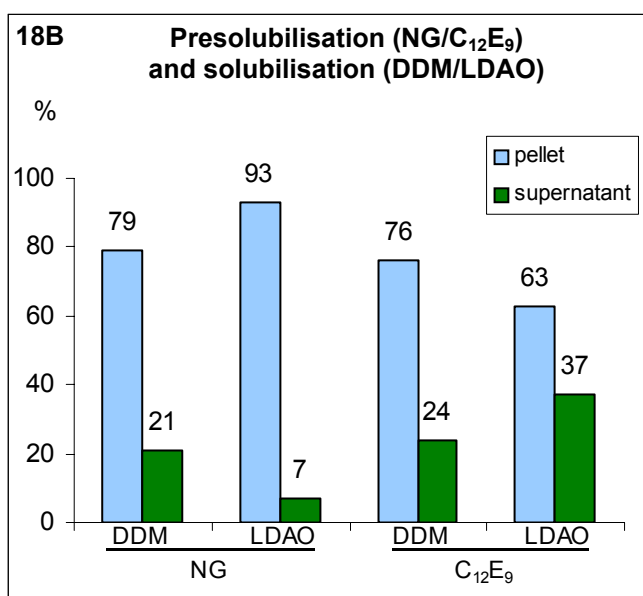
A noticeably lower amount of Ste2^{m}p was obtained after presolubilisation with NG or C$_{12}$E$_9$ followed by treatment with DDM or LDAO (21 to 37% solubilisation) than with the latter detergents alone (~50% solubilisation). Thus, the overall benefit of the two-step solubilisation procedure was negligible and we decided to go on with a single solubilisation step using DDM or LDAO.

5.5. Purification

5.5.1. One-step purification

5.5.1.1. Metal-affinity chromatography, with Ni2+-NTA beads

Metal-affinity purification using Ni^{2+}-NTA beads as a matrix, was applied after a solubilisation of 15 mg of total membrane protein. The solubilised protein was incubated overnight at 4°C with 1 ml of Ni^{2+}-NTA beads. Beads were then packed in a column and the flow-through collected. The bound protein was treated with a gradient between 20 mM and 250 mM imidazole. Ste2^{m}p eluted with approximately 220 mM imidazole. A silver-stained SDS gel (Fig. 19A) shows that Ste2^{m}p was retrieved quite pure in the eluate, although not homodisperse, as observed in the corresponding Western-blot (Fig. 19A). Densitometric analysis of the Western-blot (Fig. 19B) unveiled that more than 90% of Ste2^{m}p could be recovered after the chromatography. Unfortunately, this result was not reproducible in up-scale experiments.
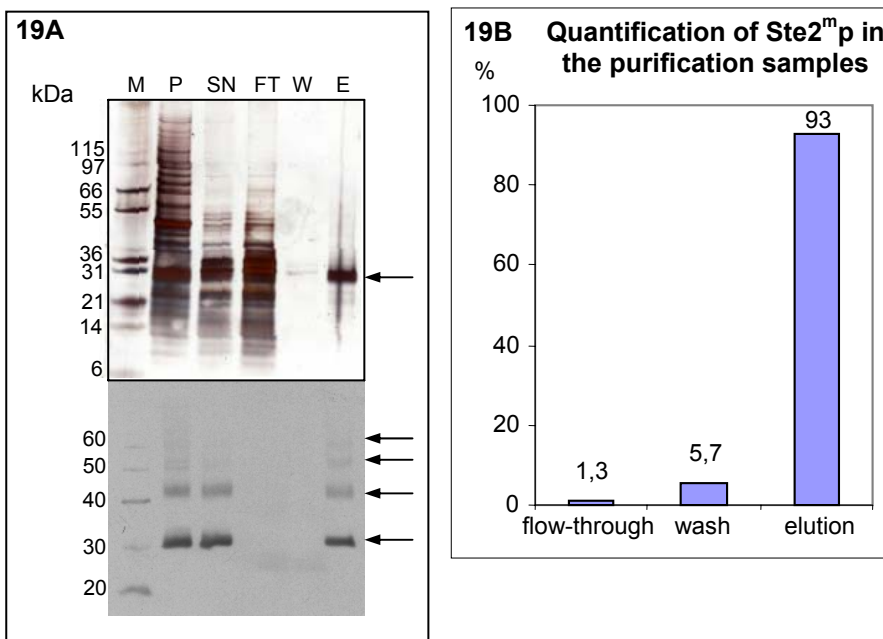
Fig. 19: **Purification trial of Ste2^{m}p by metal-affinity chromatography after solubilisation in DDM. 19A**: Silver-stained SDS gel and corresponding Western-blot of the concentrated one-step purification samples after a solubilisation from 15 mg total membrane proteins with DDM. M: Size marker, P: pellet, SN: Supernatant, FT: Flow through, W: Wash, E: Eluate. Arrows indicate oligomeric Ste2^{m}p. **19B**: Estimation of the amount of Ste2^{m}p in the purification samples by densitometric analysis of the Western-blot in Fig. 19A.

A similar one-step purification was also performed after solubilisation in LDAO (Fig. 20). The silver-stained SDS gel shows that the purification was not as efficient as after the solubilisation with DDM, as there were still a lot of contaminanting proteins in the eluate.
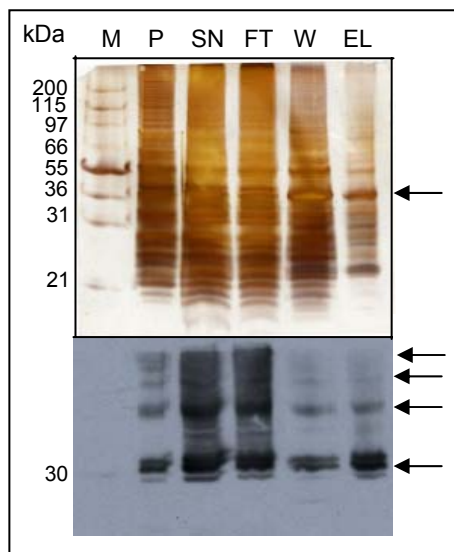
Fig. 20: **Purification of Ste2^{m}p by metal-affinity chromatography after a solubilisation in LDAO:** Silver-stained SDS gel and corresponding Western-blot of the concentrated purification samples after solubilisation of 15 mg total membrane proteins with LDAO. M: Size marker, P: Pellet, SN: Supernatant, FT: Flow through, W: Wash, E: Eluate. Arrows indicate oligomeric Ste2^{m}p.

When different amounts of eluate from 50 µl of Ni^{2+}-NTA beads were loaded onto an SDS-gel, we observed that two bands, a prominent one at slightly higher molecular weight and a faint lower band were visible around 30 kDa, as shown by arrows on Fig. 21A. Only the upper band was detectable on a Western-blot with an anti-His antibody (Fig. 21B), suggesting that this band would be Ste2^{m}p, and the lower band was some unspecific contaminant.
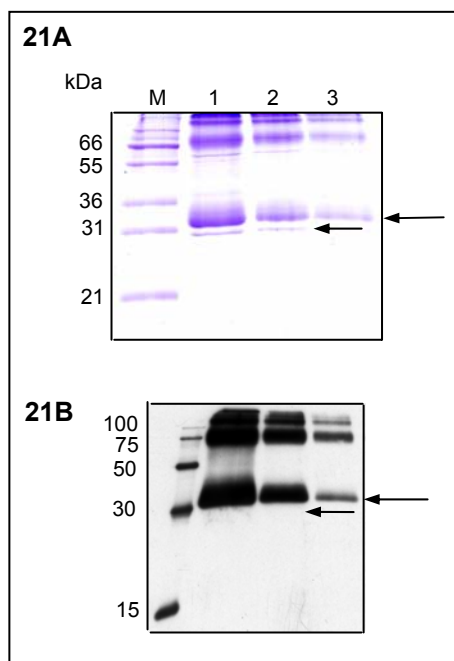
Fig. 21: **Determination of the nature of the prominent purified band.** Coomassie-stained SDS gel (**21A**) and corresponding Western-blot (**21B**) showing different amounts (1, 2 and 3) of the purification sample (M: Size marker). Arrows indicate the two bands of interest.

In order to optimise the purification conditions, the effects of different parameters on the efficiency of the chromatography, i.e., Ste2^{m}p purity and binding to the beads, were checked the beads volume, the β-mercaptoethanol concentration and the EDTA concentration. These trial experiments were performed in a small scale, i.e., in a final volume of 2 ml, after solubilisation of 10 mg of total membrane proteins in DDM.

5.5.1.1.1. Beads volume

The effect of the beads volume was assessed after solubilisation of Ste2^{m}p from 10 mg of total membranes. Different volumes of beads were tested: 10 µl, 25 µl and 50 µl. A Western-blot (Fig. 22) showed that there was approximately no protein in the flow through when using 50 µl of beads, in contrast to 10 µl and 25 µl of beads. This demonstrated that 50 µl of beads seemed to be the minimal amount needed to bind all Ste2^{m}p solubilised from 10 mg of total membrane protein.
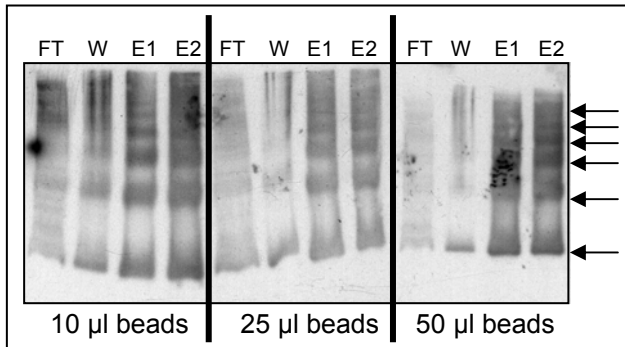
Fig. 22: **Effect of different Ni^{2+}-NTA beads volumes on the binding of Ste2^{m}p.** Comparison by immunoblotting of the Ste2^{m}p binding to different amounts of Ni^{2+}-NTA beads (10 µl, 25 µl and 50 µl). The beads were incubated with 2 ml supernatant after a solubilisation from 10 mg of total proteins. FT: Flow through, W: Wash, E1, E2: successive eluate samples.

5.5.1.1.2. β-mercaptoethanol and EDTA concentration

β-mercaptoethanol is generally used in purification buffers as a disulfide bridge reducing agent and an anti-oxydant, as many proteins are more stable in a reduced state. By reducing the disulfide bridges, the amount of oligomers can be decreased and, so, the heterogeneity. The adsorption of the protein to the matrix is also influenced by the reducing or oxidizing conditions, and an alteration of these conditions could promote the protein binding and/or elution (Hunte *et al.*, 2000) EDTA is a proteases inhibitor. However, EDTA is a chelating agent for metal-ions, and can chelate and, hence, remove the Ni^{2+} ions from the matrix. EDTA can, therefore, be used to elute proteins by stripping the metal-ions from the matrix together with the bound proteins. We checked what EDTA concentration could be used as a protease inhibitor without impairing the binding of Ste2^{m}p to the Ni^{2+}-NTA beads.

Ste2^{m}p was incubated with the Ni^{2+}-NTA beads in the presence of 20 mM β-mercaptoethanol and up to 0,75 mM EDTA. On a Western-blot (Fig. 23), we observed that neither 20 mM β-mercaptoethanol nor 0,25 mM EDTA during incubation with the Ni^{2+}-NTA beads or 0,75 mM EDTA during wash and elution noticeably affected Ste2^{m}p binding or heterogeneity in comparison to the standard conditions with in 1 mM β-mercaptoethanol and no EDTA.
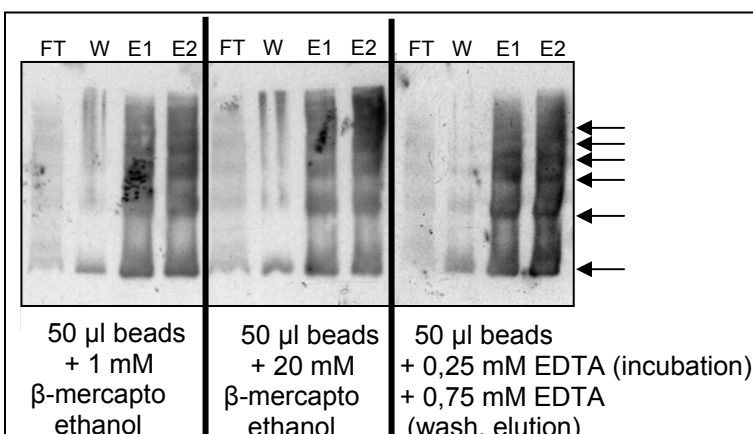
Fig. 23: **Effect of β-mercaptoethanol and EDTA on the binding of Ste2^{m}p to Ni^{2+}-NTA beads and the heterogeneity.** Comparison by immunoblotting of the binding of Ste2^{m}p to 50 µl of Ni^{2+}-NTA beads, in the presence of 20 mM β-mercaptoethanol, and of up to 0,75 mM EDTA. Incubation with 2 ml of supernatant after a solubilisation of 10 mg of total proteins. FT: Flow through, W: Wash, E1, E2: successive eluate samples. Arrows indicate oligomeric Ste2^{m}p.

With this volume of 50 µl of Ni^{2+}-NTA beads, it was then checked if the addition of 20 mM β-mercaptoethanol and 0,75 mM EDTA would improve the purity of Ste2^{m}p. The coomassie-stained SDS gel in Fig. 24 shows that there was no difference in the number of higher molecular weight bands in addition to the one corresponding to Ste2^{m}p monomer (~30 kDa). This suggests that the purity of Ste2^{m}p was not affected by the addition of the indicated concentrations of β-mercaptoethanol or EDTA.
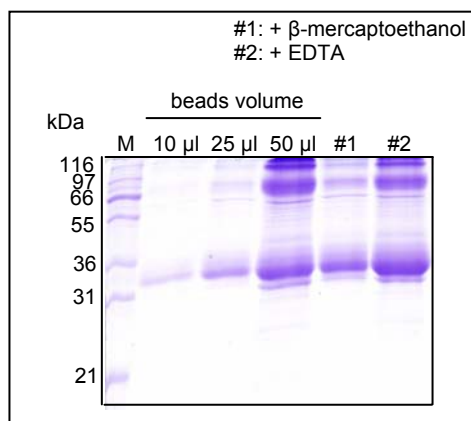
Fig. 24**: Effect of β-mercaptoethanol and EDTA on the purity of Ste2^{m}p after the metal-affinity chromatography.** Comparison of the purity of Ste2^{m}p on a Coomassie-stained SDS gel under different conditions: after binding to 10 µl, 20 µl and 50 µl of Ni^{2+}-NTA beads, and with 50 µl of Ni^{2+}-NTA beads in the presence of 20 mM β-mercaptoethanol (lane #1), or 0,75 mM EDTA (lane #2). The beads were incubated with 2 ml supernatant after solubilisation of 10 mg total membrane proteins. (M: Size Marker).

5.5.1.1.3. Urea

The several Ste2^{m}p oligomers visible on Western blots as well as Coomassie-stained SDS-gels might have been due to aggregation of the Ste2^m proteins. It is known, that SDS in some cases stabilises the secondary structure of membrane proteins. Therefore, we checked the effect of another native denaturing agent, urea, on aggregation of Ste2^{m}p. We added 8 M urea to the purified Ste2^{m}p after metal-affinity chromatography and to the separating gel (Fig. 25). There was no evident difference in the amount of oligomeric forms observed on the gel, indicating that urea was not able to prevent Ste2^{m}p aggregation. Since neither reducing agents such as β-mercaptoethanol, nor denaturing substances as SDS or urea changed the appearance of oligomeric Ste2^{m}p, this suggests that the observed oligomers were an artefact of the SDS gel.
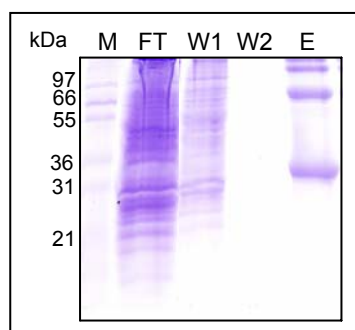
Fig. 25**: Effect of urea on the heterogeneity of Ste2^{m}p.** Analysis of the effect of urea on the aggregation of Ste2^{m}p as observed on a Coomassie-stained SDS gel after metal-affinity chromatography. M: Size marker, FT: Flow through, W1,W2: Wash1, Wash2, E: Eluate.

5.5.1.1.4. Deglycosylation

As it was intended by its construction (see chapter 5.1.2), Ste2^{m}p was not expected to be glycosylated. However, there is a third potential glycosylation site (Asn^{105}) in Ste2p which is present in Ste2^{m}p and may become glycosylated in the modified receptor (Mentesana and Konopka, 2001). Indeed, a smear and additionnal faint bands were observed running slightly higher than the one at ~30 kDa supposed to correspond to the Ste2^{m}p monomer. In order to check if this was an effect of some residual glycosylation, an attempt to deglycosylate Ste2^{m}p was performed. Isolated membranes were treated with the enzyme PNGase F. PNGase F is an amidase from *Flavobacterium meningosepticum* that hydrolyses the N-glycans of glycoproteins. The Western-blot in Fig. 26 shows no difference in the Ste2^{m}p signal between the treatment with or without amidase, suggesting that there is no clear evidence whether the smear above the Ste2^{m}p band of ~30 kDa appearing upon overexposure was due to a residual glycosylation. We concluded that the prominent band on the gel was Ste2^{m}p, and that Ste2^{m}p did not present residual glycosylation. A positive control with the bovine fetuin, a serum glycoprotein known to contain neuraminic acid and O-linked sugars, was also performed that proved that the enzyme was working (data not shown).

It is noticeable as well that the Western-blot in Fig. 26 does not show strong signals of oligomeric Ste2^{m}p in addition to the single band corresponding to monomeric Ste2^{m}p. This band pattern resembles that on the Western-Blot with isolated membranes with or without stripping (Fig. 12). Both Western blots involving isolated membranes are in stark contrast to the band pattern of the Western-blots showing Ste2^{m}p after isolation, during solubilisation and purification. On these blots, oligomeric Ste2^{m}p was always observed. This suggests that the several strong oligomeric bands observed on the immunoblots could be generated during membrane solubilisation and/or Ste2^{m}p purification.
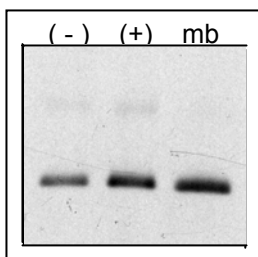
Fig. 26: **Analysis of the glycosylation state of Ste2^{m}p.** Immunoblot after treatment of Ste2^{m}p with the deglycosylase PNGase F. 0,25 µg of membranes were loaded onto the gel. (-): membranes after treatment without enzyme, (+): membranes after treatment with enzyme, mb: membranes without treatment.

5.5.1.2. Other metal-affinity purifications: Cu^{2+}-NTA, Co^{2+}-NTA, Zn$^+$-NTA

To optimise the purity and the homogeneity of Ste2^{m}p, metal-affinity chromatographies were performed with different metal ions, Copper (Cu^{2+}-NTA), Cobalt (Co^{2+}-NTA) and Zinc (Zn$^+$-NTA), using the same conditions as for the Ni^{2+}-NTA purification. The different samples (flow through, wash and eluate) of each chromatography were then analysed on silver-stained SDS gels and immunoblots. The amount of Ste2^{m}p in each sample was quantified from the immunoblots by denstitometric.

The degree of purity of Ste2^{m}p present in the eluate was not improved as observed on the silver-stained SDS gels in Fig. 27A. The graph in Fig. 27C quantifies the efficiency of the different chromatographies in terms of recovery of Ste2^{m}p from the supernatant (SN in Fig. 27A; set to 100%).

In the case of the matrices Cu^{2+}-NTA, Co^{2+}-NTA and Zn^{+}-NTA, less Ste2^{m}p was recovered in the eluate (47%, 12% and 35%, respectively) than with Ni^{2+}-NTA (84%), and more Ste2^{m}p was lost in the flow through and in the wash (53%, 73% and 30% respectively) than with Ni^{2+}-NTA (16%).

The quantification graph in Fig. 27D shows a comparison (by densitometric analysis of the Western-blot in Fig. 27B) of the efficiency of the different chromatographies. The relative amount of Ste2^{m}p in each purification samples (flow through, wash, eluate) is given as relative band intensity. The graph shows clearly that, although in the different chromatographies nearly the same amount of Ste2^{m}p was lost in the flow through and the wash samples, the most efficient metal-ion chromatography was the Ni^{2+}-NTA chromatography by which most Ste2^{m}p was recovered in the eluate (1670 units versus 296, 398 and 264 for the Cu^{2+}-NTA, Co^{2+}-NTA and the Zn^{2+}-NTA chromatographies, respectively).
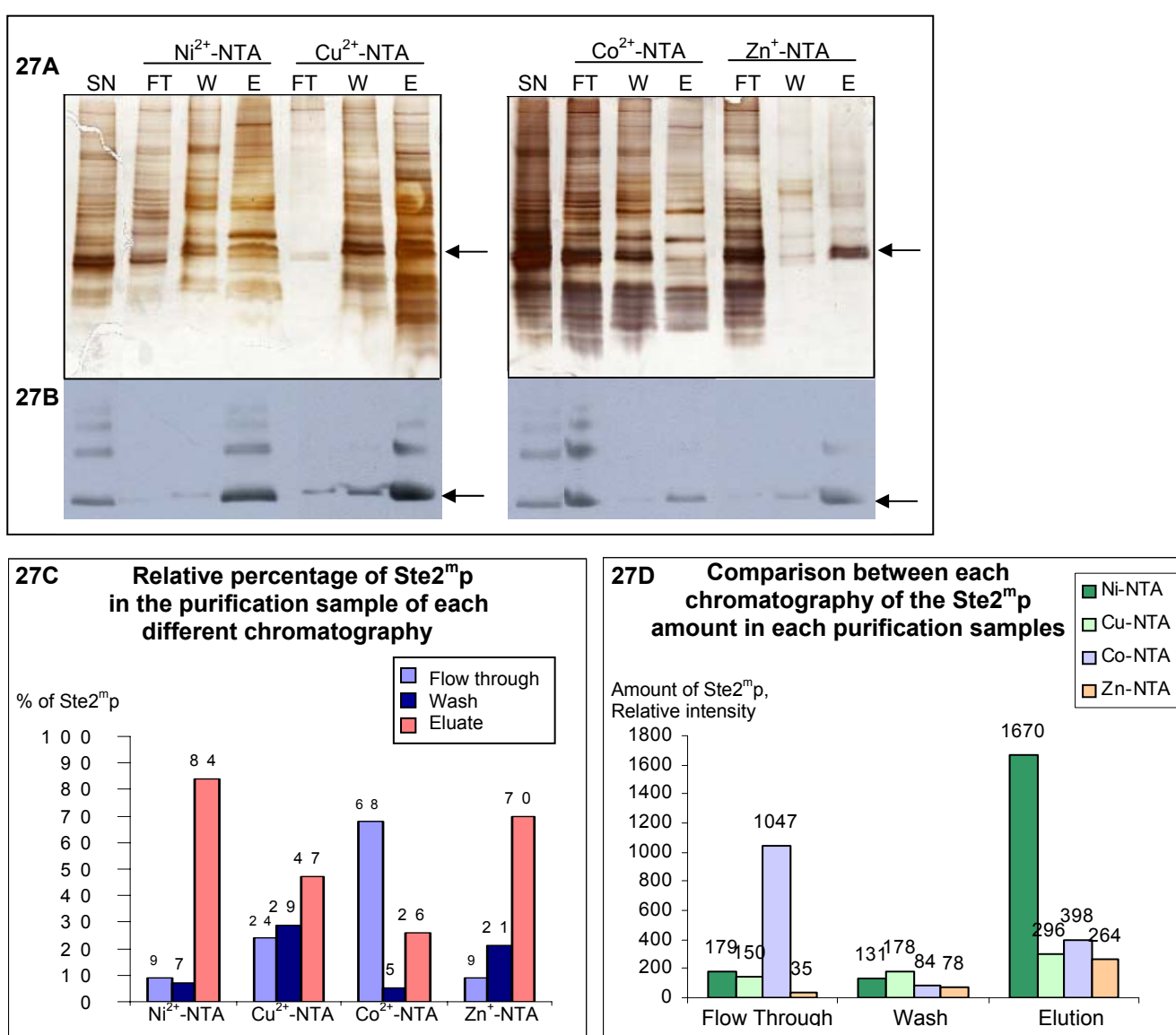
Fig. 27: **Comparison of the Ste2^{m}p amount recovered in the 4 different metal-affinity chromatographies**. **27A**: Silver-stained SDS gels of the purification samples of each different chromatography. SN: Supernatant, FT: Flow through, W: Wash, E: Eluate. **27B**: Corresponding Western-blots of the purification samples, probed with a anti-His$_6$ antibody labelling specifically Ste2^{m}p. Arrows indicate monomeric Ste2^{m}p. **27C**: Quantification graph showing for each different chromatography the relative percentage of Ste2^{m}p in each purification samples (flow through, wash, eluate). **27D**: Quantification graph showing a comparison by densitometric analysis of the Ste2^{m}p amount in each purification samples, between the different chromatographies.

5.5.2. Two-step purification

In order to improve the purity and the homogeneity of Ste2^{m}p, a two-step purification involving different chromatographies was performed.

5.5.2.1. FLAG-affinity chromatography

As outlined in chaper 0, Ste2^{m}p carries a FLAG-tag in addition to the His$_6$ tag. Thus, the pooled eluates from the first Ni^{2+}-NTA step were submitted to subsequent FLAG-affinity chromatography. All Ni^{2+}-NTA purification samples were analysed on a Coomassie-stained SDS-gel and a corresponding immunoblot (Fig. 28A).

Three successive eluates (E1, E2 and E3) from the Ni^{2+}-NTA purification were collected, pooled and loaded onto the FLAG-affinity matrix. After washing, bound Ste2^{m}p was eluted with 50 µg/ml FLAG peptide. The eluate was collected, and the column was then stripped with 0,1 M Glycine-HCl pH 3,5 to eventually elute residual Ste2^{m}p. The FLAG-chromatography samples were analysed on a Coomassie-stained SDS-gel and a Western-blot (Fig. 28B).
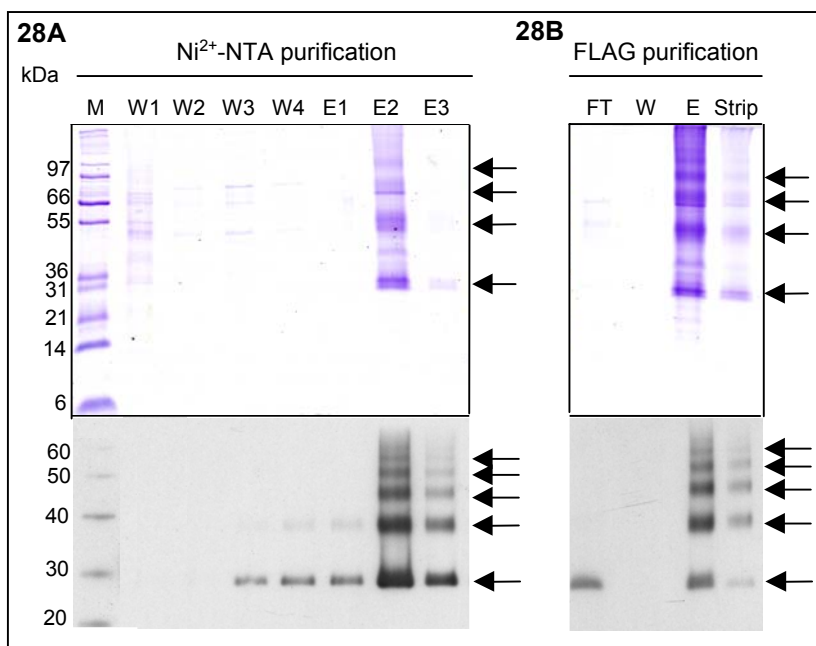
Fig. 28: **Purification of Ste2^{m}p by Ni^{2+}-NTA-affinity chromatography (28A) and subsequent FLAG-affinity chromatography (28B).** Coomassie-stained SDS-gel and corresponding Western-blot of the concentrated purification samples are shown. M: size marker, FT: flow through; W, W1, W2, W3, W4: successive washes 1, 2, 3 and 4; E1, E2, E3: successive eluates from the Ni^{2+}-NTA chromatography; E: eluate from the FLAG chromatography. Strip: flow through after the stripping of the column. Arrows indicate oligomeric Ste2^{m}p.

By comparing the purity and the heterogeneity of Ste2^{m}p in the eluate of the Ni^{2+}-NTA purification and that of the FLAG–affinity chromatography, it was clear that the FLAG-affinity chromatography did not improve the result: Neither could be the purity enhanced nor the heterogeneity reduced. Moreover, the stripping of the FLAG column revealed that elution was inefficient, since proteins were still desorbed by the stripping step.

5.5.2.2. Anion-exchange chromatography

As the FLAG chromatography was inefficient, we tried another chromatography as the second step to further improve the purity of Ste2^{m}p. We performed an anion-exchange chromatography after the Ni^{2+}-NTA chromatography. The concentrated Ni^{2+}-NTA eluate was loaded onto an anion-exchange resin. Ste2^{m}p appeared not to bind tightly to the resin and was eluted in the wash step. We, therefore, tried to optimise the binding conditions in small-scale trial experiments by testing different resin volumes (20 µl, 100µl), different buffers at different pH values (20 mM phosphate buffer at pH 6,5 and pH 7, 20 mM HEPES buffer at pH 7,5 and pH 8, 20 mM Bicine buffer at pH 8,5) and different NaCl concentrations.

In a batch procedure, for each condition 20 mg of total membranes were solubilised with 2% DDM. A Ni^{2+}-NTA purification was performed, the eluate was concentrated and finally diluted in 500 µl of each of the following buffers: 20 mM phosphate buffer pH6,5, 20 mM phosphate buffer pH7, 20 mM HEPES buffer pH7,5, 20 mM HEPES buffer pH8, or 20 mM bicine buffer pH8,5. All buffers contained 20 mM NaCl. Each sample was incubated with 20 µ or 100 µll of anion-exchange resin for 10 minutes. After a gentle centrifugation step, the supernatants were collected and analysed on a Western-blot. The determination of the amount of Ste2^{m}p in the supernatants relative to that in the Ni^{2+}-NTA eluate allowed an evaluation of the binding quality.

Fig. 29 shows that with 20 µl of resin, none of the tested buffers permitted an optimal binding of Ste2^{m}p to the resin, as most of the Ste2^{m}p was still present in the supernatants (comparison with the Ni^{2+}-NTA eluate). A volume of 100 µl of resin seemed to be the minimal quantity required to efficiently bind Ste2^{m}p solubilised from 20 mg of total membranes at a pH 7,5 to 8 (20 mM HEPES buffer). We then went on with these conditions.
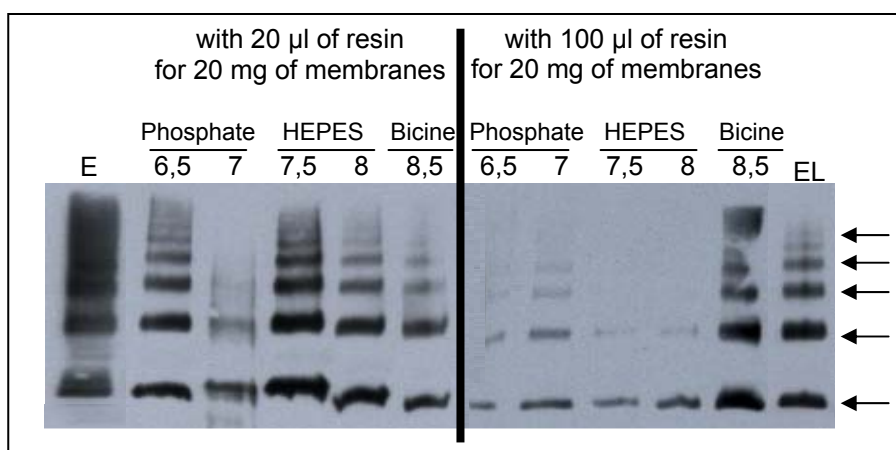
Fig. 29: **Effect of the resin volume and the pH on the binding of Ste2^{m}p to the anion-exchange matrix.** The Ni^{2+}-NTA eluate was incubated with different resin amounts, and in different buffers at different pH values. After centrifugation, the supernatants were collected and analysed on Western-blot E: Ni^{2+}-NTA purification eluate. Arrows indicate oligomeric Ste2^{m}p.

NaCl is used to elute the protein from the anion-exchange matrix, as its counterion Cl⁻ competes by displacement with the protein. We determined the optimal NaCl concentration for elution of Ste2^{m}p. After a solubilisation of 20 mg of total membranes with 2% DDM, a Ni^{2+}-NTA purification was performed. We exchanged the buffer of the eluate to 20 mM HEPES buffer pH 7,5 containing different NaCl concentrations (50, 100, 150, 200, 250, 300, 350, 400, or 450 mM). All samples were then incubated for 10 minutes with 100 µl of anion-exchange resin. After the incubation, the samples were gently centrifuged and the supernatants analysed on a Western-blot (Fig.30). It appears very clearly that Ste2^{m}p was desorbed from the resin in a buffer containing a NaCl concentration higher than 0,3 M.
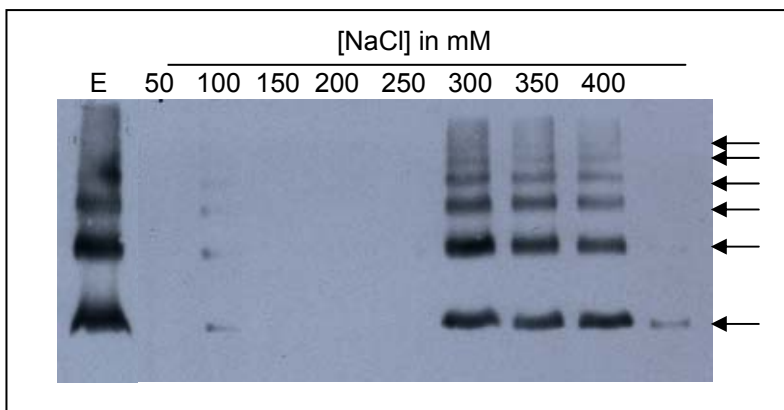
Fig. 30. **Optimisation of the NaCl concentration on the elution of Ste2^{m}p from the anion-exchange resin.** Ni^{2+}-NTA purified Ste2^{m}p was incubated with the resin in different NaCl concentrations. After centrifugation, the supernatants were analysed on a Western-blot. E: Ni^{2+}-NTA eluate (in phosphate buffer pH7 containing 20 mM NaCl). Arrows indicate oligomeric Ste2^{m}p.

The extracted conditions for an optimal anion-exchange chromatography were, after solubilisation of Ste2^{m}p from 20 mg of total membrane proteins and Ni^{2+}-NTA chromatography, a 10 minutes incubation of the Ni^{2+}-NTA eluate with 100 µl of anion-exchange resin, in 20 mM HEPES buffer pH 7,5, performing a washing step with 100 mM of NaCl and the elution with 300 mM NaCl.

Applying these conditions, the anion-exchange chromatography was performed after the Ni^{2+}-NTA chromatography in a large scale purification involving solubilisation of 700 mg total membrane proteins with 2% DDM. The buffer of the Ni^{2+}-NTA eluate was exchanged for a 20 mM HEPES buffer pH7,5 with 20 mM NaCl, and concentrated. The eluate was incubated for 10 minutes with the anion-exchange resin, washed with the same buffer containing 100 mM NaCl, and the elution was preformed with 300 mM NaCl. Coomassie-stained SDS gel and corresponding immunoblot of the purification samples (Fig. 31) show that, although Ste2^{m}p was inefficiently bound to the anion-exchange resin and washed off with 100 mM NaCl. Almost no protein was recovered with 300 mM NaCl in the eluate. Therefore, we did not go on with the anion-exchange chromatography.
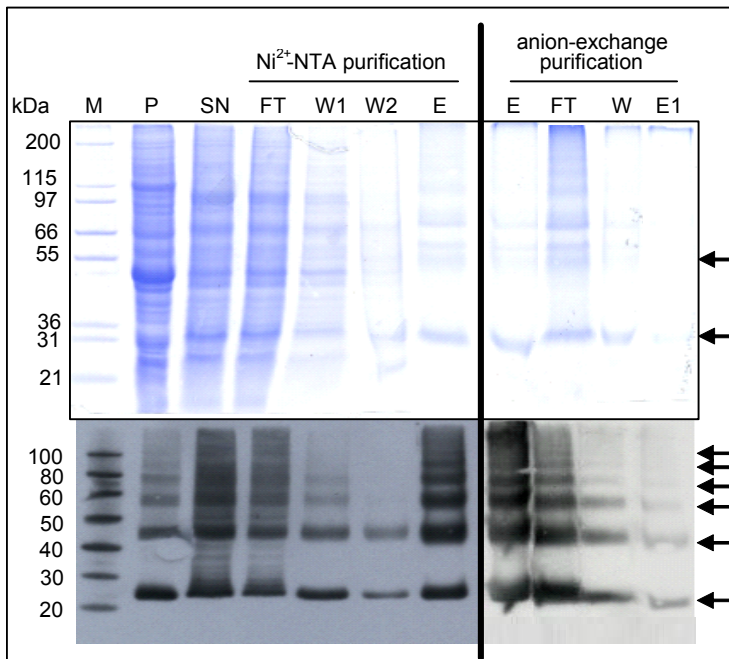
Fig. 31: **Purification of Ste2^{m}p by Ni^{2+}-NTA and anion-exchange chromatographies.**
Analysis on a Coomassie-stained SDS gel and corresponding Western-blot of the concentrated purification samples after a solubilisation from 700 mg of total membrane proteins with 2% DDM. M: Size marker, P: Pellet, SN: Supernatant, FT: Flow through, W1,W2: successive wash1,wash2, E: Ni^{2+}-NTA eluate, E1: anion-exchange eluate. Arrows indicate oligomeric Ste2^{m}p.

5.5.2.3. Size-exclusion chromatography

In order to separate the different oligomers of Ste2^{m}p, size-exclusion chromatography (SEC) was performed. The eluate from the Ni^{2+}-NTA purification was concentrated and loaded on a gel filtration column. The elution fractions corresponding to the single peak on the chromatogram were pooled and analysed for Ste2^{m}p. After SEC, the amount of Ste2^{m}p was insufficient for detection on a Coomassie-stained SDS gel (Fig. 32, sample Ese). Nevertheless, it could be detected on the corresponding immunoblot (Fig. 32) which is more sensitive. The immunoblot shows that Ste2^{m}p was still heterogenous and that the different oligomers were not separated by SEC.
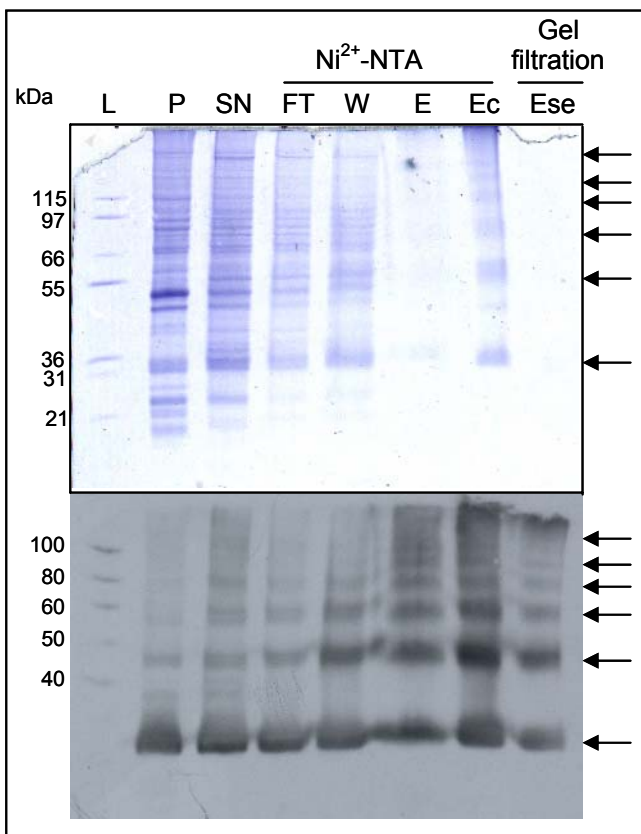
Fig. 32:.**Purification of Ste2^{m}p by Ni^{2+}-NTA and size-exclusion chromatography.**
Coomassie-stained SDS gel and corresponding Western-blot of the concentrated purification samples are shown. M: Size marker, P: Pellet, SN: Supernatant, FT: Flow through, W: Wash, E: Eluate, Ec: Concentrated eluate from the Ni^{2+}-NTA purification, Ese: Eluate of the size-exclusion chromatography. Arrows indicate oligomeric Ste2^{m}p

5.5.3. Final purification protocol

A purification protocol with a single step was finally chosen, using a Ni^{2+}-NTA chromatography with the conditions described in Fig. 33C. On the Coomassie stained SDS gel (Fig. 33A), apart from two major bands of higher molecular weight, only few contaminants were visible in comparison with the flow through and the wash samples, suggesting that an elevated concentration of imidazole (50 mM) during the wash step of the column removed a lot of them. Densitometric (Fig. 33B) of the Western-blot revealed that, from the total amount of solubilised Ste2^{m}p loaded onto the column, around, 85,5% was retrieved in the eluate, 14,5% were lost in the intermediate steps (12,5 in the flow through and 2% in the wash). However, a Schägger and a Laemmli gel systems were used for the Western-blot and the Coomassie-stained SDS gel, respectively. This could have led to the different band patterns observed in the Coomassie-stained SDS-gel and the Western-blot. N-terminal sequencing of the proteins in the Ni^{2+}-NTA eluate (see chapter 5.6.1), confirmed that the additional bands in the Coomassie-staind SDS-Gel as well as the Western-blot constitute oligomeric Ste2^{m}p. The purity of Ste2^{m}p in the eluate was estimated to be approximately 90%.

33A: Coomassie-stained gel and a Western-blot of the concentrated purification samples. M: Size marker, FT: Flow through, W1,W2: successive wash1,wash2, E: Eluate. Arrows indicate oligomeric Ste2^{m}p.

33B Quantification of Ste2^{m}p in the purification samples (relative percentage)

33C

	Solubilisation	Purification		
		wash 1	wash 2	elution
Imidazole	0 mM	50 mM		500 mM
NaCl	400 mM	400 mM		
Tris-HCl	50 mM	50 mM		
Glycerol	20%	20%		
2-mercaptoethanol	1 mM	1 mM		
DDM	2%	0,2%		

Fig. 33: **Final purification protocol. 33A:** Coomassie-stained gel and a Western-blot of the concentrated purification samples. M: Size marker, FT: Flow through, W1,W2: successive wash1,wash2, E: Eluate. Arrows indicate oligomeric Ste2^{m}p. **33B**: Quantification of the amount of Ste2^{m}p in each purification sample by densitometric analysis of the Western-blot. **33C:** Composition of the solubilisation and purification buffers.

5.6. Characterisation of Ste2ᵐp

5.6.1. N-terminal sequencing analysis

The Ni2+-NTA eluate was analysed by N-terminal sequencing. It was found that the first 9 amino-acids of the analysed protein sample exactly matched the first 9 amino-acids composing the N-terminus of the Ste2ᵐp sequence (MSDAAPSLS). This confirmed that the observed band on the SDS-gel and the immuoblot was Ste2ᵐp, and that the sample was 90% pure.

5.6.2. MALDI-TOF mass spectrometric analysis

All bands of the eluate were cut from an SDS-gel, digested with trypsin and analysed by MALDI-TOF mass spectrometry. On the Coomassie-stained SDS gel (Fig. 33B) the band corresponding to monomeric Ste2ᵐp migrated around 30 kDa. MALDI-TOF confirmed the N-terminal sequencing result, attesting that this 30 kDa band corresponds to Ste2ᵐp. Its molecular mass was determined to be 38694 Da.

5.7. 3D-crystallisation experiments: hanging-drop method

Manual crystallisation trials were performed with several commercial solutions (purchased from Hampton Research), e.g., MembFac, Index, Crystal Screen 1 and Crystal Screen 2. The method used was the hanging-Drop method, as described in the Material and methods section (chapter 13.7.3.1). So far, no protein crystals were obtained.

6. Heterologous overexpression of the hyperthermophilic putative amino acid transporter (Aatp) of Methanococcus jannaschii in Saccharomyces cerevisiae. Isolation and purification for crystallisation experiments.

This work presents the cloning of the putative amino-acid transporter Aatp from *Methanococcus jannaschii*, its heterologous overexpression in *Saccharomyces cerevisiae* and its purification by chromatography to perform crystallisation trials. Two different expression constructs and several different culture conditions were tested in order to yield the best Aatp expression. For the purification of hyperthermophilic proteins, one usually takes advantage of their hyperthermostability. Indeed, by overexpression in a mesophilic organism, their purification can be greatly facilitated and optimised by heat treatment to which, in contrary to the mesophilic proteins, they are resistant. Previously, this purification procedure proved successful for other hyperthermophilic integral membrane proteins, for instance, for the Ca^{2+}-ATPase of *Methanococcus jannaschii* (Morsomme *et al.*, 2002) or the H^{+}-PPase of *Thermotoga maritima* (López-Marqués *et al.*, 2005). Both membrane proteins had been overexpressed in *S.cerevisiae*.

6.1. Cloning strategy

6.1.1. Construction of the Aatp expression vector pAAT and the expression strain YpAAT

We intended to clone the AAT gene from *Methanococcus jannashii* genomic DNA. Routine cloning strategies allow DNA molecules to be precisely combined by ligation between suitable restriction endonuclease sites, which can be quite annoying if such sites are not available. Indeed, this is a crucial issue for genomic DNA sequences. An as yet largely unexploited approach for cloning genes directly from genomic DNA is gap-repair cloning, a method that uses *in vivo* homologous recombination in the yeast *Saccharomyces cerevisiae*. Gap-repair is a simple and inexpensive cloning method, in which a linearized yeast cloning vector bearing sequences at its termini homologous to the ends of a target genomic sequence (termed homology arms) is co-transformed into yeast cells with donor genomic DNA. The homology arms, which are usually ≤ 50 bps, are generated by PCR with tailed primers. The linear DNA strands that share sequence overlaps undergo recombination *in vivo* to incorporate the desired genomic sequence, e.g., a gene into the vector (Noskov *et al.*, 2003; Bhargava *et al.*, 1999). This method greatly simplifies the construction of cloning vectors. A sequence that is cloned in this manner is proofread by the yeast cell's replication machinery (unlike that generated by PCR) and is unlikely to contain unwanted mutations. Using this method, we cloned the intronless AAT gene from the *M.jannaschii* genome.

The transporter gene AAT was inserted into the multi-copy *E.coli* / yeast shuttle vector pITy-QC to yield expression vector pAAT. Homologies to the 5' and 3' termini of the AAT gene were introduced into pITy-QC by PCR. *M.jannaschii* genomic DNA was digested with *Xho*I and co-transformed with the linear vector into yeast expression strain BJ5464. The resulting uracil-prototrophic expression strain was designated YpAAT. The expression of the cloned AAT gene is driven by the strong galactose-inducible *GAL1* promoter. The pITy-QC *in vivo* cloning / expression vector carries the yeast 2µ replication origin for stable plasmid maintenance in yeast. The promoterless *URA3* selection marker (*ura3d)* triggers very high plasmid copy numbers per cell (Griffith *et al.*, 2003; Okkels, 1996; Loison *et al.*, 1989) The neomycin/canamycin-resistance gene neo^R or can^R allows selection in *E.coli*. The principle of the Aatp cloning is outlined in Fig. 34.
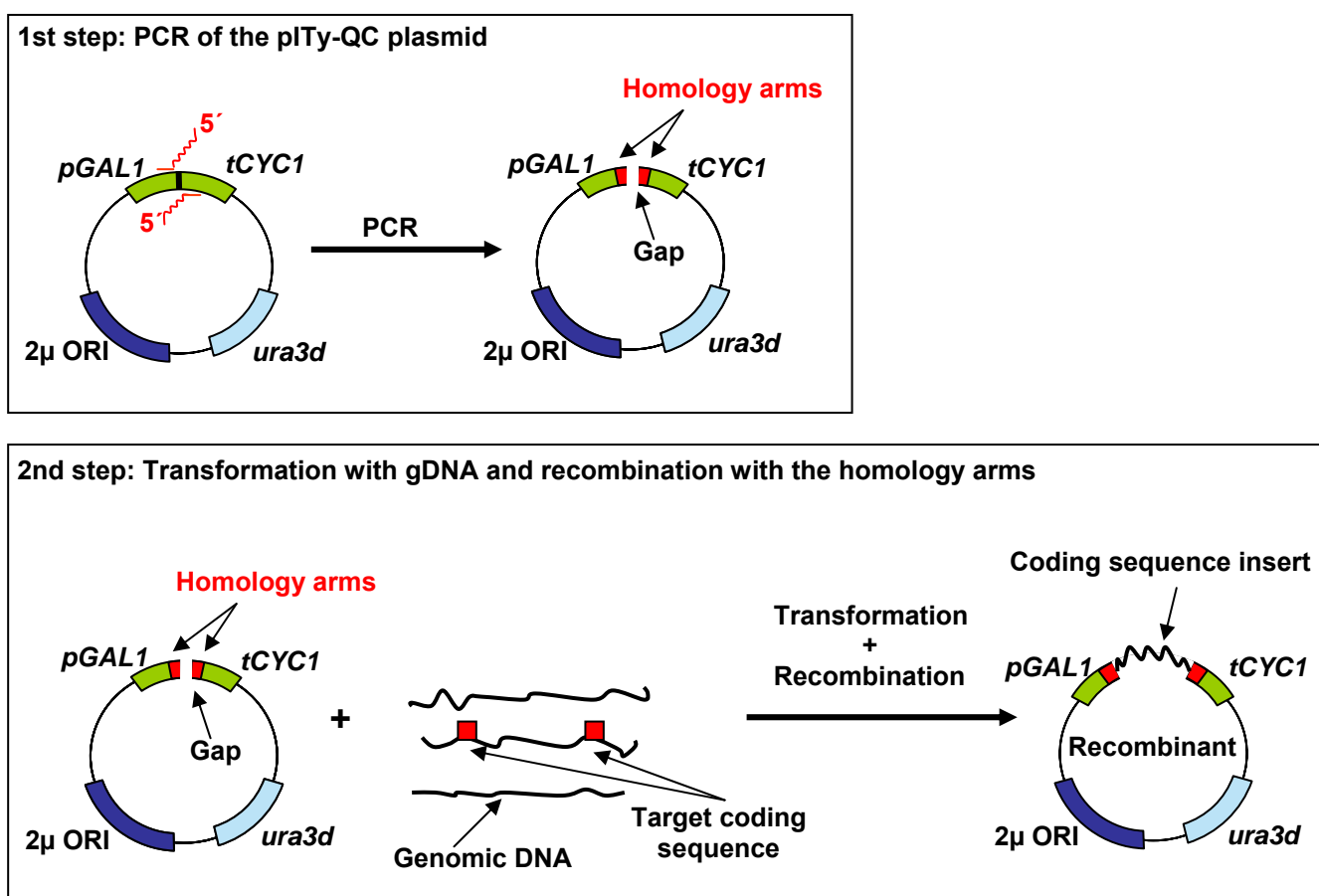
Fig. 34: **Schematic description of AAT cloning by homologous recombination. 1st step:** Introduction of the short sequences homologous to the termini of the AAT gene (homology arms) by PCR of the pITy-QC plasmid. **2nd step:**. Co-transformation of the BJ5464 yeast strain with the PCR product and the *Xho*I digested *M.jannaschii* genomic DNA. The gap in the vector is closed by homologous recombination between the AAT gene and the homogy arms. *ura3d*: promoterless yeast selection marker, 2µ: yeast origin of replication, *pGAL1*: *GAL1* promoter, *tCYC1*: terminator. gDNA: genomic DNA from *M.jannaschii,* previously digested with *Xho*I. For clarity, *E.coli* elements are not shown.

pAAT leads to the expression of a C-terminally His$_6$ tagged variant of Aatp. The Aatp expression cassette is presented in Fig. 35.
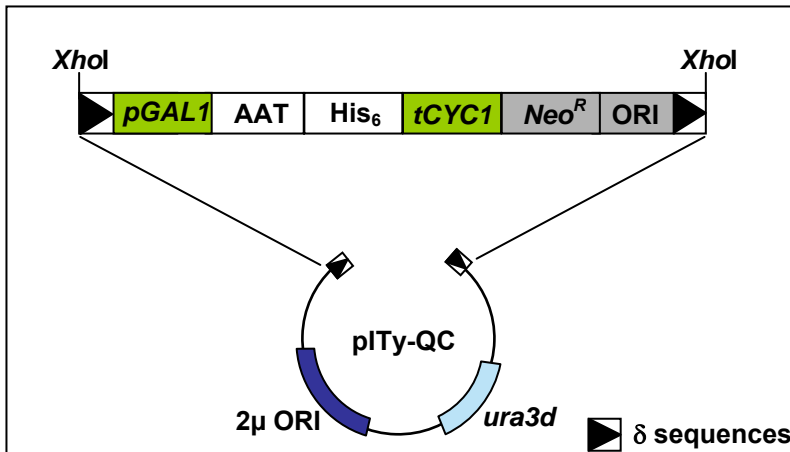
Fig. 35: **Schematic representation of the Aatp expression cassette harbored on the pITy-QC plasmid.** *pGAL1*: *GAL1* promoter; AAT: coding sequence for Aatp; His$_6$: coding sequence for the His$_6$-tag; *tCYC1*: terminator; Neo[R]: neomycin resistance gene; ORI: *E.coli* origin of replication; 2μ ORI: yeast origin of replication; *Xho*I: restriction site; δ sequences: sequences which target chromosomal integration of the expression cassette to the 150-200 copies of the Ty δ sequence present in the yeast genome.

6.1.2. Construction of a yeast strain for enhanced Aatp expression

As for Ste2^{m}p, we constructed an alternative expression strain in order to push the expression level of Aatp. For this, BJ5464 was co-transformed with the pAAT and pMEGA vectors (Sil *et al.*, 2000) and the resulting expression strain was designated YpMEGA/AAT. As previsously explained, the pMEGA vector allows overexpression of the Gal3p, Gal80p and Gal4p switch proteins that enhance transcription of the *GAL1* promoter. Co-expression of these switch proteins in a strain that already sustains high copy numbers of pAAT was expected to boost Aatp expression even further, like it did for Ste2^{m}p.

The features of the two expression strains are summarised in Table 2.

Strain	Plasmid	Important features
YpAAT	pAAT	- 2 μ origin of replication
		- promoterless *ura3d* selection marker
YpMEGA/AAT	pAAT	- 2 μ origin of replication
		- promoterless *ura3d* selection marker
	pMEGA	- enhanced transcription from the *GAL1* promoter

Table 2: **Denominations and important features of each AAT expression strain.**

6.2. Selection of suitable culture conditions and the optimal expression strain for AAT

In order to find conditions yielding an optimal expression level of Aatp, three transformants of the strain YpAAT were submitted to different conditions of growth and induction of gene expression.

For each transformant, starter cultures were first established. They grew for 48h, until an OD$_{600}$ around 11 was reached.

The strains were then inoculated to an OD_{600} of 0,02 at 30 C into a volume of 200 ml of non-inducing selective medium containing raffinose, or rich medium containing glucose, as the sole carbon source (for description of the media composition, see the Material and methods section, chapter 13.2.1).

From the 200 ml uninduced culture, 50 ml each were withdrawn at four different growth phases., i.e., at OD_{600} of 1 to 2, 4 to 5, 7 to 9, and in the stationary phase (indicated by arrows in Fig. 36). The growth curves in selective medium are shown in Fig. 36 (growth curves in rich medium presented no significant differences). The aliquots were then supplemented with 2% galactose to induce the expression of Aatp. After 4h of induction, 25 ml were collected from each culture, cells harvested and frozen. The remaining 25 ml were induced for a total of 8h before being harvested and frozen as well. The same procedure was performed in selective and rich medium for each transformant.
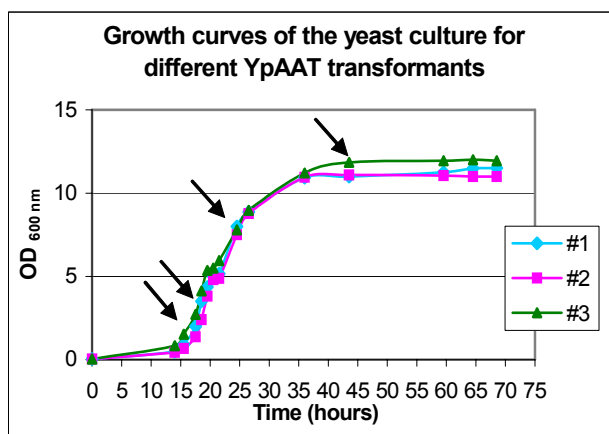
Fig. 36: **Growth curves of different YpAAT transformants in non-inducing selective medium**. Data were obtained from three different transformants, #1, #2 and #3. Arrows indicate the timepoints where samples were collected to be analysed as described above (OD_{600} of 1 to 2, 4 to 5, 7 to 9, and ~12 in the stationnary phase).

The protocol for the determination of the optimal growth and induction conditions is summarized in Fig. 37.
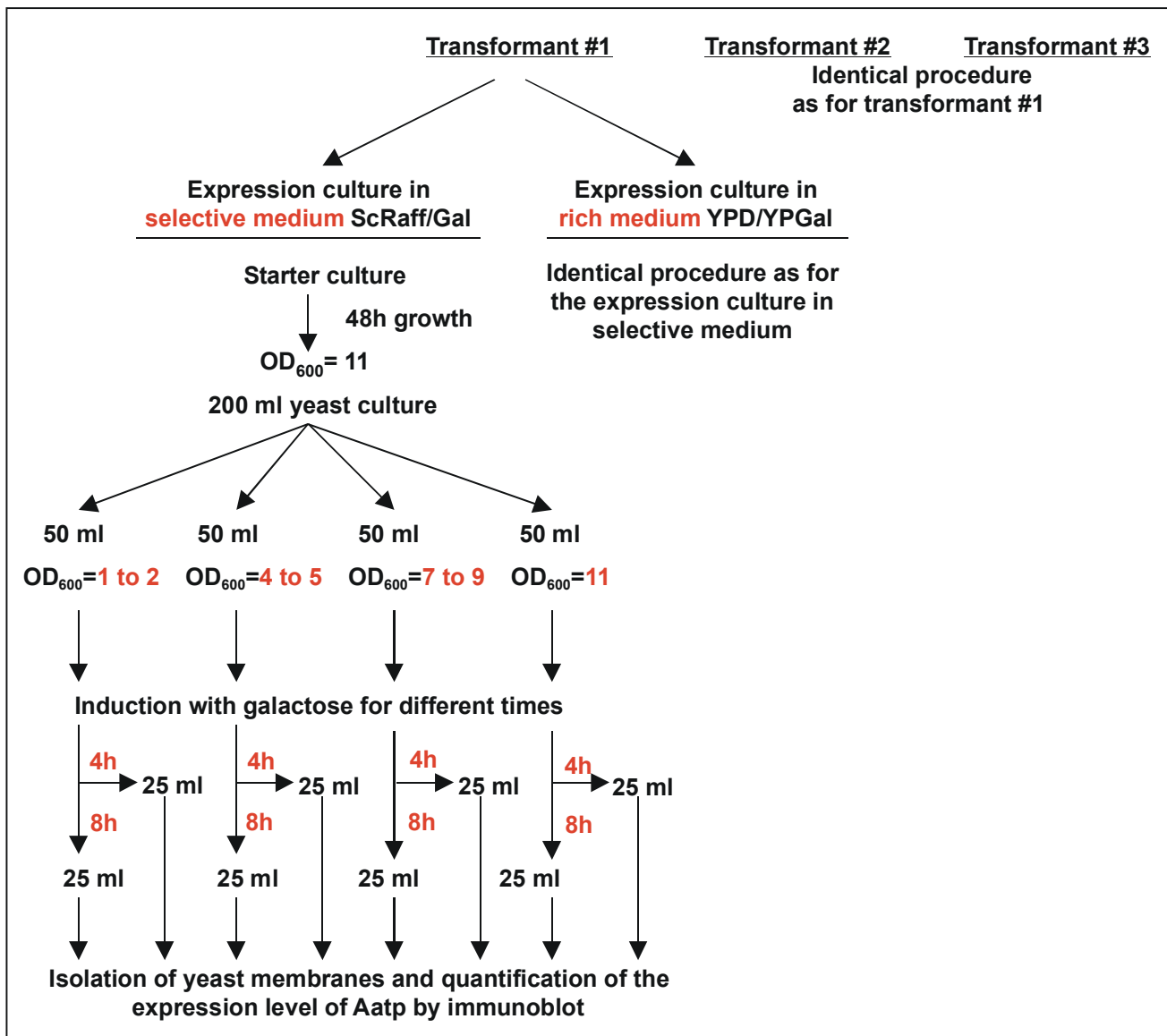
Fig. 37: **Protocol followed to determine the optimal growth conditions and concurrent high level Aatp expression.**

After the induction, yeast membranes of each yeast cells samples were isolated, and the expression level of Aatp was analysed for each of them by immunoblotting, with an anti-His antibody directed towards the His_6-tag of Aatp. During the isolation of yeast membranes, extrinsic proteins were removed by a stripping-step, to enrich the sample in Aatp. This was performed by adding 400 mM NaCl to the homogenisation buffer.

We first compared the Aatp expression level in the membranes of yeast cells grown in rich medium, at different OD_{600} and after different induction times. From the Western-blot in Fig. 38A, it is clear that, in rich medium, the highest Aatp expression level was obtained when the induction was started at an OD_{600} of 6 to 9 and performed for 8h. Densitometric analysis of the Western blot signals yielded relative intensities of Aatp expression of ~8500 to ~9000 as indicated in the corresponding quantification graph (Fig. 38B).
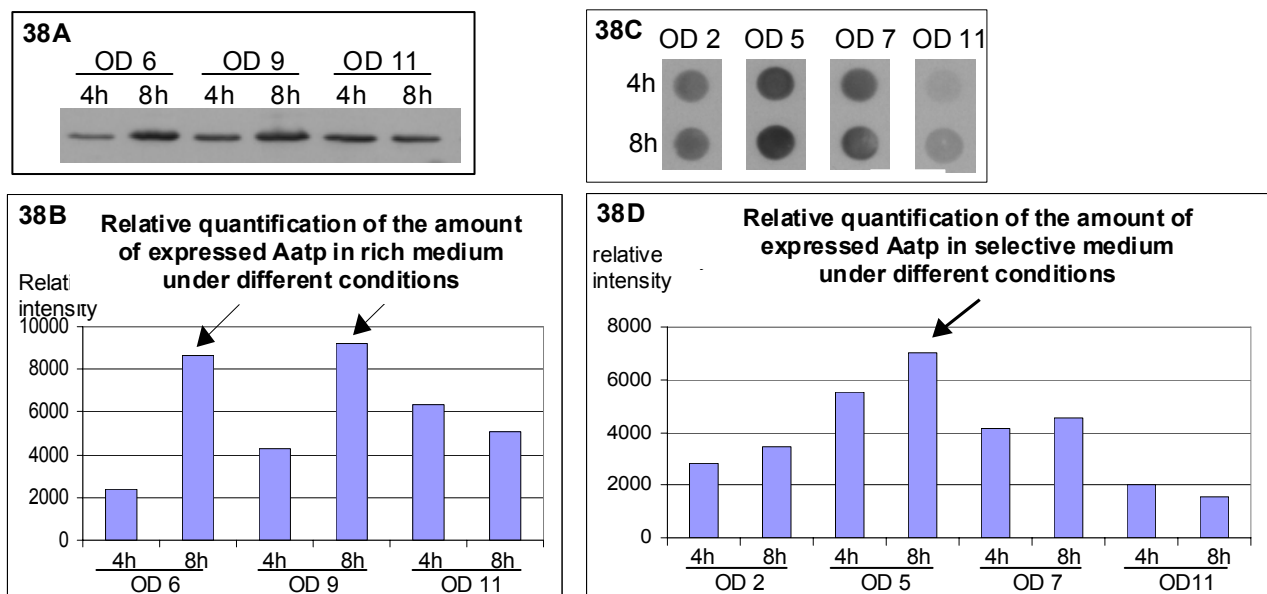
Fig. 38:**Overexpression of Aatp under different growth conditions**. Aliquots were collected from the cultures at different OD_{600} (2, 5, 6, 7, 9, 11), and induced for 4h or 8h with galactose. Ten µg of isolated total yeast membranes were analysed by Western-blot or dot-blot. **38A** and **38B**: Western-blot and corresponding quantification graph showing the amount of expressed Aatp at different times of growth in rich medium, after different times of galactose induction. Arrows indicate the best expression levels. **38C** and **38D**: Dot-blot and corresponding quantification graph showing the amount of expressed Aatp at different times of growth in selective medium, after different times of galactose induction. The arrow indicates the best expression level.

The Dot-blot of Aatp expression in selective medium in Fig. 38C shows clearly that the best Aatp expression level was obtained when the cells were at an OD_{600} of 5 at the induction start and protein expression was induced for 8h. Densitometric analysis of the Dot blot signal yielded a relative intensity of ~7000 as pointed out on the corresponding quantification graph Fig. 398D).

The best expression levels in the two different media were then directly compared on the same Western blot. (Fig. 39A). The blot and its corresponding quantification graph (Fig. 39B) show clearly that Aatp was better expressed in cells grown in selective medium than in rich medium, yielding 4500 and 9000 relative units, respectively.

The expression level of Aatp was also checked in the YpMEGA/AAT strain that carries the pMEGA vector for enhanced AAT expression from the *GAL1* promoter. As for Ste2^{m}p, it was expected that the constitutive overexpression of the Gal transcription factors from the pMEGA vector would lead to an increased transcription of the AAT gene and, consequently, to a higher Aatp expression level.

The Western blot with total membranes isolated from YpMEGA/AAT that had been grown and induced under the same conditions as the YpAAT shows that Aatp expression is not boosted by coexpression of the GAL transcription factors (Fig. 39C).

The quantification graph of the densitometric analysis of the Western-blot signals (Fig. 39D) indicates a considerably lower intensity for Aatp expressed in the YpMEGA/AAT strain (~2000 units) than in YpAAT (~6500 units).
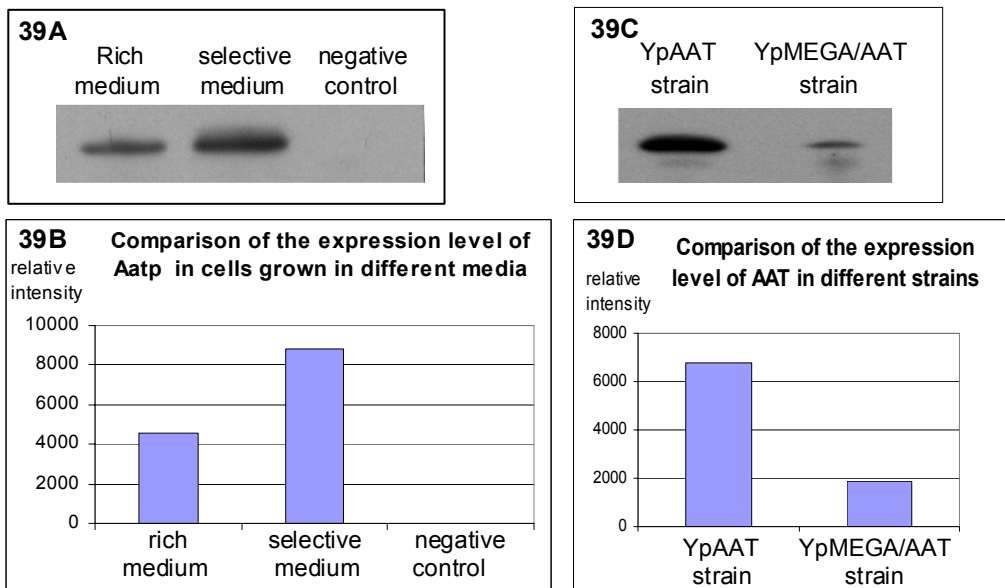
Fig. 39: **Comparison of the Aatp expression levels in cells grown in two different media and between different strains.** Comparison from same amounts of total membranes (20 µg). **39A** and **39B**: Comparison between cells giving the best level of expression in each medium in the strain YpAAT: in rich medium: OD_{600} of 6, induction 8h; in selective complete medium: OD_{600} of 4, induction 8h. **39A:** Western-blot showing the expressed Aatp in cells grown in rich medium or selective complete medium. **39B:** Corresponding quantification graph comparing the amount of expressed Aatp in the two different media. **39C**: Western-blot showing the expressed Aatp in the YpAAT strain and in the YpMEGA/AAT strain. **39D:** Corresponding quantification graph comparing the amount of expressed Aatp in the two different strains.

From the results outlined above, we chose to express Aatp in YpAAT induced in selective medium at an OD_{600} between 4 to 5 and to induce gene expression with galactose for 8h.

6.3. Solubilisation of Aatp

Once overexpression of Aatp in *S.cerevisiae* was optimised, Aatp had to be extracted from the yeast membranes.

40A
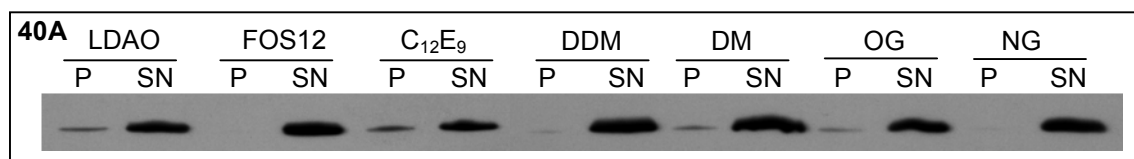
LDAO: N,N-Dimethyldodecylamine-N-oxide
FOS12: N-Dodecyl-phosphocholine
$C_{12}E_9$: Polyoxyethylene-9-laurylether
DDM: N-Dodecyl-β-D-maltoside

DM: N -Dodecyl-α-D-maltoside
OG: N-Octyl-β-D-Glucopyranoside
NG: N-Nonyl-β-D-Glucopyranoside
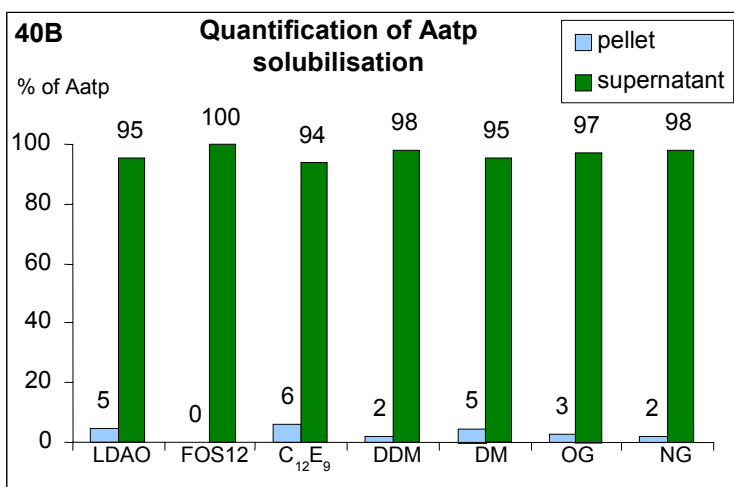
Fig. 40: **Solubilisation of Aatp with different detergents.** Solubilisation of 2 mg of total membrane proteins with 2% detergent (protein/detergent ratio of 1/4) after a 30 min incubation at 4°C. P: Pellets, SN: Supernatants. Pellets were resuspended in the same volume as supernatants, and equal volumes (15 µl) of samples were loaded onto the gel. The anti-His$_6$ antibody used to probe the blot specifically labeled Aatp. **40A**: Western-blot showing the Aatp amount in soluble or insoluble fractions. **40B:** corresponding quantification graph after densitometric analysis of the Western blot.

In order to determine the conditions yielding the best solubilisation, different detergents were tested: N,N-Dimethyldodecylamine-N-oxide (LDAO), N-Dodecyl-phosphocholine (FOS12), Polyoxyethylene-9-laurylether ($C_{12}E_9$), N-Dodecyl-β-D-maltoside (DDM), N -Dodecyl-α-D-maltoside (DM), N-Octyl-β-D-Glucopyranoside (OG) and N-Nonyl-β-D-Glucopyranoside (NG). We intended to choose one that could solubilise at least 50% of Aatp. With all detergents, the solubilisation was carried out with 2 mg of total membrane proteins. A membrane protein/detergent ratio of 1/4 was chosen and the membranes were treated with the desired detergent for 30 minutes at 4°C. The soluble membrane fraction was then separated from the insoluble material by a 1h ultra-centrifugation at 200 000 xg. The amounts of Aatp present in the supernatant and in the pellet were compared by immunoblotting with an anti-His antibody specifically labelling Aatp. The Western-blot (Fig. 40A) and its densitometric analysis in the corresponding quantification graph (Fig. 40B) clearly show that all tested detergents very efficiently solubilised Aatp from the yeast membrane, i.e., between 94 and 100% Aatp was present in the supernatant after the ultra-centrifugation step.

6.4. Purification of Aatp

6.4.1. One-step purification trial by heat treatment

Aatp was supposed to be the only heat-stable membrane protein expressed in *S.cerevisiae*. Therefore, the first purification attempt was performed by a heat treatment step that was expected to cause denaturation and precipitation of the endogenous *S.cerevisiae* proteins but not Aatp. Solubilisation was carried out with the detergents indicated above except LDAO and FOS12, and after a 1h centrifugation at 200 000 xg the supernatants containing solubilised Aatp (and other co-solubilised yeast membrane proteins) were submitted to a 5 minutes heat treatment at 40°C, 70°C or 90°C. After the heating step, the samples were kept on ice for 10 minutes in order to prevent an undesired renaturation of the denatured proteins. After a 1h centrifugation at 200 000 xg at 4°C to pellet aggregated denatured proteins, supernatants were analysed on a silver-stained SDS gel and a Western-blot (Fig. 41).
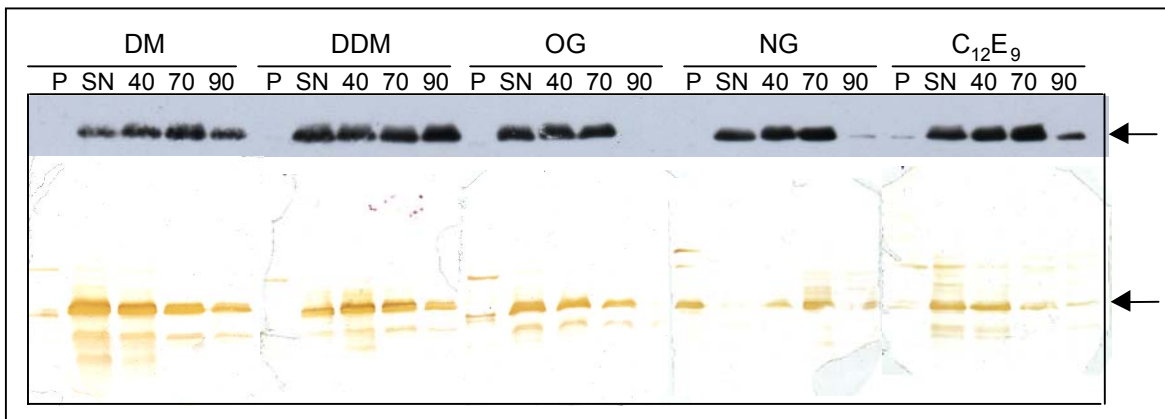
Fig. 41: **Aatp purification by heat treatment of the soluble membrane fraction.** Western-blot and corresponding silver-stained gel, showing the amount of Aatp and total membrane proteins in the original pellet and in the supernatants after a 5 minutes heat treatment at 40, 70 or 90°C. P: Pellet, SN: Supernatant (without heat treatment), 40, 70 and 90: temperature in °C applied to the SN. Samples were heated for 5 minutes and then incubated on ice for 10 minutes. After a 1h centrifugation at 200 000 xg at 4°C, 10 µl of the supernatants were loaded onto the gels. Arrows indicate putative Aatp.

In the case of solubilisation with OG, NG or $C_{12}E_9$, Aatp was denatured after 5 minutes at 90°C as no or only a faint Aatp signal was detected in the Western blot. No denaturation of Aatp was observed after solubilisation with DM or DDM.

In order to determine how long Aatp remained native at high temperatures, the protein was solubilised with DM or DDM. and incubated at 90°C for 1, 3, 5, 7 or 10 minutes followed by incubation on ice for 10 minutes to prevent undesirable renaturation of other denatured membrane proteins. After a 1h centrifugation at 200 000 xg at 4°C to pellet aggregated denatured proteins, supernatants were analysed on a silver-stained SDS gel and a Western-blot (Fig. 42).
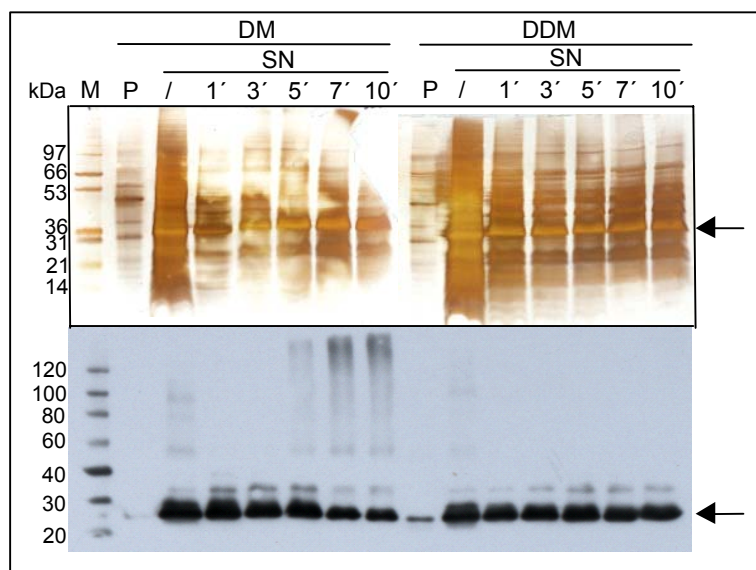
Fig. 42: **Aatp purification by heat treatment of the soluble membrane fraction: time-course of the Aatp thermostability.** Western-blot and silver-stained SDS-gel showing the amount of solubilised Aatp after heat treatment at 90°C for 1, 3, 5, 7, and 10 min. 3 mg of total membrane proteins were solubilised in DM or DDM. After a 1h centrifugation at 200 000 xg at 4°C, the supernatant was incubated at 90°C for different times, then let on ice for 10 minutes, and centrifuged for 1h at 200 000 xg at 4°C. Three µl of the supernatant were loaded onto gels. M: Size marker, P: Pellet, SN: Supernatatant, / :no heat treatment, 1´, 3´, 5´, 7´ and 10´: minutes for the heat treatment. Arrows indicate monomeric Aatp.

The Western-blot shows that Aatp solubilised with DM was stable for 5 minutes at 90°C, and aggregated afterwards as indicated by the high molecular weight bands in lanes 5', 7' and 10' (Fig. 42) and the correspondingly weaker Aatp signals in the same lanes on the Western blot. In contrast, Aatp remained in solution for 10 minutes at 90°C when solubilised in DDM. Surprisingly, the purity of Aatp was not increased by this heat treatment, as on the silver-stained gel many contaminating bands of other proteins (from *S.cerevisiae*) are still present in the soluble fraction after 10 minutes at 90°C. In comparison to the silver-stained SDS-gels in Fig. 41, the silver-stained SDS-gel in Fig. 42 present a lot more contaminating bands, this is probably due to a longer time of development in the silver-staining protocol.

Taken together, the heat treatment did not result in the desired purity of Aatp and, therefore, was abandoned in favour of an alternative 2-step purification strategy.

The calculated molecular weight of the His-tagged Aatp is around 48 kDa. However, in comparison to the size marker on the SDS-gels, it appears around 36 kDa. We used a different size marker for the immunoblot. On the immunoblot, Aatp appears to run around 25 kDa on Western-blots. The use of these different size-markers could explained this size discrepancy. Indeed, MALDI-TOF mass spectrometry analysis (see chapter 6.5.2) revealed that the protein in the bands running at these unexpected molecular weights was indeeed Aatp.

6.4.2. Two-step purification trials

6.4.2.1. Purification by metal-affinity chromatography with Ni2+-NTA beads, and subsequent heat treatment

Aatp carries a His_6-tag. This allowed us to perform metal-affinity chromatography with Ni^{2+}-NTA beads. The chromatography was performed with LDAO- or DDM-solubilised Aatp. Both detergents were chosen due to their efficiency (~100% of Aatp solubilised, Fig. 40), LDAO also for its cheap price, and DDM because it was proved efficient in the solubilisation and purification of other hyperthermophilic membrane proteins (Morsomme *et al.*, 2002), (López-Marqués *et al.*, 2005).

6.4.2.1.1. Purification after solubilisation with LDAO

Ni^{2+}-NTA chromatography was performed after a solubilisation of 100 mg of total membrane proteins with 2% LDAO. Supernatants containing solubilised Aatp were prepared as outlined above and incubated overnight at 4°C with 1 ml Ni^{2+}-NTA beads. The beads were then packed into a column, and the flow-through collected. Subsequently, the beads were washed and Aatp eluted with varying imidazole concentrations.

 The second step of purification consisted in a heat treatment of the Ni^{2+}-NTA eluates and the wash samples, at different temperatures and for different time spansAll Ni^{2+}-NTA chromatography samples were analysed on a silver-stained SDS gel and a corresponding Western-blot. Densitometric analysis of the silver-stained SDS gel (Fig. 43A) showed that Aatp was retrieved around 70% pure in the eluate. However, most of the Aatp came off the column during the wash step.

43B	Wash	Elution				
		15	20	25	250	500
Imidazole	10 mM	15 mM	20 mM	25 mM	250 mM	500 mM
NaH$_2$PO$_4$	50 mM					
NaCl	400 mM					
Glycerol	20%					
LDAO	0,2%					
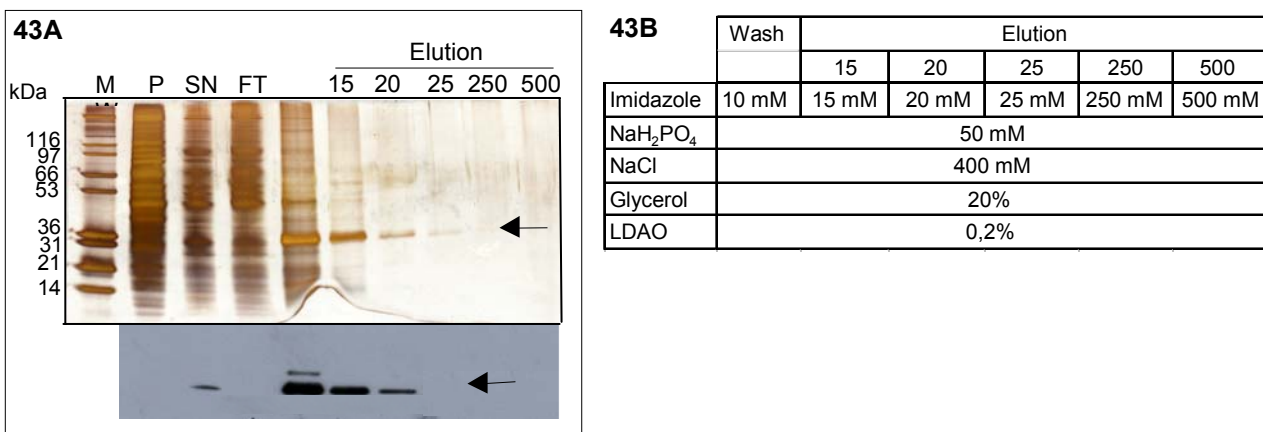
Fig. 43**: Aatp purification trial by metal-affinity chromatography with Ni^{2+}-NTA beads. 43A:** Silver-stained SDS gel and corresponding Western-blot, showing the purification samples after solubilisation of 100 mg total membrane proteins with LDAO. M: Size marker, P: pellet, SN: supernatant, FT: Flow through, W: wash. Elution with different imidazole concentrations: 15, 20, 25, 250 or 500 mM). Arrows indicate monomeric Aatp. **43B:** Composition of the purification buffers.

Unfortunately, the purity of Aatp in the Ni^{2+}-NTA eluate was not reproducible when the purification procedure was up-scaled. Therefore, we performed a heat treatment with the Ni^{2+}-NTA eluate after large scale purification. The eluate was heated to 65°C, 80°C or 90°C for 1, 2 or 5 minutes.

Fig. 44 shows the analysis of the Ni^{2+}-NTA eluate (E) after heat treatment, on a Coomassie-stained SDS gel and its corresponding Western-blot. It reveals that at 65°C, Aatp was stable for 5 minutes. Aatp did not sustain 80°C for 2 minutes as the signal on the Western blot was visibly weaker than in the original eluate (E), and it was completely denatured after 1 minute at 95°C.

Taken together, Aatp does not stay in a native state at high temperatures for longer than 1 to 2 minutes, under the conditions used above and when solubilised in LDAO. More importantly, the purity of Aatp was never improved by the heat treatment.

Surprisingly, after 5 minutes at 90°C, we could still detect a persistent band running around 17 kDa on the Coomassie-stained SDS gel. Both N-terminal sequencing and MALDI-TOF analysis identified it as the 60S ribosomal protein L28 (or L29) from *S.cerevisiae.*
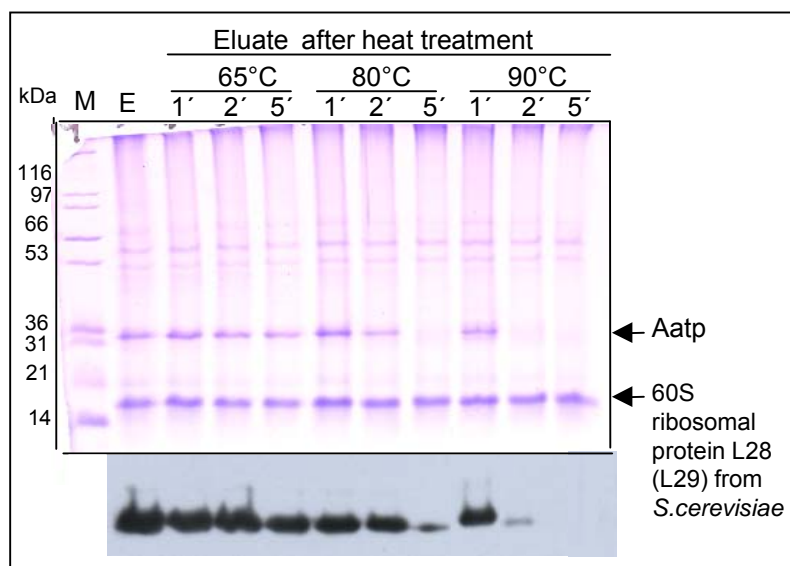
Fig. 44: **Aatp purification trial by metal-affinity chromatography with Ni^{2+}-NTA beads and subsequent heat treatment.** Coomassie-stained gel and corresponding Western-blot, showing the Ni^{2+}-NTA eluate after a heat treatment at 65, 80 and 90°C for 1, 2 and 5 min. 100 mg of total membrane proteins were solubilised with LDAO. M: Size marker, E: Ni^{2+}-NTA Eluate. Arrows indicate monomeric Aatp or 60S ribosomal protein L28 (or L29) from *S.cerevisiae.*

6.4.2.1.2. Purification after a solubilisation with DDM

Since the two-step purification of LDAO solubilised Aatp with Ni^{2+}-NTA and heat treatment was not satisfaying, the same procedure was tried after solubilisation with DDM. The metal-affinity chromatography was done as described above. A Coomassie-stained SDS gel and its corresponding Western-blot (Fig. 45A) show that 75% of loaded Aatp were retrieved, and recovered around 70% pure in the eluate (Fig. 45B). Only 25% were lost during the chromatography, 19% in the flow through and 6% during the wash. The heat treatment was carried out with the eluate at 90°C for 5, 10 and 15 minutes. DDM-solubilised Aatp remained stable at 90°C for at least 10 minutes.

However, after 15 minutes the protein starts to aggregate since the signal on the Western blot becomes weaker. Due to this result, we decided to go on with the purification of Aatp after solubilisation in DDM.

On the SDS-gel in Fig. 45A the purity of Aatp is clearly improved in the heated Ni^{2+}-NTA eluates (lanes 5', 10', 15') as indicated by the decreased number of contaminating side-bands in comparison to the unheated eluate (lane /). Complete removal of the contaminating proteins, though, was not achieved and prolongued heating (15' vs 5') did not improve Aatp purity any further.
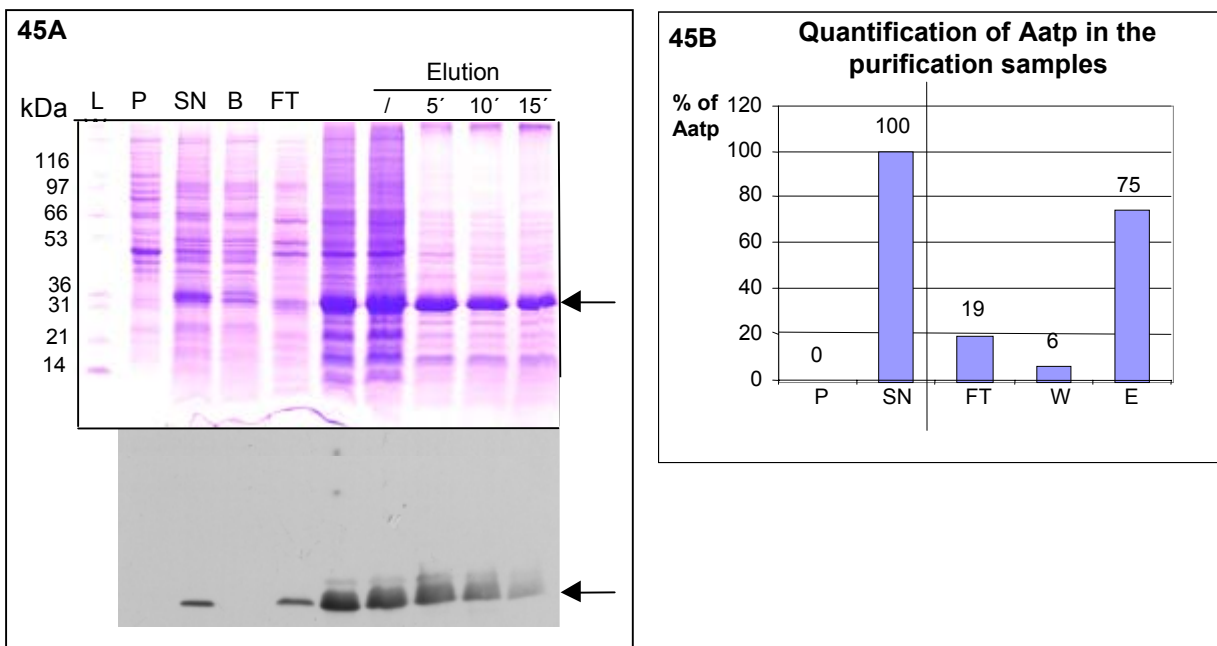
Fig. 45: **Aatp purification trial by metal-affinity chromatography with Ni^{2+}-NTA beads and subsequent heat treatment. 45A:** Western-blot and corresponding Coomassie-stained gel, showing the purification samples after a solubilisation of 100 mg of total membrane proteins with 2% DDM. Heat treatment of the eluate for 5, 10 and 15 min at 90°C. The X-ray film was exposed 30 seconds or 2 minutes to the Western-blot. M: Size marker, P: Pellet, SN: Supernatant, B: Beads, FT: Flow through, W: Wash, E: Eluate. Arrows indicate monomeric Aatp. **45B:** Quantification of the amount of Aatp in each purification sample by densitometric analysis of the Western-blot.

Although quite a number of contaminting proteins were removed by the heating step, the eluate was still not pure enough for crystallisation attempts. In order to further improve the purity, another heat treatment was applied on the supernatant just after solubilisation, and on the eluate after the Ni^{2+}-NTA chromatography. As it is shown on a Coomassie-stained SDSgel and the corresponding Western-blot (Fig. 46), it appears that Aatp denatured when submitted to a duplicate heat treatment, and in addition, its purity was not improved. Thus, Aatp was not heatstable enough to resist the duplicate heat treatment under the solubilisation and purification conditions we used.
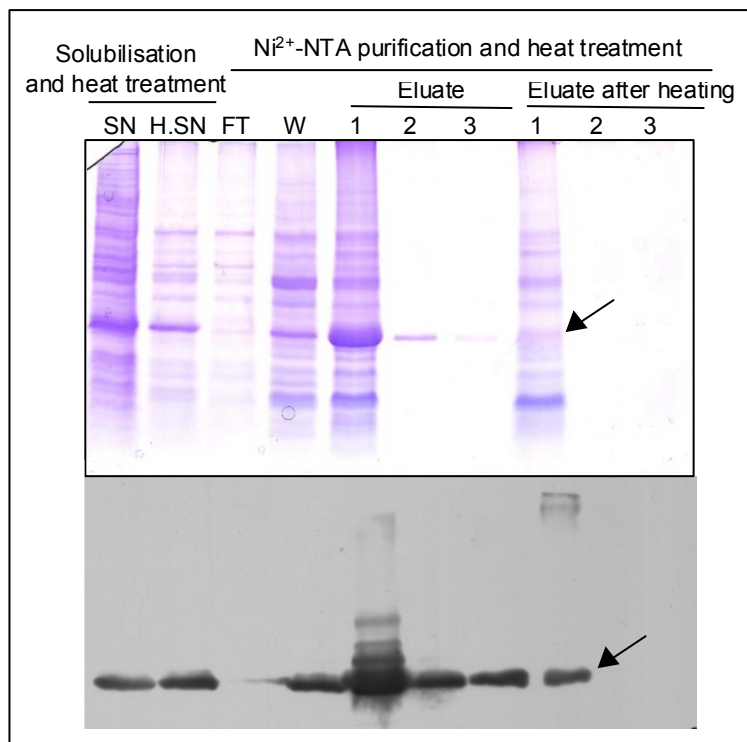
Fig. 46: **Aatp purification trial by metal-affinity chromatography with Ni^{2+}-NTA beads and duplicate heat treatment.** Coomassie-stained SDS gel and corresponding Western-blot, showing a three-step purification trial of Aatp after solubilisation of 100 mg of total membrane proteins with DDM: heat treatment of the soluble sample, Ni^2-NTA chromatography, and heat treatment on the Ni^2-NTA eluate at 90°C for 5 min, 10 min or 15 min. SN: Supernatant, H.SN: Heated supernatant, FT: Flow-through, W: wash. Eluates 1, 2 and 3: were successively collected during elution. Arrows indicate monomeric Aatp.

As it seemed inefficient in inproving Aatp purity, heat treatment was not further pursued.

6.4.2.1.3.   Purification of Aatp in different buffers

In order to improve the efficiency of the Aatp purification, different buffer conditions were tested during the Ni^{2+}-NTA chromatography. We carried out the solubilisation and the chromatography with buffers supplemented with 5 mM imidazole or without imidazole. Coomassie-stained SDS gels and the corresponding Western-blots show the samples of the two different purifications (Fig. 47A and Fig. 47B). A higher amount of Aatp was retrieved in presence of 5 mM imidazole than without imidazole.
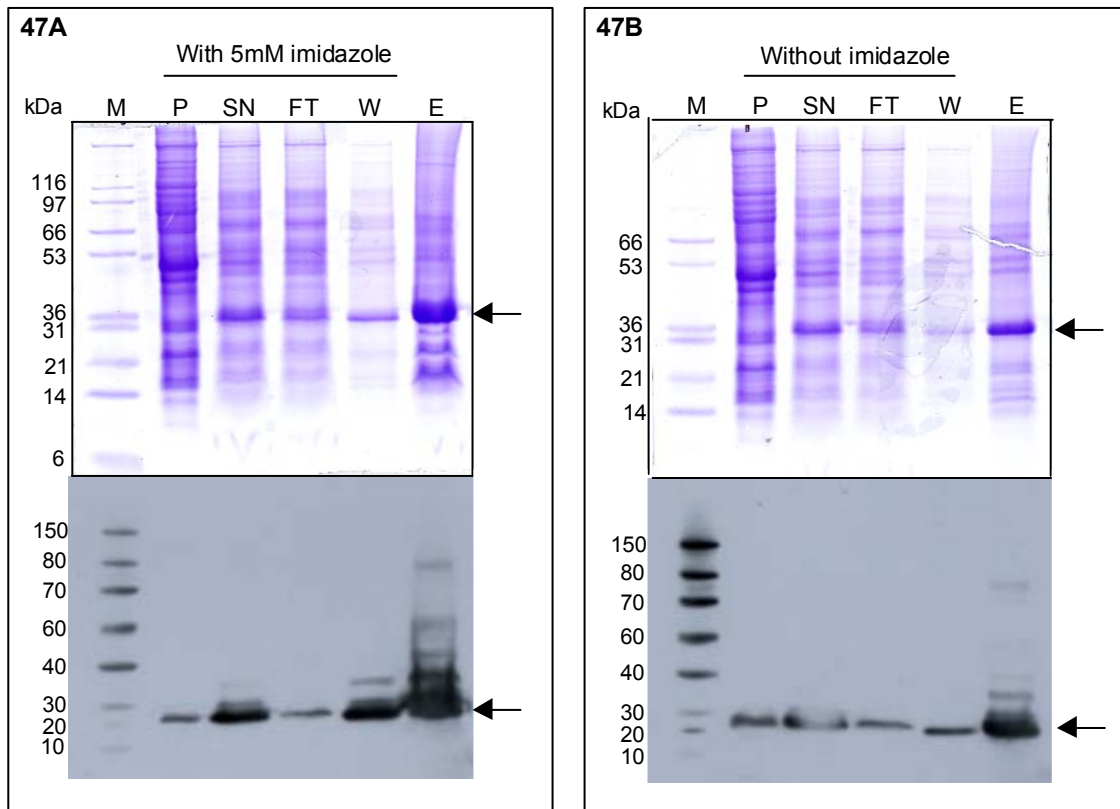
Fig. 47: **Comparison of the efficiency of the Aatp purification in buffers with and without imidazole:** Coomassie-stained SDS gel and corresponding Western-blot of the purification samples after a solubilisation and a purification in buffers containing 5 mM imidazole (**47A**) or without imidazole (**47B**). M: Size marker, P: Pellet, SN: Supernatant, FT: Flow-through, W: Wash, E: Eluate. Arrows indicate monomeric Aatp.

The buffer usually used was 50 mM Na_2HPO_4, as common buffers like Tris-HCl (above 100 mM) are not indicated for the Ni^{2+}-NTA matrix, because of the risk that secondary or tertiary amines reduce the nickel ions. However, we tested the influence of 50 mM Na_2HPO_4 and 50 mM Tris-HCl on the purification efficiency Same amounts of solubilised Aatp were incubated with Ni^{2+}-NTA beads and the usual chromatography protocol was performed. Coomassie-stained SDS gel and the corresponding Western-blot of the two different purifications (Fig. 48) show that the purification was more efficient when performed in a 50 mM Na_2HPO_4 containing buffer than in a 50 mM Tris-HCl containing buffer, in terms of recovered amounts of Aatp in the eluate. Although the purity of the Aatp preparation was better in 50 mM Tris-HCl containing buffer we continued to purify Aatp in 50 mM Na_2HPO_4 containing buffer in order to increase the yield.
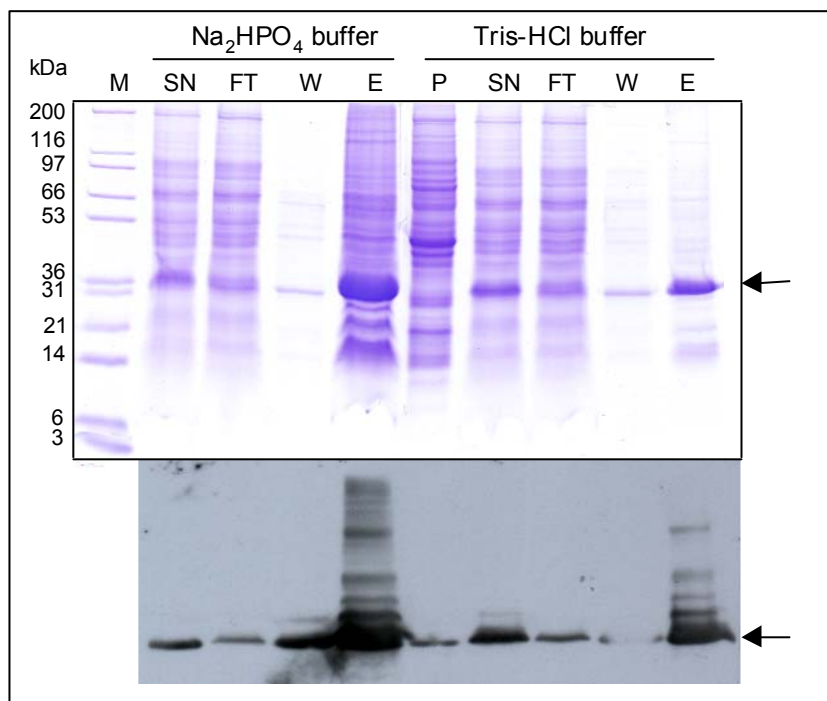
Fig. 48: **Comparison of the efficiency of the Aatp purification in a phosphate and a Tris buffer.** Purification carried out in 50 mM Na_2HPO_4 or in 50 mM Tris-HCl buffer. Coomassie-stained gel and corresponding Western-blot show the purification samples of a purification where same amounts of solubilised Aatp and used for the Ni^{2+}-NTA chromatography in the two different buffers. M: Size marker, SN: Supernatant, FT: Flow-through, W: Wash, E: Eluate. Arrows indicate Aatp.

6.4.2.2. Purification of Aatp by metal-affinity chromatography with Ni^{2+}-NTA beads followed by size-exclusion chromatography

As the purity of Aatp after Ni^{2+}-NTA chromatography was not sufficient to proceed to crystallisation experiments, a second chromatographic purification step was performed. It was our goal to obtain 80-90% pure Aatp in a homogenous state. This second step was a size-exclusion chromatography (SEC) with the concentrated and filtered Ni^{2+}-NTA eluate. The Na_2HPO_4 buffer is inappropriate for crystallisation as phosphate crystals grow very easily, thus, we exchanged it for 50 mM Tris-HCl buffer during the size-exclusion step.

The SEC samples were analysed on a Coomassie-stained SDS gel, and the peak observed on the chromatogram was correlated with the presence of a band corresponding to the calculated molecular weight of Aatp. The purest samples were pooled and concentrated.
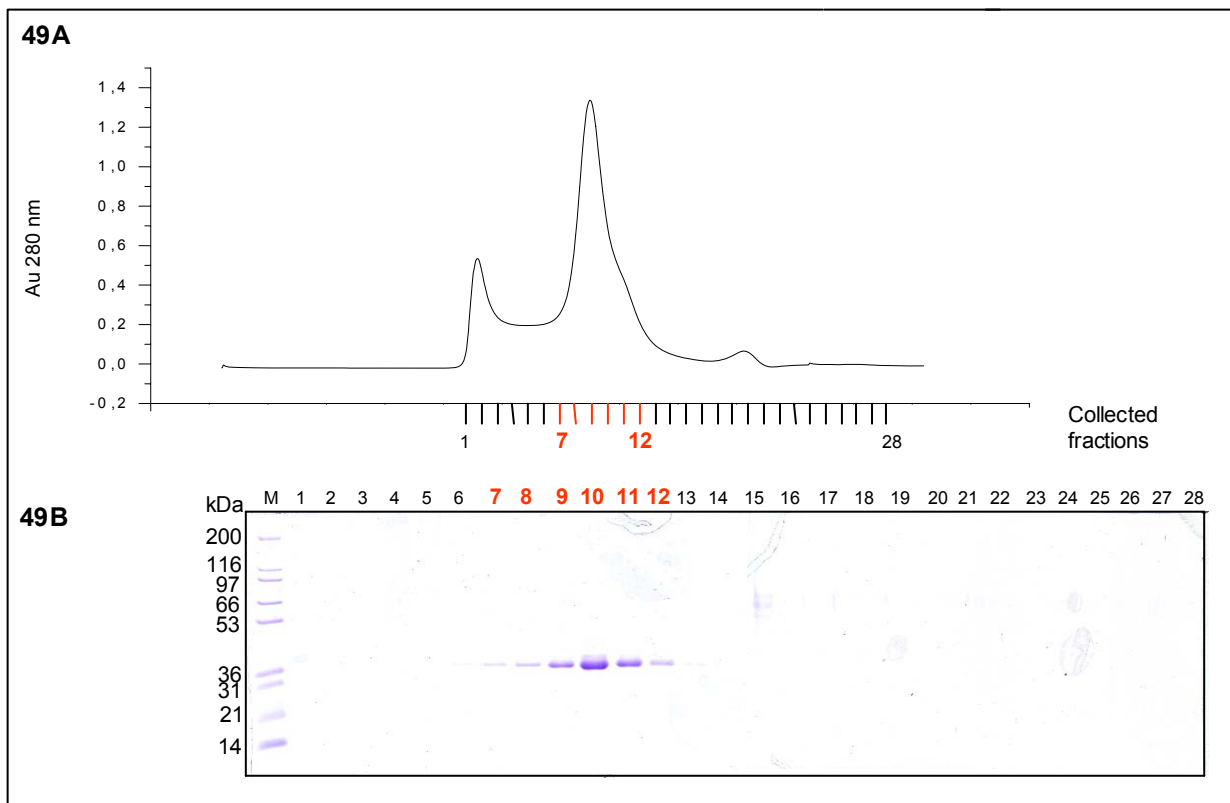
Fig. 49: **Aatp purification by size-exclusion chromatography**. **49A**: Chromatogram of the size-exclusion chromatography. **49B**: Coomassie-stained gel analysing the collected fractions of the size-exclusion chromatography. M: Size marker, 1...28: successive collected fractions.

6.4.3. Final purification protocol for Aatp

All the samples of this two-step purification were analysed on a Coomassie-stained SDS gel and a corresponding Western-blot. This analysis permitted to define the final purification Aatp.

The final purification protocol for Aatp involved two steps: Ni^{2+}-NTA affinity chromatography followed by size-exclusion chromatography. Samples of this two-step purification were analysed on a Coomassie-stained SDS gel and its corresponding Western-blot (Fig. 50A). Purification conditions are described in Fig. 50C.

As shown in the quantification graph (Fig. 50B), appoximately 100% of Aatp were solubilised in DDM. During Ni^{2+}-NTA affinity chromatography, DDM-solubilised Aatp efficiently bound to the beads: only 1% of the protein was lost in the flow through. Aatp bound tightly to the Ni^{2+}-NTA beads as only 4% were lost in the washing step. Almost 95% of the loaded Aatp were retrieved in the eluate. Elution was 100% efficient and no Aatp retained on the beads after elution (0%). Finally, the eluate was concentrated and filtered, and subjected to size-exclusion chromatography. After SEC, approximately 90% pure Aatp (as estimated by densitometric analysis of the Coomassie gel) was retreived in 50 mM Tris-HCl buffer.

50A

solubilisation | Ni²⁺-NTA purification | gel filtration

kDa M   P   SN   B   FT   W   Eni   Ese
200
116
97
66
53
36
31
21
14

50B: Quantification of Aatp in the purification samples

% of AAT

100% | 100% | 100%
98 | | 95 | 95

100
80
60
40
20
0

2   98   0   1   4   95   95
P   SN   B   FT   W   ENI   ESe

50C

	Solubilisation	Purification		
		Ni²⁺-NTA affinity		Size-exclusion
		Wash	Elution	
Imidazole	5 mM	10 mM	500 mM	500 mM
NaH₂PO₄	50 mM	50 mM		/
Tris-HCl	/	/		50 mM
Buffer pH	8	8		7,5
DDM	2%	0,2%		
NaCl	400 mM			
Glycerol	20%			

Fig. 50: **Final purification protocol for Aatp. 50A:** Coomassie-stained SDS gel and corresponding Western-blot showing the purification samples. M: Size-marker, P: Pellet, SN: Supernatant, B: Beads, FT: Flow-through, W: Wash, E: Eluate from the Ni²⁺-NTA chromatography, Ese: Eluate from the size-exclusion chromatography (gel filtration). **50B:** Corresponding quantification graph. **50C:** Composition of the purification buffers. All buffers contained 20% glycerol as chemical chaperone for Aatp.

6.5. Characterisation of Aatp

6.5.1. N-terminal sequence analysis

The major single band of the eluate (Fig. 50A) was cut from an SDS gel and analysed by N-Terminal sequencing. On the Coomassie-stained SDS gel (Fig. 50A) the band corresponding to the putative Aatp migrated around 36 kDa. N-terminal sequencing determined that the 6 first amino-acids of the sequence of this band were MELKNK, which exactly matches the first 6 amino-acids of the sequence of Aatp. This confirmed the nature of the band.

6.5.2. MALDI-TOF mass spectrometry analysis

The major single band of the eluate (Fig. 50A) was cut from an SDS gel, digested with trypsin and analysed by MALDI-TOF mass spectrometry. On the Coomassie-stained SDS-PAGE (Fig. 50A) the band corresponding to the putative Aatp migrated around 36 kDa. MALDI-TOF confirmed the N-terminal sequencing result, attesting that this 36 kDa band corresponded to Aatp. Its molecular mass was determined to be 48149 Da.

6.6. Crystallisation of Aatp

In order to optimise the protein preparation for the crystallisation experiments, as much detergent (DDM) as possible hat to be removed. As DDM can not be dialysed, it was removed by incubation with absorbent biobeads, and a time-course of the Aatp stability against removal of DDM was established.

After Aatp had been purified with the two-step procedure described above (see Fig. 51A for the analysis of the purification samples on an SDS-gel), the SEC eluate was incubated with biobeads with gentle agitation. After 15, 30, 45 minutes, 1h, 1h30, 2h or 2h30, the agitation was stopped to sediment the beads, aliquots of the supernatant were collected and analysed on a Coomassie-stained SDS gel (Fig. 51B). It shows that the amount of Aatp in the supernatant decreased after 30 minutes of incubation with biobeads. After 1h no Aatp band was detected which indicates that too much DDM had been withdrawn from Aatp by adsorption to the beads.

Finally, we continued with a 15 minutes incubation with the biobeads for removal of excess DDM.
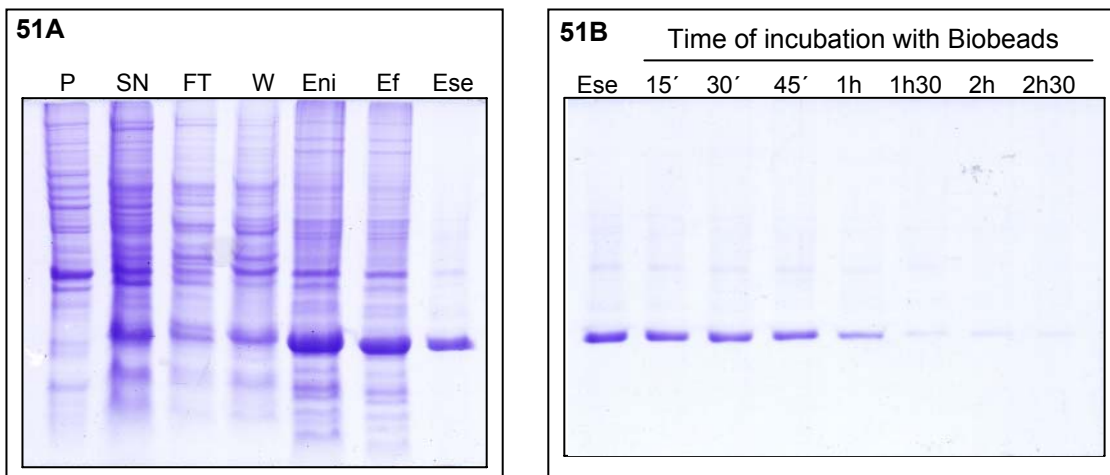
Fig. 51: **Aatp solubility during removal of DDM. 51A**: Coomassie-stained SDS gel of the purification samples from the final purification procedure. P: Pellet, SN: Supernatant, FT: Flow-through, W: Wash, Eni: Eluate of the Ni^{2+}-NTA chromatography, Ef: Eluate Eni Filtered, Ese: Eluate of the size-exclusion chromatography. **51B:** Coomassie-stained SDS gel showing the amount of Aatp still in solution at the indicated time points during incubation with biobeads.

6.6.1. 3D-Crystallisation experiments

6.6.1.1. Manual 3D-crystallisation

We carried out manual crystallisation experiments with several commercially available crystallisation kits: MembFac, Index, Crystal Screen 1 and Crystal Screen 2. The method used was the hanging-Drop method, as described in the Material and methods section (chapter 13.7.3.1).

So far, no protein crystals were obtained.

6.6.1.2. Automated 3D-crystallisation

Automated crystallisation experiments covering 576 different conditions were performed by Crelux GmbH.

No protein crystals were obtained with any of those conditions.

6.6.2. 2D-crystallisation experiments

2D-crystallisation experiments were performed on a Ni^{2+}-lipid monolayer. The principle of this 2D-crystallisation method is based on the use of a Ni^{2+}-lipid layer spread at an air-buffer interface. Proteins present in this lipid phase are concentrated by specific interactions with Ni^{2+} residues carried on the lipid molecules. The Ni^{2+}-chelating lipid is employed as an adapter molecule to bind histidine residues of His_6-tagged modified proteins. Thus, a rigid mixed protein-lipid monolayer is formed on the surface. The monolayer rigidity is directly correlated with the amount of protein bound to it. The more rigid the monolayer, the more proteins are bound and the better ordered they are, which leads to a better chance to obtain protein crystals.

This method consumes only very little pure protein and has already been successful for 2D-crystallisation of different macromolecules and membrane proteins (Lebeau *et al.*, 2001; Asturias and Kornberg, 1999; Brisson, 1999; Levy *et al.*, 1999; Leuther *et al.*, 1996).

Pure Aatp was sent to Dr. Patrick Bron, UMR-CNRS 6026 "Interactions cellulaires et moléculaires", Rennes, France for preliminary 2D-crystallisation experiments. The trials were performed according to the protocol of Levy and coworkers (Levy *et al.*, 1999).

Unfortunately, too few proteins were bound to the monolayer and no order was observed at the surface of the monolayer. Consequently, no protein crystals formed.

Classical 2D-crystallisation experiments with proteoliposomes were also performed. For this, DDM-solubilised Aatp was reconstituted into liposomes made of a classical mixture of *E.coli.* lipids. However, no crystals were observed under all tested conditions (see Materials and Methods section for details).

7. Overexpression of other putative membrane transporters of *Methanococcus jannaschii* in *Saccharomyces cerevisiae*

Four other membrane transporters of *Methanococcus jannaschii* were as well studied: a putative phosphate permease transporter (designated Phopp), a sodium-decarboxylate transporter (designated Dassp), a sodium transporter (designated Nssp) and a potassium uptake protein (designated Trkp). These four transporters were cloned using the same method as for Aatp, and we tried to heterologously overexpress them in *Saccharomyces cerevisiae*, with the final aim to purify them and perform crystallisation trials. As for Aatp, the hyperthermophilic nature of these transporters was expected to facilitate the purification in a heat treatment step.

7.1.1. Expression constructs

As with the AAT gene, each transporter genes PHOP, DASS, NSS and TRK were inserted into the multi-copy *E.coli* / yeast shuttle vector pITy-QC resulting in expression vectors pPHOP, pDASS, pNAA and pTRK (see the section material and methods, chapter 13.1.1.2). The constructs were generated so as to encode a C-terminally His$_6$ tagged variant of each gene for facilitated purification by metal-affinity chromatography. Yeast expression strain BJ5464 was transformed with all of these constructs.

7.1.2. Selection of suitable culture conditions by expression level

The expression of the 4 putative membrane transporters was tested under the same conditions as those described for Aatp (see chapter 6.2): growth in selective medium to an OD_{600} between 4 to 5, and induction with galactose for 8h.

As with Aatp, total membranes were isolated from each induced yeast strain and stripped under high salt conditions in order to remove extrinsic proteins, and to enrich the sample in the desired transport protein. On a Western-blot, the total (stripped) membranes were analysed for expression of the transporters and total stripped membranes of a strain expressing Aatp were used as the reference in the densitometric analysis (Fig. 52). There is clear evidence that Phopp, Dassp, Trkp and Nssp were extremely poorly expressed in comparison to Aatp.
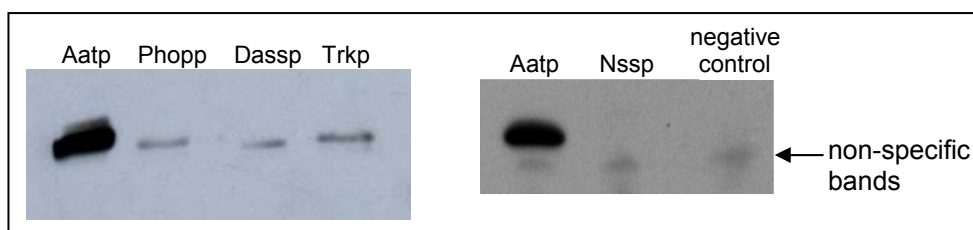
Fig. 52: **Comparison of the expression level of Aatp with that of Phopp, Dassp, Trkp and Nssp in total stripped yeast membranes**. Total membranes were isolated from induced expression strains and 5 µg were loaded on a Western-blot gel. The anti-His$_6$ antibody used to probe the Western-blot labeled specifically the proteins of interest. The negative control presents membranes from untransformed yeast cells.

In the expression system and under the conditions we used, none of the 4 putative membrane transporters of *Methanococcus jannashii* was overexpressed, or even expressed at a level sufficient to obtain enough material for further investigations. It seems that our *Saccharomyces cerevisiae* expression system was only efficient for Aatp.

In consequence, we did not perform further investigations with these four transporters.

Discussion

Membrane proteins are vital elements in the communication of the cell with its environment.

Among them, the G-protein coupled receptors (GPCRs) have raised a great deal of interest lately since they comprise around one third of the pharmaceutically promising drug targets. Their structural analysis is of outstanding medical and pharmaceutical interest in order to understand the mechanism of drug action. However, we have limited knowledge of membrane protein structure and function in general and of GPCRs in particular. So far, there is only one 3D-structure of a GPCR resolved, which is that of the bovine rhodopsin (Palczewski *et al.*, 2000).

The membrane proteins from extremophiles such as hyperthermophilic archaea are also of scientific interest. It was found that many of them could be phylogenetically related to membrane proteins of eukaryotic organisms. As these membrane proteins naturally function in organisms that are extremely resistant to high temperatures, high pressure and extreme pH, they are expectedly more robust than their mesophilic counterparts. This robustness can be very useful to overcome the problems usually encountered during solubilisation and purification of integral membrane proteins.

Hyperthermophilic proteins usually contain a higher proportion of amino-acid residues capable of forming intrinsic forces of stabilisation like salt bridges, hydrogen bonds or hydrophobic interactions, this leading to an expected higher stability of the transmembrane domain interactions under high temperatures (Shiraki et al., 2001; Jaenicke and Bohm, 1998; Vetriani et al., 1998; Jaenicke et al., 1996). For example, a comparison between the glutamate dehydrogenase of the hyperthermophile *Thermococcus litoralis* and the one from *Pyrococcus furiosus* showed that the less stable *T.litoralis* enzyme has a decreased number of ion pair interactions, modified patterns of hydrogen bonding, and substitutions that decrease its packing efficiency (Britton et al., 1999). Hyperthermophilic membrane proteins are also thought to present a better helical packing, making them more resistant to the decrease of lateral pressure (Engelman et al., 2003; Schneider et al., 2002).

So, thermostability is possibly caused by numerous subtle sequence differences modifying the intrinsic stabilisation forces in the proteins. If these forces are disturbed during the solubilisation and/or the purification procedure, loss of hyperthermostability would result (Arnott et al., 2000).

Until now, several soluble proteins from hyperthermophilic organisms have been overexpressed, purified and crystallised. However, only 7 structures of hyperthermophilic membrane proteins (López-Marqués *et al.*, 2005; Ferreira *et al.*, 2004; Van den Berg *et al.*, 2004; Kamiya and Shen, 2003; Jiang *et al.*, 2002b; Jiang *et al.*, 2002a; Nogi *et al.*, 2000; Soulimane *et al.*, 2000b; Soulimane *et al.*, 2000a)), and only one structure of a hyperthermophilic amino-acid transporter, the glutamate transporter homologue from *Pyrococcus horikoshii* (Yernool *et al.*, 2004) have as yet been resolved.

Though there is plenty of experience with the expression, purification and crystallisation of soluble proteins, we are indeed far from having the same possibilities for membrane proteins. Only few generally applicable methods and protocols have been developed that can be referred to, so that the field of membrane protein study appears rather vague, and every new study is actually pioneering work. The challenge to produce high amounts of correctly folded, biologically active, and pure protein for biophysical, biochemical and structural analyses becomes even more demanding with integral membrane proteins that are naturally low abundant and whose overexpression is confined to the biomembrane as the natural environment.

This study's goal was to acquire high resolution 3D structural data of integral membrane proteins. For the crystallisation experiments, we had to provide chemically and structurally homogenous, and highly purified membrane protein preparations in high quantities (mg).

8. Overexpression of integral membrane proteins in *S.cerevisiae*

The choice of a suitable organism for the overexpression of recombinant membrane proteins is an important determinant for its success. In this study, *Saccharomyces cerevisiae* turned out to be an ideal host organism for the overexpression of two integral membrane proteins from different kingdoms of life.

8.1. Overexpression of Ste2^{m}p and assessment of its functional activity

The *S.cerevisiae* alpha-factor pheromone receptor Ste2p, a GPCR, was previously functionally overexpressed in *S.cerevisiae,* and successfully purified (David *et al.*, 1997). Mentesana and Konopka observed that wild-type Ste2p is glycosylated at two consensus N-glycosylation sequences present in the extracellular N-terminal domain of the protein (Mentesana and Konopka, 2001). In addition, they observed on immunoblots a high molecular weight band, due to phosphorylation in the receptor´s C-terminal domain. These post-translational modifications were shown to cause heterogeneity of the Ste2p preparation (Mentesana and Konopka, 2001), which is especially undesirable for protein crystallisation experiments.

However, post-translational modifications, in particular N-glycosylations and phosphorylation, are essential for some membrane proteins and GPCRs for proper folding, regulation and/or stability (Katada *et al.*, 2004; von Zastrow, 2002; Imperiali and O'Connor, 1999; O'Connor and Imperiali, 1996; Imperiali and Rickert, 1995), and activation (Duran-Avelar *et al.*, 2001). Obviously, the modifications are not essential for Ste2p function since unphosphorylated and/or unglycosylated (truncated after Ser^{326} and/or mutated at Asn^{25} and Asn^{32}) Ste2p mutants could be functionally expressed in *S.cerevisiae*. Mutation of the two Asn glycosylation sites into Gln, and removal of the phosphorylation sites does not alter receptor function or subcellular localisation (Mentesana and Konopka, 2001). Although the truncation of the C-terminal part after Ser^{326} reduces the receptor ability of mating projection orientation (Vallier *et al.*, 2002), this modification results in a 4- to 5-fold increase in cell surface expression and a 10-fold increase in the cell sensitivity to pheromone (Mentesana and Konopka, 2001). The truncation is supposed to remove residues that are phosphorylated in the receptor´s basal state (Konopka *et al.*, 1988), and it was shown that it does not affect the G-protein activation (Chen and Konopka, 1996). Dhami and coworkers (Dhami *et al.*, 2002) showed that the phosphorylation of an other GPCR, the metabotropic glutamate receptor, was also prevented by the truncation of its C-terminus.

Taken these observations together, we mapped out a strategy to homologously overexpress an unglycosylated and unphosphorylated mutant Ste2p receptor, Ste2^{m}p, in *S.cerevisiae*. We aimed at the production of high amounts of protein that would facilitate purification and permit subsequent crystallisation studies.

In accordance to the literature and in order to prevent carbohydrate attachment at the two N-glycosylation sites, Asn^{25} and Asn^{32} were exchanged to Gln residues. We also truncated the C-terminal part containing the phosphorylation sites, after Ser^{326}. Two different affinity tags were also introduced at the C-terminus of Ste2^{m}p for facilitated protein purification by affinity-chromatography, and detection on immunoblots.

We attached the FLAG- and His$_6$-tags to the C-terminus of Ste2^{m}p since Lee and Altenberg had previously shown that FLAG- or His$_6$-tags at the C-terminus have no effect on the expression of the multidrug-resistance protein 1 (MRP1) in *S.cerevisiae*, whereas they impair it when hooked onto the N-terminus (Lee and Altenberg, 2003). Moreover, signals for protein translocation and localisation to the target membrane are usually included in the N-terminal part of integral membrane proteins (Jackson *et al.*, 1985).

The *ste2^{m}* gene was cloned into a yeast expression vector, downstream of the galactose-inducible *GAL* promoter (p*GAL*). We pursued two different strategies to optimise Ste2^{m}p expression:

Two expression strains were constructed in order to test whether increased p*GAL*-*ste2^{m}* copy numbers alone or in combination with overexpression of the GAL transcription factors would lead to improved protein expression.

One strain harboured the p*GAL-ste2^m*-expression plasmid with a promoterless *ura3d* selection marker instead of the standard *URA3* marker. Uracil-auxotrophic *ura3* yeast strains that carry plasmids with the *ura3d* marker must replicate the plasmid in higher copy numbers in order to be able to grow on uracil-free medium. Expectedly, gene expression is pushed by plasmid copy number. The second strain was co-transformed with the same p*GAL-ste2^m*-*ura3d* expression plasmid and the pMEGA plasmid (Sil *et al.*, 1999), which allows simultaneous and constitutive overexpression of the GAL transcription factors or "switch proteins" Gal4p, Gal80p and Gal3p. *S.cerevisiae* responds to galactose as the sole carbon source by activating the *GAL* genes that encode the enzymes of the Leloir pathway. The switch from repressed to activated gene expression involves the interplay of the three galactose-dependent switch proteins and two small molecules, galactose and ATP (Sil *et al.*, 1999). Gal4p, the activator, binds to the upstream activating sequence (UAS$_{gal}$) in the promoter of GAL-regulated genes. However, gene expression is not activated as long as Gal4p is bound to its repressor Gal80p. In the absence of galactose, Gal80p binds to Gal4p and prevents it to activate transcription, whereas in the presence of galactose and ATP, galactose interacts with the inducer Gal3p and the complex binds to Gal80p in an ATP-dependent manner. When Gal3p binds to Gal80p, it relieves the inhibition of Gal4p and transcription from the *GAL* promoter is induced. Sil and coworkers showed that cells co-transformed with the pMEGA vector express 15- to 20-fold more Gal4p and 30 to 40-fold more Gal3p and Gal80p (Sil *et al.*, 2000). They also showed that high levels of the switch proteins do not perturb the integrity of galactose-inducible regulation, though their expression levels must be balanced. Indeed, Platt and Reece suggested that Gal3p must still be present in excess over Gal4p levels for the induction process to occur (Platt and Reece, 1998).

Optimal cell growth conditions were established in order to accumulate cell mass for subsequent strong induction of *ste2^m* gene expression. We grew the two different expression strains in selective and rich growth media and tested different growth phases for induction. After varying induction times with galactose, the expression level of Ste2^{m}p was assessed during a time-course. As expected, we obtained the best expression level with the strain that retained high copy numbers of p*GAL-ste2^m*-*ura3d* in selective growth medium. The co-expression of the GAL switch proteins clearly optimised Ste2^{m}p expression even further. David and co-workers expressed the wild-type Ste2p in *S.cerevisiae* at 350 pmol/mg of total membrane proteins (David *et al.*, 1997). This was the highest expression level ever obtained for a GPCR in yeast. Comparable, though lower expression levels were found for the human β$_2$-adrenergic receptor (115 pmol/mg), and the human μ-opioid receptor expressed in *Pichia Pastoris* at 100 pmol/mg (Sarramegna *et al.*, 2003). In comparison to those, the expression level of 143 ± 14 pmol Ste2^{m}p/mg of total membrane proteins that we obtained is superior.

Why we did not achieve similar expression levels as David and co-workers might be due to the glyceraldehyde-3-phosphate promoter (*GAP* or *GPD*) they used, which is noticeably stronger than the inducible *GAL1* promoter (Romanos *et al.*, 1992). However, we cannot rule out that the C-terminal truncation in Ste2^{m}p adversely affects its expression.

Binding of the pheromone ligand to its functional receptor leads to the arrest of cell growth (see introduction section, chapter 3.1.1). In order to demonstrate that Ste2^{m}p was functional, we performed a halo assay that assesses the ability of a yeast strain to undergo growth arrest in response to α-factor, the natural ligand of Ste2p. The inhibition of cell growth is indicated by halos that form around an α-factor soaked filter disk which is placed on agar mixed with haploid yeast cells. With constant α-factor concentration the halo size mirrors α-factor receptor activity.

The halos formed by yeast cells expressing either full length Ste2p fused to a FLAG- and a His$_6$-tag or the modified Ste2^{m}p receptor with the same tags were comparable in size to the halo formed by wild-type yeast cells. This indicates that all mutants responded with a comparable sensitivity to α-factor than the wild-type receptor did. This indirectly demonstrates that the truncation after Ser^{326}, the mutation of the N-glycosylation sites and the introduction of the FLAG- and His$_6$-tags at the C-terminal part of Ste2p did not alter the *in vivo* function of the receptor.

The result of the halo-assay demonstrates that Ste2^{m}p is not only able to bind its ligand but also to couple the G-protein. Almost all GPCRs so far expressed in yeast were shown to bind their ligand, however, coupling of the G-protein was only rarely observed (Erickson *et al.*, 1998; Kajkowski *et al.*, 1997; Price *et al.*, 1995; King *et al.*, 1990).

In order to test the ligand binding activity of Ste2^{m}p *in vitro*, we performed activity assays with native membranes from the Ste2^{m}p expression strain or membranes that were stripped of peripheral membrane proteins, and tritium-labelled α-factor. [^{3}H]α-factor binding-assays showed that Ste2^{m}p in stripped membranes bound approximately twice the amount of labelled ligand in comparison to Ste2^{m}p in unstripped membranes (143 ± 14 versus $73{,}8 \pm 5{,}4$ pmol/mg protein respectively). This suggests that the Ste2^{m}p is active in isolated membranes and, moreover, the stripping-step results in an enrichment of Ste2^{m}p by effectively removing extrinsic and peripheral (membrane) proteins.

The K_d of 87 nM for Ste2^{m}p is 4- to 5- fold higher than that reported by David and coworkers for the wild-type Ste2p (David *et al.*, 1997)., suggesting that the modifications that we introduced into the receptor do affect its ligand binding capacities. The findings of Dosil and coworkers who observed that the integrity of the Ste2p C-terminus affects pheromone binding affinity (Dosil *et al.*, 2000) confirm our conclusion.

The slightly different ligand binding capacities of mutant and wiltd-type pheromone receptors might have been obscured in the halo assays in which we observed similar halos with cells expressing either mutant or wild-type Ste2p. However, the apparently lower affinity of the mutant receptor could be due to the high ionic stripping-step which David and coworkers did not apply when they assessed the K_d of Ste2p. The stripping may have removed, in addition to peripheral membrane proteins, the peripheral membrane G-protein, thus accounting for the observed lower affinity of the mutant receptor to its ligand. This had indeed previously been observed with Ste2p in isolated stripped yeast membranes, where the physical removal of G proteins during receptor purification or the addition of a non-hydrolysable GTP analog results in a decreased affinity for the ligand (Blumer and Thorner, 1990).

It is also possible that the presence of even very small populations of inactive receptors may adversely affect ligand binding affinity.

Competitive ligand binding studies were performed in order to assess the stereoselectivity of Ste2^{m}p. The capacity of Ste2^{m}p to distinguish between two chemically identical but stereoisomeric competitors of the natural α-factor was tested with D-Ala^9 and L-Ala^9 α-factors. In these ligands the Gly at position 9 is mutated to Ala either in D- or L-conformation, thus they display identical hydrobicities.

The observed apparent affinity of Ste2^{m}p for D-Ala^9 (K_d of 102 ± 38 nM) was lower than that of the wild-type Ste2p (K_d of ~ 10 nM, (David *et al.*, 1997)), and the affinity for L-Ala^9 (K_d of 1580 ± 210 nM) was higher (David and coworkers, K_d of ~ 4000 nM). There is a 16-fold difference in affinity of Ste2^{m}p for these peptides in contrast to the ~ 400-fold difference observed for Ste2p by David and coworkers. Nevertheless, the affinity of Ste2^{m}p for the competitors was lower than for the α-factor (K_d of 102 and 1580 nm versus 87 nM), which is similar to the results of Xue (Xue *et al.*, 1996; Xue *et al.*, 1989) and Liu (Liu *et al.*, 2000) for the interaction of Ste2p with other competitors. Taken together, Ste2^{m}p still can still distinguish between two stereoisomeric competitors, though the modifications introduced into the receptor do alter its stereoselectivity.

A possible explanation for the altered ligand binding affinity and stereoselectivity of Ste2^{m}p might be offered by the mutated N-glycosylation sites Asn^{25} and Asn^{32} in the N-terminal part of the receptor (Mentesana and Konopka, 2001). The ligand binding-site of Ste2p is actually located in its N-terminal part, similar to most other GPCRs (Bockaert and Pin, 1999). Since Ste2p interacts with the C-terminus of the α-factor peptide, the overall topology of the receptor N-terminus relative to the α-factor C-terminus is critical for strong receptor binding (Naider and Becker, 2004).

In the native Ste2p, the glycosyl-moieties at Asn^{25} and Asn^{32} might be involved in ligand binding, thus, the mutations could have altered the shape of the binding pocket and/or the access of the ligand. Indeed, point mutations, such as the exchange of two highly conserved Cys residues for Val in the second and third extracellular loops of rhodopsin and the β-adrenergic receptor resulted in a destabilisation of the tertiary structure of these GPCRs and altered their ligand binding characteristics (Dohlman and Thorner, 2001).

8.2. Overexpression of the hyperthermophilic putative transporter Aatp

We intended to overexpress five putative transporters from the hyperthermophilic organism *M.jannashii* in *S.cerevisiae*. Obviously, only AAT was expressed in sufficient amounts to allow subsequent purification.

Full length wild-type Aatp was produced in *S.cerevisiae* with a similar overexpression system as for Ste2p, exploiting a promoterless *ura3d* selection marker for high plasmid copy number, strong inducible transcription intitiation by the *GAL* promoter and constitutive and simultaneous overexpression of the GAL transcription factors from the pMEGA plasmid. The AAT gene was cloned directly from genomic *M.jannashii* DNA into a suitable expression vector by homologous recombination in *S.cerevisiae*. In the final expression construct AAT carried a FLAG- and a His_6-tag at its C-terminus.

However, in contrast to $Ste2^{m}p$, co-expression of the GAL transcription factors did not improve Aatp expression. Although overexpression was not analyzed at the transcription level, we speculate that AAT mRNA is instable and prematurely degraded, which leads to no obvious overexpression. Premature degradation might be due to the altered GC base content of *M.jannaschii* genes in comparison to those from mesophilic organisms, although we did not find any examples in the literature that could corroborate this speculation.

As the proteome is the entire complement of cellular proteins at a given time under certain environmental conditions, Aatp expression was assessed during a time-course under various growth conditions and gene expression was induced in different growth phases. We observed that the amount of Aatp produced in the cells varied substantially with the used conditions.

Aatp was best expressed in selective medium when galactose was added at an OD_{600} of 4 to 5 and gene expression induced for 8h. After overexpression and purification, we obtained approximately 6 mg of pure Aatp from 10 litres of culture.

Since Aatp is a putative amino-acid transporter of which the substrate is entirely unknown, we were unable to assess whether the protein was functionally expressed in *S.cerevisiae*. Most probably, the development of a functionality test would have gone beyond the scope of this thesis.

9.   Solubilisation

The purification and characterisation of membrane proteins rise several problems usually not encountered with soluble proteins. Since the techniques used to liberate integral membrane proteins from the membrane destroy or at least disturb the native membrane structure, it is important to preserve the membrane-associated function of the protein.

Membrane proteins are extracted from their native membranes by solubilisation with detergents. The biophysical features of the detergent molecules are similar to those of the lipids forming the lipid bilayer: both species present a hydrophobic tail and a hydrophilic head. Above their critical micelle concentration (CMC), detergent monomers self-assemble into micelles that can penetrate the lipid bilayer and form mixed protein-lipid-detergent micelles without denaturing integral membrane proteins (Garavito and Ferguson-Miller, 2001).

Choosing a suitable detergent for the solubilisation of an integral membrane protein in the native and functional form is a matter of balancing its efficiency with the capability to preserve the functional properties of the protein. Non-ionic detergents are preferred because they contain uncharged hydrophilic head groups and are generally considered mild and relatively non-denaturing. They efficiently break lipid-lipid and lipid-protein interactions rather than protein-protein interactions. This facilitates solubilisation of membrane proteins in their biological active form without affecting their structural features.

As detergents solubilise membrane proteins with varying efficiencies (Schuck *et al.*, 2003), the appropriate compound is to be screened for each membrane protein. Efficient protein solubilisation corresponds to successful crystallisation of membrane proteins (Rosenow *et al.*, 2002).

In ligand binding assays, David and coworkers (David *et al.*, 1997) demonstrated that the wild-type Ste2p retained its native structure when they solubilised the protein in 2% N-Dodecyl-β-D-maltoside (DDM). Indeed, DDM was the most successful detergent for the solubilisation of half of the 45 GPCRs solubilised to date (Sarramegna *et al.*, 2006). Moreover, it proved very efficient for the solubilisation and the isolation of two hyperthermophilic membrane proteins, the Ca^{2+}-ATPase from *M.jannaschii* (Morsomme *et al.*, 2002) and the H^+-PPase from *T.maritima maritima* (López-Marqués *et al.*, 2005; Perez-Castineira *et al.*, 2001)*.*

DDM is generally very popular for the solubilisation of membrane proteins, since it is appropriate for crystallisation studies as well as for reconstitution experiments. However, DDM does present some disadvantages, e.g. it cannot be dialysed because of its low CMC (0,2 mM), the working temperature is to be kept at 4°C, and, last but not least, the detergent is rather expensive. The commercially available detergent is quite pure which allows its use for chromatography.

For reconstitution experiments, that normally require high CMC detergents allowing dialysis, low CMC detergents such as DDM can still be used, since it is possible to remove them fast and efficiently with polystyrene beads (Biobeads) (Lanfermeijer *et al.*, 1998; Lanfermeijer *et al.*, 1997; le Maire *et al.*, 1987).

DDM was the first choice for solubilisation of both, Ste2^{m}p and Aatp, though we screened as well other detergents such as N-Dodecyl-α-D-maltoside (DM), N,N-Dimethyldodecylamine-N-oxide (LDAO), N-Octyl-β-D-Glucopyranoside (OG), Polyoxyethylene-9-laurylether ($C_{12}E_9$), Triton X-100 (TX100), N-Nonyl-β-D-Glucopyranoside (NG) and N-Dodecyl-phosphocholine (FOS12).

While almost no differences were observed in the solubilisation efficiency of Aatp (around 100% of the protein were solubilised) with any of these detergents at the standard concentration of 2% (w/v), there were clear differences in the solubilisation efficiency of Ste2^{m}p. Again, DDM solubilised Ste2^{m}p most efficiently, around 50%, while the other detergents were far less efficient.

We can only speculate on the inability of the other detergents to solubilise Ste2^{m}p efficiently. The solubilisation capacity of a given detergent might be dependent on the lipid environment of the membrane protein to be isolated. Ste2^{m}p was homologously expressed, that means, in its native lipid environment. This might represent the ideal environment in terms of hydrophobic interactions between protein and lipid which are only inefficiently broken by the other detergents. Aatp, on the other hand, was heterologously expressed and easily extracted from the membrane with all tested detergents. This could indicate that the yeast membrane provides a suboptimal hydrophobic environment for Aatp and the interactions with the neighbouring lipid molecules are, thus, easier broken.

A second explanation for the efficiency differences of the detergents can be related by their interaction with the used buffers. For example, phosphate may cause some detergents to precipitate. In addition, other detergents like OG or NG, although described in the literature as mild and efficient for solubilisation of membrane proteins, possess a more abrasive nature, implying that proteins have to be robust enough to survive the solubilisation process in their native form. This was maybe not the case for Ste2^{m}p, upon interaction with, e.g. OG or NG, the protein denatured, aggregated and subsequently precipitated which rendered solubilisation with these detergents inefficient.

For all the reasons outlined above, DDM was ultimately chosen as the detergent to extract Aatp and Ste2^{m}p from the yeast membranes.

A presolubilisation step with NG or $C_{12}E_9$, aimed at the removal of contaminating membrane proteins and concomitant enrichment of Ste2^{m}p failed. Probably, the membrane was too much disturbed after the first extraction step with NG or $C_{12}E_9$. which might have caused unordered yet very strong hydrophobic interactions between the membrane lipids and the remaining Ste2^{m}p molecules that could not be dissolved in the second solubilisation step with DDM. However, the presolubilisation strategy seems to be ineffective with GPCRs since it failed as well with the olfactive receptor OR5 (Eva Lemker, personnal communication).

10. Purification

Even if the overexpression and solubilisation of an integral membrane protein are successful, usually one has to run the gauntlet in terms of preserving its native function during the subsequent purification procedure. With the lipid molecules more or less quantitatively replaced by detergent molecules, the native hydrophobic environment of the protein is indeed severely modified. The lipid-substituting environment is not only a mediocre preserver of protein structure integrity, it also cannot protect the protein against the attack of endogenous proteases as does the intact lipid bilayer, thus necessitating the addition of protease inhibitors to all used buffers. Moreover, the covert abrasive or denaturing nature of the detergents can lead to aggregation of solubilised membrane proteins, which reduces the efficiency of most separation techniques.

10.1. Purification of Ste2^{m}p

Affinity chromatography was performed by exploiting the presence of the FLAG and His$_6$ affinity tags genetically engineered into the protein.

10.1.1. Ni^{2+}-NTA chromatography

With an optimised Ni^{2+}-NTA chromatography procedure, we obtained 90% pure Ste2^{m}p. Although only 50% of the protein could be solubilised from the yeast membranes, roughly 85% of the material loaded onto the chromatography column was recovered after a single purification step. Around 5,6 mg of pure Ste2^{m}p were regularly obtained per 10 litres of yeast culture. This equals 1 mg from 1,8 litres, a yield superior compared to that obtained by David and coworkers, who could purify 1 mg of the wild-type Ste2p only from 20 litres of yeast culture (David *et al.*, 1997). However, although the group of David managed to overexpress twice as much Ste2p per mg total membrane protein as we did with Ste2^{m}p (350 versus ~145 pmol pure protein per mg of total membrane protein, respectively), they ended up with far less pure protein in the end (~0.05 versus ~0.6 mg of pure protein per litre of yeast culture, respectively).

When we separated the Ni^{2+}-NTA purified Ste2^{m}p preparation on SDS-gels, we always observed two prominent bands of ~30 kDa and ~60 kDa and other oligomers which were multiples of 30 kDa. A similar band pattern was detected on immunoblots with a monoclonal anti-His antibody.

Mass-spectrometric analysis of the Ste2^{m}p preparation confirmed that the sidebands were not contaminating yeast proteins but Ste2^{m}p oligomers. We sought to diminish this heterogeneity in order to optimise the Ste2^{m}p preparation for subsequent crystallisation.

The purification conditions, such as the concentrations of β-mercaptoethanol, EDTA, NaCl and urea, and the amount of Ni^{2+}-NTA beads were thus varied in order to prevent protein aggregation. Unfortunately, we were unable to increase the homogeneity of the Ste2^{m}p preparation by any of these means, indicating that the heterogeneity neither resulted from ionic interactions (which would have been disturbed by the high salt conditions we applied) nor did it involve disulfide bridges which would have been broken by high β-mercaptoethanol concentrations. Addition of the mildly denaturing agent urea as well did not prevent aggregation of Ste2^{m}p.

One might speculate that the persistent band pattern of the Ste2^{m}p preparation was the result of residual glycosylation of the protein. Indeed, in addition to the two N-glycosylation sites Asn^{25} and Asn^{32}, Mentesana and Konopka identified three other potential N-glycosylation sites (Asn^{46}, Asn^{105} and Asn^{205}) in the consensus sequence Asn-X-Ser/Thr by detailed sequence inspection of the extracellular domains of Ste2p (Mentesana and Konopka, 2001). By systematically mutating the putative glycosylation sites, they demonstrated that Asn^{25} and Asn^{32} were exclusively glycosylated in Ste2p. Our deglycosylation experiment with Ste2^{m}p confirmed their result, which excludes residual glycosylation as the cause for the high molecular weight sidebands in the Ste2^{m}p preparation.

All purification buffers contained 20% glycerol to protect Ste2^{m}p protein structure and integrity. When the glycerol concentration was lowered to 10% for facilitated concentration of the protein preparation, this led to a substantially lower yield of purified Ste2^{m}p suggesting a chemical chaperone role of glycerol for Ste2^{m}p.

Although the purity of the Ste2^{m}p preparation was satisfying after the one step purification with Ni^{2+}-NTA beads, we sought to improve the heterogeneity of the product by further chromatography steps. Affinity chromatographies with other metal-ions than Ni^{2+}, FLAG-affinity chromatography, cation-exchange chromatography and size-exclusion chromatography were tested to achieve the goal.

Unexpectedly, FLAG-affinity chromatography did neither improve the purity of Ste2^{m}p nor decrease the heterogeneity, as it did, for example, with the human dopamine D2S receptor (de Jong *et al.*, 2004). A possible explanation is that the Ste2^{m}p did not efficiently bind to the matrix-immobilised anti-FLAG antibody due to the arrangement of the FLAG- and the His$_6$-tags in the recombinant protein. As FLAG is inserted upstream of the C-terminal His$_6$-tag in Ste2^{m}p, it might have been poorly accessible for binding by the antibody on the matrix.

However, there is an example for the efficient purification of the dopamine D1A receptor from *S.cerevisiae* with the same combination of the two tags (Andersen and Stevens, 1998).

Metal ions, such as Ni^{2+}, Cu^{2+}, Co^{2+} or Zn^{2+} interact with His-tagged proteins with varying selectivity. We intended to exploit this selectivity to favour binding of $Ste2^mp$ over other yeast background proteins. For example, in comparison to Ni^{2+}, Co^{2+} displays a higher affinity for His_6-tagged proteins, yet a lower affinity for untagged proteins (Yip *et al.*, 1989; Porath and Olin, 1983; Porath *et al.*, 1975). His_6-tagged proteins bound to Co^{2+}-NTA can therefore be eluted under less stringent conditions than from Ni^{2+}-NTA. A disadvantage of divalent cations other than Ni^{2+} is their non-specific binding to other amino-acids like Cys, Asp, or Glu.

Affinity chromatographies with immobilised Cu^{2+}, Co^{2+} or Zn^{2+}, unfortunately, did not lead to an improvement of $Ste2^mp$ recovery nor homogeneity.

Ion-exchange chromatography with $Ste2^mp$ was also inefficient. This is in contrast to reports on other GPCRs like the rat and human olfactory receptors, which could be readily purified with this method (Nekrasova *et al.*, 1996). Even optimised separation conditions, such as pH, resin volume, or NaCl concentration, would not improve the ion-exchange performance. The main problem was that detergent-solubilised $Ste2^mp$ did not bind efficiently to the matrix. Most probably, the detergent molecules masked possible surface charges of $Ste2^mp$.

Surprisingly, size-exclusion chromatography did not separate oligomeric forms of $Ste2^mp$ from the desired monomers. The probability that this heterogeneity was due to persistent ionic interactions was low, since the running buffer contained 400 mM NaCl and, in addition, 1 mM β-mercaptoethanol to reduce disulfide bridges. Most probably, the $Ste2^mp$ oligomers were held together by hydrophobic interactions that could not be broken by the non-denaturating detergent DDM. Not even boiling the sample in the strongly denaturing detergent SDS would disintegrate the aggregates as the oligomers were well detectable on denaturing protein gels.

The numerous oligomeric forms of $Ste2^mp$ are in stark contrast to the band patterns of Ste2p observed by David's group and by Mentesana and Konopka. They also detected multiple protein species in their purified samples, however, these were due to post-translational modifications such as glycosylation or phosphorylation and did not originate from oligomerisation of the receptor. Possibly, the removal of the hydrophilic C-terminus exposed previously obscured hydrophobic domains in $Ste2^mp$. If these were only insufficiently solubilised by DDM this could have led to the observed aggregation of adjacent receptors by hydrophobic interactions during the extraction from the yeast membrane. This notion is corroborated by the detection of predominantly monomeric but very little dimeric $Ste2^mp$ on immunoblots of isolated yeast membranes. Blumer and coworkers made similar observations with wild-type Ste2p (Blumer *et al.*, 1988)

Neither FLAG-affinity chromatography, nor cation-exchange chromatography, metal-affinity chromatography with alternative metal ions nor size-exclusion chromatography were effective in diminishing Ste2^{m}p heterogeneity. Thus, the purification protocol for Ste2^{m}p finally comprised a one-step Ni^{2+}-NTA chromatography. Ste2^{m}p purified in that way was pure and monodisperse enough to subject it to crystallisation experiments.

Further optimisation of the Ste2^{m}p purification procedure might deal with other high affinity-tags, such as the Streptavidine-tag, or a bulkier tag, like the glutathion-S-transferase (GST). A longer poly-histidine tag including 10 or 12 residues as well as insertion of the affinity tag at the N-terminus, though not too promising for the reasons outlined above, could be worth trying.

10.2. Purification of Aatp

With our developed purification protocol, we routinely obtained 0.6 mg of ~ 90% pure and homogenous Aatp from 1 litre of yeast culture. Although this yield was lower than that for the *M.jannaschii* Ca^{2+}-ATPase (1,6 mg/litre (Morsomme *et al.*, 2002)) and the *T.maritima* H+-PPase (1,5 mg/litre (López-Marqués *et al.*, 2005)), our preparation fulfilled the requirements for subsequent crystallisation experiments.

10.2.1. Single-step purification by heat treament on solubilised protein

To purify Aatp, we tried to take advantage of its thermal stability. The optimal growth temperature for *M.jannaschii* is 85°C whereas *S.cerevisiae* thrives at 30°C. Thus, the proteins of the hyperthermophilic archaeon are expected to withstand high temperatures at which S.cerevisiae proteins would grossly denature. We assumed that a drastic heat treatment of the detergent-solubilised protein extract from yeast membranes would denature most of the yeast proteins and cause them to aggregate, so that they would be easily separated from Aatp.

Previously, heat treatment had turned out as a fast and convenient tool for the purification of other hyperthermophilic membrane proteins, such as *M.jannaschii* Ca^{2+}-ATPase (Morsomme *et al.*, 2002) and *T.maritima* H$^+$-PPase (López-Marqués *et al.*, 2005).

In this study, DDM-solubilised Aatp was stable at 90 °C for 10 min, whereas it appeared more heat-labile in all other tested detergents.

However, the heat-shock of the DDM-solubilised membranes did not yield pure Aatp, as numerous contaminanting sidebands were detected in the soluble fraction on Coomassie-stained SDS-gels. These bands could originate from yeast proteins that expose hydrophobic domains during the heat denaturation step. These domains may interact with excess detergent molecules in the sample, leading to their solubilisation instead of aggregation and separation from Aatp.

10.2.2. Multistep purification by Ni^{2+}-NTA chromatography and heat treatment

As the heat treatment resulted in very low purity of the Aatp preparation, we combined it with a Ni^{2+}-NTA chromatography, thus, exploiting the His$_6$-tag on the Aatp C-terminus.

Two different protocols were performed: first, we tried Ni^{2+}-NTA chromatography after the heat treatment of DDM-solubilised Aatp; in the second attempt not only the solubilisate but also the Ni^{2+}-NTA eluate was heated.

Unfortunately, none of both protocols improved the purity of the Aatp sample. Conversely, Aatp appeared to become heat-labile after Ni^{2+}-NTA chromatography. Possibly, the high imidazole concentration from the elution step adversely affected the stability of the detergent-solubilised Aatp at elevated temperatures.

10.2.3. Ni^{2+}-NTA chromatography and size-exclusion chromatography

Since the heat treatment of detergent-solubilised Aatp did not meet our expectations, we chose to quit this strategy and focussed our efforts on the Ni^{2+}-NTA chromatography . Although the on-step purification yielded quite pure Aatp, we performed a subsequent size-exclusion chromatography, which has been a popular "polishing" step in the purification procedures of other hyperthermophilic membrane proteins (López-Marqués *et al.*, 2005; Morsomme *et al.*, 2002; Lanfermeijer *et al.*, 1998).

The combination of both chromatographies indeed facilitated the production of highly pure, homogenous and monodisperse Aatp, as attested by a single band on the Coomassie-stained SDS-gel and its corresponding immunoblot. These results allowed us to undertake crystallisation trials with purified Aatp.

Although N-terminal sequencing and Mass-spectrometry analysis confirmed that the band on Coomassie-stained SDS-gels and immunoblots was Aatp, it is obvious that the protein runs at much lower size, e.g., ~36 kDa on SDS-gels and ~25 kDa on immunoblots, than expected from its calculated molecular mass of ~48 kDa. The discrepancy between SDS-gels and immunoblots can be explained by the use of two different molecular weight standards. We tested different commercially available molecular weight markers and observed that standard bands signifying the same molecular weight do not necessarily display the same mobility in SDS-gels. However, it is well known, that in some instances SDS does not entirely denature integral membrane proteins. On the contrary, the detergent stabilises the helical transmembrane domains leading to only partial disintegration of the three-dimensional structure of the protein (le Maire *et al.*, 2000). Thus, the incompletely unfolded molecule shifts to higher mobility in SDS-gels than one would expect from its calculated mass.

11. Crystallisation

Although several thousand 3D-structures of cytosolic proteins are resolved, only 93 structures of membrane proteins are to date described, most of them are structures of bacterial proteins. This amount discrepancy is clearer when one consider that 20 to 30% of all ORFs from bacteria, archea and eukaryote code for membrane proteins (Wallin and von Heijne, 1998).
These figures mirror the technical challenge of crystallising integral membrane proteins.

X-ray crystallography is one of the most efficient methods to determine high resolution structures of membrane proteins. Electron microscopy is also a powerful technique, along with NMR (Rigaud, 2002; Hasler *et al.*, 1998; Walz and Grigorieff, 1998). The rate-limiting step in the process of structure determination is usually the production of crystals suitable for diffraction experiments.

Several prerequisites lead the way to a successful crystallisation process of membrane proteins (Caffrey, 2003). In general, the high hydrophobic segments of membrane proteins hamper the efforts to stably keep them in a native state, and the challenge is to find a suitable temporary environment that preserves their structure and function until they are fixed in a crystal lattice. By any means, the structural integrity of the protein has to be maintained (conformational homogeneity) and there should not be non-specific aggregates. The protein must not denature during the process. Heterogeneities by post-translational modifications are also interfering, and in addition, in a protein-detergent complex, it is crucial that the non-protein components of the complex are homogenous (Wiener, 2004; Caffrey, 2003; Wiener, 2001). It is of outstanding importance that the membrane protein to be crystallised is very pure and available in high concentration, ideally, 5 to 15 mg/ml.
Taken together, these prerequisites absolutely require a systematic search for ideal crystallisation conditions.

3D-crystallisation experiments with purified Ste2^{m}p and Aatp were performed manually using the hanging-drop method,. Alternatively, the sitting-drop method was chosen in automated trials. During the course of this PhD study, these 3D-crystallisation trials have not succeeded in the growth of Ste2^{m}p or Aatp crystals so far under the conditions we used. Although automated crystallisation experiments allow to screen thousands of different crystallisation conditions in a reasonable time (Stevens, 2000b; Stevens, 2000a), this approach was unsuccessful in our case.

For membrane proteins, 2D-crystallisation is a convenient alternative to the classical 3D-crystallisation. This method, first described in technical detail by Levy and collaborators (Levy *et al.*, 2001; Levy *et al.*, 1999), was originally developed by the group of Kornberg (Kornberg, 1991) and further developed by other groups (Courty *et al.*, 2002; Brisson, 1999; Brisson *et al.*, 1994).

In principle, a Ni^{2+}-lipid monolayer is set up to enhance the formation of crystals. Detergent-solubilised His_6-tagged membrane proteins selectively attach to a Ni^{2+}-lipid monolayer. Fixing the His_6-tagged proteins to the Ni^{2+} residues of the monolayer enriches and orders them, which favours the formation of a crystal lattice. A major advantage is the minute amount of protein needed, e.g., a concentration of 1 mg/ml is enough to get crystals.

This method proved to be especially successful for the crystallisation of membrane proteins such as, e.g., FhuA, a phage receptor from *E.coli*, the F_0F_1-ATP synthase from *Bacillus* PS3 (Levy *et al.*, 1999), or the H^+-ATPase from the plant plasma membrane (Lebeau *et al.*, 2001).

We tried 2D-crystallisation with Aatp. Unfortunately, Aatp hardly bound to the monolayer, no order was observed in the vesicles formed at the surface.

In order to exchange the detergent for a more native lipid environment, reconstitution experiments were also performed with Aatp, using lipids from *E.coli.* However, reconstituted protein did not yield better results in the 2D-crystallisation experiments. Other membrane proteins that had been heterologously and functionally expressed in *S.cerevisiae*, like the rabbit Ca^{2+}-ATPase SERCA1a (Jidenko *et al.*, 2005) or the dog kidney Na^+/K^+-ATPase (Mohraz, 1999) could be successfully crystallised from reconstituted proteoliposomes.

We have several explanations for the so far unsuccessful crystallisation experiments with Ste2^{m}p and Aatp. We added 20% (v/v) glycerol as a stabiliser to the purification buffers and a lower concentration (10%) was not appropriate during the purification process. This concentration of 20% could, however, have complicated the crystallisation, as glycerol can behave either as a precipitant or an additive, and, therefore, severely influence the outcome of a crystallisation experiment.

Even traces of phosphate in the protein sample can interfere with crystallisation, cause protein precipitation under certain screening conditions or promote the formation of salt crystals. As phosphate buffer was used for Ni^{2+}-NTA chromatography of Aatp, we cannot rule out that the final protein preparation contained trace amounts of phosphate that negatively affected crystallisation.

Temperature is also an important variable for crystal growth. Although proteins in high salt solutions are generally better soluble at cold than at warm temperatures, maybe the proteins were not stable at 18°C, the temperature we used, although it is a common temperature for crystallisation.

The introduction of excess detergents into the crystallisation sample can also present a problem for the growth of crystals, so that one has to choose specific additives like salts or precipitants to aid the crystallisation (Caffrey, 2003; Rosenbusch, 2001; Rosenbusch *et al.*, 2001; Rosenbusch, 1990). Although the Aatp preparation was depleted for excess detergent by treatment with Biobeads, which is a common procedure for detergent removal from membrane protein preparations (Mosser, 2001; Rigaud *et al.*, 2000; Lacapere *et al.*, 1997; Rigaud *et al.*, 1997), there might still have been to much DDM for the crystallisation process to succeed.

More importantly, although we carefully optimised the purification conditions, our protein concentrations never exceeded 2,5 mg/ml and crystal growth occurs very slowly in insufficiently concentrated protein solutions.

Taken together, more elaborate screening of crystallisation conditions is still to be done for Ste2^{m}p and Aatp, which would have gone beyond the scope of this PhD thesis.

General conclusion

To conclude, in this study, we have developed a successful system for the efficient overexpression of two membrane proteins from different kingdoms of life in *S.cerevisiae.* We set up a fast large-scale purification protocol that permits the isolation of milligram quantities of homogeneous and monodisperse protein at a purity around 90%. Solubilisation of Ste2^{m}p and Aatp from yeast membranes with DDM was 50% and 100% efficient, respectively. This protocol involves a one step purification by metal-affinity chromatography for Ste2^{m}p and a two step procedure for Aatp (metal-affinity chromatography followed by a size-exclusion chromatography). Applying these purification strategies, we routinely recovered 85 to 95% of the solubilised proteins, corresponding to 5,6 mg of pure Ste2^{m}p and 6 mg Aatp from approximately 10 litres of yeast cell culture.

Preliminary crystallisation experiments indicate that more crystallisation conditions need to be explored.

Material and methods

12. Organisms, vectors and oligonucleotides

12.1. Organisms

Strain	Relevant geno or phenotype	Reference
Saccharomyces cerevisiae BJ5464	MATα; ura3-52; trp1; leu2Δ1; his3Δ200; pep4::HIS3; prb1Δ1.6R; can1; GAL1	ATCC #208288
Saccharomyces cerevisiae BY4741	Mat a; his3Δ1; leu2Δ0; met15Δ0; ura3Δ0; YIL015w::kanMX4; YFL026w (STE2)::LEU2	Euroscarf #Y00000
Escherichia coli Dh5α	FΦ80d/*lacZ* M15 (*lacZYA-argF*) U169 *recA1 endA1 hspR17* ($r_k^-m_k^+$) *supE44* λ *thi-1 gyrA96*	Hanahan, D., 1983

Table 3: **Genotype of the organims used**

12.2. Vectors

Plasmids	Relevant features	Source
pYES2-FT.HT	2μ, *URA3, ORI*, Amp^R; *GAL1*, tCYC1, FLAG- and His$_6$-tags	Invitrogen
pYES-*ura3d*-FT.HT	2μ, *ura3*d, *ORI*, Amp^R; *GAL1*, tCYC1, FLAG- and His$_6$-tags	Dr. James Hopper
pMEGA2-ΔURA3	Gal4p, Gal80p, Gal3p, 2μ, Δ*URA3*, *LEU2*, Amp^R	Dr. Douglas Griffith
pITy-QC	δ-integration vector; 2μ; *ura3d*; *ORI*, can^R; *GAL1*, tCYC1	Jason Burbank

Table 4: **Main features the vectors used**

Maps of the vectors are represented above (Fig. 53).
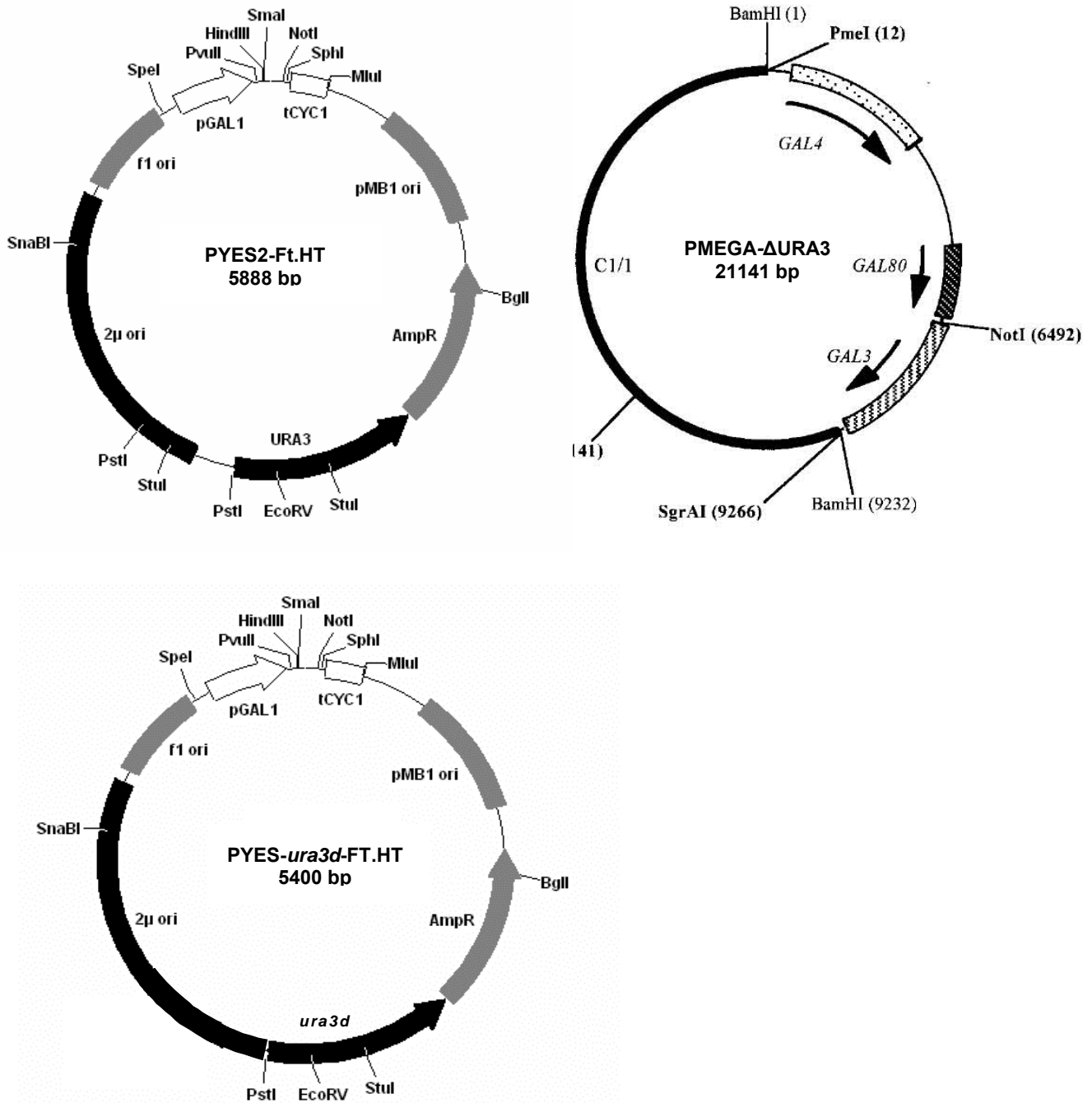
Fig. 53: **Maps of the vectors pYES2-FT.HT, pYES2-*ura3d*-FT.HT and pMEGA2-ΔURA3**

12.3. Oligonucleotides used for the cloning of the hyperthermophilic proteins

Cloning of the *M. jannaschii* integral membrane proteins into an expression vector was based on a direct homologous recombination strategy. The target genes were directly cloned from genomic DNA of *M.jannaschii* which was purchased from ATCC (#43067), Wesel, Germany.

The expression vector pITY-QC was modified by PCR based introduction of 45bp/50bp homologies to the target genes on either side of the expression cassette. The integral membrane proteins were expressed with a C-terminal His$_6$-tag

The following primer pairs were used to generate the receiving expression vector pITY-QC for the cloning of MJ0609 (AAT), MJ0630 (PHOP), MJ0672 (DASS), MJ1319 (NSS), and MJ1485 (TRK).

Primers combinations for each proteins:

MJ0609 (AAT):   DG204 / DG209
MJ0630 (PHOP):   DG205 / DG210
MJ0672 (DASS):   DG206 / DG211
MJ1319 (NSS):   DG207 / DG212
MJ1485 (TRK):   DG208 / DG213

DG204 MJ0609	5'-<u>AGA AAC AGC TTC CCA CAA ACT AAG CTT TTT ATT TTT TAA CTC CAT</u> TTT TTT AAT ATT CCC TAT AGT GAG TCG TAT TAC AG -3'
DG205 MJ0630	5'-<u>ACT TAT GAT TAG CTC TAA ATT TAT AGA AAT CTC TAT AGT AAT CAT</u> TTT TTT AAT ATT CCC TAT AGT GAG TCG TAT TAC AG -3'
DG206 MJ0672	5'-<u>AGC TGT AAT TAT CCC TAA GCC TAT AAA TTC TTT GGA TAA TCT CAT</u> TTT TTT AAT ATT CCC TAT AGT GAG TCG TAT TAC AG -3'
DG207 MJ1319	5'-<u>AAA TCC CAA GTT AGA GCT CCA GCT TTC TCT TTC CAT ATA ACT CAT</u> TTT TTT AAT ATT CCC TAT AGT GAG TCG TAT TAC AG -3'
DG208 MJ1485	5'-<u>TAA AAT TCC TTC AAT GTC TTT TTT TGT TAA TCT ACA GAT TCC CAT</u> TTT TTT AAT ATT CCC TAT AGT GAG TCG TAT TAC AG -3'

Table 5: **Forward primers used for the cloning of the hyperthermophilic proteins**

DG209 MJ0609	5'-<u>ATA GAA AAG TAA CAA AAA GAA CAT TCT CCA ACA ATA TGT ATG TTA AAA GC</u> GAT TAT AAA GAT GAT GAT GAT AAA ACT GGT-3'
DG210 MJ0630	5'-<u>TAG CTC CAA TAA TAG CTT TAA TAA TTG GTT TTA TAA TAA ATA GGA TGA TA</u> GAT TAT AAA GAT GAT GAT GAT AAA ACT GGT-3'
DG211 MJ0672	5'-<u>TAT CAA TAC TAT CTG CAG CTG TAA TAA CTC TAT ATT CCA TTC TTT ATC TA</u> GAT TAT AAA GAT GAT GAT GAT AAA ACT GGT-3
DG212 MJ1319	5'-<u>CGT TTG TTG TAA GTG TAA TTC TTC AAA AAA TGA AAA CGA TTA AAG GTT GG</u> GAT TAT AAA GAT GAT GAT GAT AAA ACT GGT-3'
DG213 MJ1485	5'-<u>TTG TTT TAT TTG CTA CTT TGT ATT TTA AAA CTC TGA GAC TTT TAA AAA AA</u> GAT TAT AAA GAT GAT GAT GAT AAA ACT GGT-3'

Table 6: **Reverse primers used for the cloning of the hyperthermophilic proteins**

13. Methods

13.1. Molecular biology methods

13.1.1. Cloning method

13.1.1.1. Cloning of the G-Protein Coupled Receptor Ste2^{m}p

The procedure was carried out by Dr. Douglas Griffith (2001, Max-Planck-Institute of Biochemistry, Martinsried, Germany) with the following procedure:

The multicopy vector for the expression of functional C-terminally tagged Ste2p was constructed using a modified version of plasmid pYES260 (purchased from EUROSCARF, Frankfurt, Germany). Two sequences functioning as affinity tags, encoding a FLAG-tag (FT) and a His$_6$-tag (HT), were ligated into *Hind*III/*Not*I-digested pYES260. The 484-bp *Pst*I fragment containing the entire *URA3* selection gene promoter was removed. The *Xho*I site in the vector was then removed by *Xho*I digestion, T4 polymerase fill-in and religation which eventually led to the modified expression vector pYES-*ura3d*-FT-HT, into which the STE2 gene was cloned. The STE2 gene was amplified by polymerase chain reaction (PCR). All constructs were confirmed by dye terminator sequencing.

The STE2 gene was cloned into pYES2-FT.HT by *in vivo* homologous recombination in yeast. It was amplified by PCR from yeast genomic DNA (from strain S288C; Research Genetics, Huntsville, AL, USA) using a commercially available kit (High Fidelity PCR Master; Roche Applied Science, Mannheim, Germany) according to the manufacturer's instructions, and the primers:
5'-CTGTAATACGACTCACTATAGGGAATATTA<u>AAAAA</u>**ATG**TCTGATGCGGCTCCTTCAT-3' (forward) and 5'-ACCAGTTTTATCATCATCATCTTTATAATCTAAATTATTATTATCTTCAGTCCAG AACTTTCTG GC-3' (reverse).
These primers added 30-bps of sequence to the 5' and 3' ends of the gene that targeted it to the desired point of insertion in pYES2-FT.HT. The forward primer also introduced five A nucleotides (underlined) immediately preceding the gene's initiation codon (in bold) to provide an optimal nucleotide context for start codon recognition by yeast ribosomes. The reverse primer, lacking the gene's stop codon, directed the fusion of the STE2 sequence to that for the tags. pYES2-FT.HT was prepared for recombination-mediated cloning by digestion with *Sma*I. BJ5464 was then transformed to Ura$^+$ with 0.1 µg of *Sma*I-cut pYES2-FT.HT and 1 µg of the STE2 PCR product by electroporation using a Bio-Rad Gene-Pulser. This method results in > 98% of yeast transformants harbouring a vector with insert. Total yeast DNA was prepared from a pool of approximately 2000 Ura$^+$ transformants and used to transform *E.coli*.

Plasmids (pDG-STE2) were isolated from ampicillin-resistant colonies and the integrity of the expression cassette (*GAL1* promoter-STE2 gene-*CYC1* terminator) verified by sequencing.

Codon 269 of STE2 was AAA (Lys) and not GAA (Glu), potentially as a result of phylogenetic variation. The STE2 gene was cloned into the plasmid pYES2-*ura3d*-FT.HT in an identical manner to generate pDG-*ura3d*-STE2.

The Ste2p-N25/Q32-T326 sequence was constructed from two overlapping PCR products. A small portion of the 5' end of the *STE2* gene, whose entire length is 1.296 bps, was amplified from pDG-STE2 with the forward primer used to clone the wild type gene and 5'-GGTAGATCCCTGCCCATATATGGAAGTGTACTGAATGGTGCTTTGACCAGG-3' which straddled the two Asn codons (25 and 32) in the two utilised N-glycosylation sequences. The product had at its 5' end a sequence homologous to that at the desired point of insertion downstream of the *GAL1* promoter in the pYES2-FT.HT and pYES2-*ura3d*-FT.HT vectors. A portion of the 3' end of the gene, lacking 315 bps encoding the last 105 amino acids of the protein's C-terminus, was amplified with primers 5'-CCTGGTCAAAGCACCATTCAGTACACTTCCATATATGGGCAGGGATCTACC-3' and 5'-ACCAGTTTTATCATCATCATCTTTATAATCGCTAGACAGCGTGCCTGGATAAAAC-3'. This PCR product overlapped with the first at its 5' end and had at its 3' end 30 bps that allowed fusion to sequences encoding the tags in the vectors. Underlined in the primers are the mutated Asn codons which were originally AAC and AAT for Asn25 and Asn32, respectively, and were replaced by the Gln codon CAG. The expression vectors pDG-Ste2p-N25/Q32-T326 and pDG-*ura3d*-Ste2p-N25/Q32-T326 were assembled by cotransformation of BJ5464 with 1 µg each of the two PCR products and 0.1 µg of *SmaI*-digested pYES2-FT.HT and pYES2- *ura3d* -FT.HT, respectively.

The plasmid pMEGA2-ΔURA3 was generously provided by James Hopper (Pennsylvania State University, USA).

The BY4741bar1ΔSte2Δ strain was constructed by Dr. Douglas Griffith with the following procedure: The *STE2* gene in BY4741 *bar1Δ* was deleted by a PCR-mediated method. Primers to incorporate the genomic flanking sequences of the *STE2* gene (5'-ACTTAAAAATGCACCGTTAAGAACCATATCCAAGAATCAAAAATGCTGTGCGGTATTTCACACCGC-3' and 5'-CCGAAGGTCACGAAATTACTTTTTCAAAGCCGTAAATTTTGATCAGCGGCATCGAGCAGATTGTACTGAG–3'), were used to PCR amplify the *LEU2* selection marker from the pRS405 plasmid (ATCC, # 87516) with a commercially available kit (High Fidelity PCR Master; Roche Applied Science, Mannheim, Germany) according to the manufacturer's instructions. The PCR product was used to transform BY4741 *bar1Δ* to Leu⁺ by a high-efficiency lithium acetate method.

13.1.1.2. Hyperthermophilic transporters Aatp, Phopp, Dassp, Trkp and Nssp.

13.1.1.2.1. Construction of the original vector pITy-QC

The construction of the pITy-QC vector was performed by Dr. Douglas Griffith (2001, Max-Planck-Institute) with the following procedure:

Plasmid construction steps were performed using standard methods for recombinant DNA work (Sambrook, 1989) in *E.coli* strain DH5α and by recombination in BJ5464. A 50 µl aliquot of transformation competent BJ5464 cells was co-transformed with 0,1 µg of vector and ~ 1 µg of DNA fragments. Recombinant plasmids from yeast transformants were shuttled into *E.coli* as described previously by Hoffman and coworkers (Hofmann, 1993). A recombination competent version of pITy-3 (provided by Karl Wittrup, Massachusetts Institute of Technology, USA; (Parekh and Wittrup, 1997; Parekh *et al.*, 1996)) was constructed by introducing the 2µ sequence and promoterless *ura3d* marker from plasmid pYES2-*ura3d*-FT.HT, amplified by PCR as a single product containing flanking *XhoI* sites, at the unique *XhoI* site in pITy-3 (unique *XhoI* site of a fragment carrying the yeast 2µ replication origin). This fragment also contained a promoter-less *URA3* selection marker (*ura3d*). The portion of the pITy vector containing the multiple cloning site (MCS) between the end of the Neo^R gene and start of the δ sequence was then replaced with a sequence comprising the *GAL1* promoter and the tCYC1 terminator separated by a *SmaI* site and sequences encoding FLAG and His$_6$ affinity tags (pGAL1-SmaI-tCYC1). This was done by recombination between a PCR amplified pGAL1-SmaI-tCYC1 fragment from pYES2-*ura3d*-FT.HT and SphI/KpnI-digested vector. The PCR primers used added 30 bp homology arms to the 5' and 3' ends of the pGAL1-SmaI-tCYC1 product that targeted it to the desired point of insertion in the vector. The integrity of the pGAL1-SmaI-tCYC1 sequence was confirmed by dye-terminator sequencing.

Another dispensable sequence supF encoding a tRNA suppressor that can on multicopy expression inhibit *E.coli* cell growth was also deleted by recombination between BamHI/EcoRI-digested vector and a 50 bp double stranded DNA linker (formed from primers SupF-del-F and SupF-del-R) with homologies to the sequences flanking SupF. Deletion of this sequence removed one unwanted *SmaI* site. The last unwanted *SmaI* site in the vector, in the canamycin resistance (NEO) gene, was destroyed by a single silent mutation. Finally, using the QuickChange Site-Directed Mutagenesis Kit (Stratagene, La Jolla, CA, USA) and primers SmaI-del-F plus SmaI-del-R, the SmaI site within the coding sequence of the Neo^R gene was removed with a single base substitution causing a silent mutation in a glycine residue.

13.1.1.2.2. Linearisation of the plasmid pITy-QC

The linearisation of the pITy-QC vector was achieved with the restriction enzyme *SmaI* ,a blunt cutter. The reaction was carried out with buffers and enzymes purchased from New England Biolabs, Frankfurt am Main, Germany.

Reaction setup for 1 µg of pITy-QC vector, total volume 20 µl:

pITy-QC vector	3,6 µl (stock at 0,28µg/µl)
SmaI restriction enzyme	1 µl (stock at 20 u/µl))
NEB 4 buffer 10x	2 µl
H_2O	13,4 µl

The reaction was incubated at 25°C for 1h, following the digestion the enzyme was heat inactivated at 60°C for 20 minutes. One µl of the reaction was analyzed by agarose gel electrophoresis (0.7% agarose, 60 min at 60 V) to test for success and completeness of the reaction.

13.1.1.2.3. PCR of pITy-QC

The PCR was performed with the High Fidelity PCR Master from Roche Diagnostics GmbH, Penzberg, Germany. Fifty ng of template vector was used with oligonucleotides at a final concentration of 0,3 µM.

Reaction setup, total volume: 50 µl:

pITy-QC pector (linearized)	1 µl (50 ng)
Forward primer	2 µl (stock at 7,5 µM)
Reverse primer	2 µl (stock at 7,5 µM)
H_2O	20 µl
Roche Master Mix	25 µl

Cycling conditions

1. Initial denaturation	94 °C	3 min
2. denaturation	94 °C	30 sec
3. annealing	55°C	30 sec
4. elongation	68°C	4 min repeat 9 times from step 2
5. denaturation	94°CV	30 sec
6. annealing	55°C	30 sec
7. elongation/polymerisation	4 min + 5 sec/cycle	repeat 24 times from step 5
8. polishing	68°C	10 minutes
9. storage	4°C	∞

13.1.1.2.4.   PCR purification of pITy-QC

All solutions were from the PCR purification kit purchased from Qiagen, Hilden, Germany. The purification was performed with slight modifications of the supplied PCR purification protocol from Qiagen. Three 50 µl PCR mix were pooled and added to 5 volumes (750 µl) of binding buffer. A volume of 450 µl was placed onto a spin column and spun down once by a 30 seconds centrifugation at 14000 rpm, and after reloading with the remaining 450 µl, a second time for 60 seconds. A volume of 750 µl of wash buffer was then added and the suspension was centrifuged twice at 14000 rpm for 60 seconds, after having discarded the flow through from the first spin. Products were eluted by adding 53 µl of low salt elution buffer (EB, 10 mM Tris at pH 8,5) to the centre of the Qiagen column membrane, and let stand for 60 seconds, to be finally spun down for 60 seconds at 14000 rpm.

13.1.1.2.5.   Analysis and quantification of PCR products

The analysis and the quantification of the PCR products was performed by loading a 1 µl sample of the reaction (added to 4 µl of loading buffer (LB-XL composition)) onto a 0.7% agarose gel which was run for 90 minutes at 45 V. The standards used for the quantification were at the following concentrations: 200 ng/µl, 100 ng/µl, 50 ng/µl and 10 ng/µl. One µl of each standard was loaded onto the gel in order to densitometrically determine the dsDNA concentration of the sample.

13.1.1.2.6.   BJ5464 strain culture

Five ml of YPD medium were inoculated with 10 µl of a BJ5464 freezer stock, and cells were grown overnight at 30°C under agitation (220 rpm).

13.1.1.2.7.   Digestion of genomic DNA (gDNA)

Two µg of *M.jannaschii* genomic DNA was digested with restriction endonuclease to release the fragments bearing the genes of interest (*XmnI* for PHOP and DASS, *HindIII* for TRK and NSS) to be cloned into pITY-QC. Note: AAT was cloned from undigested genomic *M. jannaschii* DNA.

Reaction setup, final volume 50 µl:

M.jannaschii gDNA	10 µl (~2 µg)
BSA (100x)	0,5 µl
Restriction enzyme	5 µl (stock at 10 u/µl))
NEB 2 buffer 10x	5 µl
H_2O	29,5 µl

The suspension was incubated overnight at 37°C, the endonuclease was inactivated by a 20 minutes incubation at 60°C.

13.1.1.2.8. Transformation in BJ5464 yeast strains, plasmid construction via homologous recombination

Fifty ml of YPD were inoculated with overnight starter culture to give an intial OD_{600} of 0,2. The culture was then incubated at 30°C and agitated at 220 rpm for 3,5 h until an OD_{600} of around ~ 1 (anywhere between 0,8–1,2) was reached. Cells were then spun down for 5 min by a 4000 rpm centrifugation at room temperature. The supernatant was discarded and the pellet resuspended in 25 ml sterile H_2O. Cells were spun down again, the supernatant discarded, and the pelleted cells resuspended in 1 ml of 100 mM Lithium acetate (LiAc). Cells were spun down a third time by a brief 15 second centrifugation at 4000 rpm at RT, the pellet was finally resuspended in ~ 450 µl of 100 mM LiAc, to reach a final volume of 500 µl (allowing up to 10 transformations). The suspension was divided into 50 µl aliquots, these were again centrifuged for 15 seconds at 14000 rpm at RT. After removing of the supernatant from the transformation competent cells, a transformation mix was sequentially (see table: from top to bottom) added to the pellet.

Plates / Chemicals	protein	Empty	Trafo control
PEG 50% (w/v) (µl)	240	240	240
LiAc 1M (µl)	36	36	36
SSS-DNA (µl)	10	10	10
pITy-QC (at 25 ng / µl) (µl)	4	4	---
digested *M.jannaschii* genomic DNA (at 40 ng / µl) (µl)	25	---	---
pCD-P2 (µl)	---	---	1
H_2O (µl)	45	70	73
V_{total} (µl)	360	360	360

Table 7: **Composition of the transformation mix.** PEG: Polyethylene glycol, LiAc: Lithium acetate, SS-DNA: Salmon Sperm DNA, pCD-P2: transformation control plasmid

Cells were then vortexed until they were „more or less" resuspended, and incubated first 30 minutes at 30°C, then 60 minutes at 42°C. They were spun down for 15 seconds by a 7000 rpm centrifugation at RT. The transformation mix was discarded and the pelleted cells very carefully resuspended in 1 ml of YPD medium. The culture grew overnight at 30 °C and 220 rpm.

The transformed cells were then spun down and resuspended in 500 µl of sterile water. SCØUracil/ 2% Glucose plates were inoculated with 250 µl of culture and incubated at 30°C for 3 to 4 days until colonies appeared.

13.1.1.2.9. Colony plasmid rescue of the transformant BJ5464+pITy-QC into *E.coli*

One ml of sterile H_2O was added on plates to resuspend the cells. Cell suspension was then centrifuged 1 minute at 14000 rpm. Supernatants were discarded and the pelleted cells resuspended in 100 µl of buffer TSN-TE8 (Tris-HCl 50 mM/EDTA 50 mM pH 8). The suspension was then mixed with glass beads (1/3 of the volume) with an addition of 50 µl phenol and 50 µl chloroform. The mixture was vortexed for 10 minutes at 14000 rpm at 4°C, and finaly centrifuged for 5 minutes at 14000 rpm at RT. The 50 µl of the aqueous phase was collected.

13.1.1.2.10. Transformation of *E. coli* cells by electroporation

E.coli DH5α competent cells were transformed with the aqueous solution of the phenol/choroform extraction from the previously described colony plasmid rescue, to test if the recombination reaction was successful. From the 50 µl extract (DNA and plasmid), 5 µl were used (the resting 45 µl were stocked at –20°C) and added to 70 µl of competent DH5α cells. The mixture was transfered in a pre-chilled electroporation cuvette and cooled 10 minutes on ice. The electroporation was then performed in a BioRad Gene Pulser with one pulse, at 1.5 kV, 400 Ω, 25 µF. Then 0.5 ml of cold LB media were immediately added. Cells were carefully resuspended and incubated 45 minutes at 37°C, to allow regeneration of the cells, without selective pressure. Two LB/amp[100] plates were inoculated with the cell suspension (with selective pressure), each with 250 µl of cell suspension, and the plates were incubated overnight at 37°C, and let afterwards at 4°C until sufficient growth.

13.1.1.2.11. Colony PCR of plasmids rescue into *E.coli*, analyse on agarose gel

Since the yeast colony PCR appears to be neither very robust nor reliable, the plasmids from the yeast transformation/homologous recombination gap closure cloning (gapture) experiments were previously shuttled into *E.coli* DH5α.

Extensive screening is thought to facilitate the reliable detection of successfully gaptured plasmids. The number of insert positive clones might not reflect the true transformation efficiency in yeast. DG29 and DG30 oligonucleotides were used to help discrimination between parental plasmid or non-homologous end joined (NHEJ) plasmid.

Colony PCR reaction mix:

10 x Taq buffer	55 µl
DG 29 (stock 182.5 µl)	1.51 µl
DG 30 (stock 141.8 µM)	1.94 µl
dNTPs (stock 4 mM)	27.5 µl
Taq. pol. (5.5 U / µl)	11 µl
H$_2$O	343.1 µl
Loading buffer	110 µl

Each reaction has a 10 µl final volume, colonies were picked with sterile toothpicks, restreaked onto LB/kan[100] and subsequently rolled in the reaction mix.

Name	Sequence	bps	Tm
DG29	5'- GGG TAA TTA ATC AGC GAA GCG –3'	21	~ 61
DG30	5'-GCG TGA ATG TAA GCG TGA CA –3'	20	~ 61

Table 8: **Primers used for the colony PCR**

PCR cycling conditions

1.melting	96°C	120"	
2.melting	96°C	30"	
3.annealing	55°C	30"	
4.elongation	72°C	150"	repeat 39 x from 2.
5.polishing	72°C	600"	
6.storage	4°C	∞	

The entire reaction mix was loaded onto a 7% agarose gel, the migration was performed for 1h at 60V.

13.1.1.2.12. Culture of positive clones

After identifying positive clones from the colony PCR, the restreaked colonies were used to inoculate 6 ml of LB/kan[100] medium. The cultures grew overnight at 37°C / 200 rpm.

13.1.1.2.13. Mini-preparation of *E.coli* and sequencing for verification

Minipreps were prepared from each culture (4,5 ml) according to the protocol of Qiagen. A volume of 1,5 ml was kept for freezer stocks (925 µl culture + 75 µl DMSO).

To further verify the proper insertion of the genes, sequencing was performed. To verify that the gene of interest was captured during homologous recombination, the appropriate PCR primers (DG29 and DG30) were used, further to verify the homologous recombination junctions (HR junctions), the promoter and the terminator (the primers will read into the genes from outside the promoter and terminator respectively).

Reaction setup:

Primer dilutions at 3,2 pmol/µl , 50 µl (3,2 µM)

	1 rxn	42 rxn
Big DyeV3.1:	2 µl	84 µl
5M betaine:	2 µl	84 µl
Seq. Buffer (2.5x)	2 µl	84 µl
H_2O:	2 µl	84 µl

Eight µl were dispensed into each PCR tube, then mixed with 1 µl of oligonucleotide and 3 µl of plasmid (~ 500 ng).

cycle sequencing conditions:

1. denaturation:	95°C	3'	
2. denaturation:	95°C	30"	
3. annealing:	55°C	30"	
4. elongation:	60°C	4'	repeat 50 x from step 2
5. storage:	4°C	∞	

13.1.1.2.14. Purification of sequencing products

Ten µl of sterile H_20 were added to the 10 µl of the cycle sequencing reaction. Nucleotide and enzyme removal was done with Autoseq G-50 micro-spin columns (Amersham Biosciences, Freiburg, Germany) The columns were vortexed to mix the gel-matrix, and centrifuged for 1 minute at 2000 g. The 20 µl volume was then placed on the top of the column, without disturbing the matrix. The column was centrifuged again, and the supernatant discarded. Samples were dried in a speed vac for 20 min and then sent to the in-house sequencing service.

The yeast cells were afterwards retransformed with positive plasmids (whose the sequence was confirmed).

13.1.2. Turbidity measurements

An Ultrospec 200A Spectrophotometer (Amersham Biosciences, Freiburg) was used to determine the culture turbidity at a wavelength of 600 nm. In general the samples were diluted with a 1:40 ratio in H_2O and measured in a disposable plastic cuvette with 10 mm pathlength, the blank was H_2O.

13.1.3. Agarose gel

We routinely used TAE electrophoresis buffer, whose composition is described below:

Buffer Tris-Acetate (TAE)

Working solution1x :	Tris-Acetate	0,04 M
	EDTA	0,001 M

Concentrated Stock (per Litre) 50x:	Tris base	242 g
	glacial acetic acid	57,1 ml
	EDTA (pH 8.0)	100 ml 0,5 M

For a 1% gel in the small mold (10 x 7 cm), 3 g Agarose (Sigma-Aldrich, Munich, Germany) were mixed to 300 ml of 1xTAE to it. Agarose boiled in microwave, until being completely dissolved. It was then cooled down on the bench for a few minutes. From this molten agarose, 40 ml were transferred to a 50 ml centrifuge tube and ethidium bromide was added to a final concentration of 0,5 µg/ml. The mixture was then poured into the small mold and left to set for 15 minutes. The gels were run routinely for 1h at 60 V.

Preparation of the samples:

Glycerol 87%	5.8 ml
H_2O	3.8 ml
Bromophenol Blue	100 µl (saturated solution in water)
Xylencyanol	100 µl (saturated solution in water)
1 M Tris-HCl,pH 7.5	200 µl (20 mM final)

13.1.4. Pheromone halo-assay for growth arrest in *S.cerevisiae*

The response of yeast cells expressing the mutant Ste2^{m}p to α-factor was analysed by halo-assay. This method was compiled from a number of different sources: Dohlman Lab protocols (http://www.med.unc.edu/~hdohlman/haloassay.html); (Liu *et al.*, 2000; Abel *et al.*, 1998a; Abel *et al.*, 1998b; Raths *et al.*, 1988)

This method requires to use sterile techniques and sterile solutions throughout.

Four starter culture of different yeast strains were grown at 30°C and 150-250 rpm until saturation. Saturation is important because cell density can affect the size of the halos. Sterilised solution of 2% Noble agar (containing 2% glucose, rich medium YPD or appropriate selective medium Sc) was microwaved until melted and placed in a 55°C to 60°C water bath.

Four paper disks (Difco) were distributed into a sterile petri dish, and spotted each with 5 to 15 µl of α-factor (from 1 to 5 mg/ml), corresponding to 0,1 µg, 0,5 µg, 1 µg and 10 µg of α-factor respectively. Immediately before performing the assay, a small volume of the four different saturated starter cultures was transferred into a 15 ml sterile centrifuge tube containing 2,4 ml of sterile water, 200 µl of culture from selective medium and 20 µl from rich medium (~ 1x10^6 cells). To this suspension, 1,6 ml of the 2% agar solution were added, the tube was inverted a few times and poured onto a pre-warmed plate containing the appropriate solid media, evenly covering the plate by swirling. The disks impregnated with α-factor were then placed on the plate. The plates were then let at 30°C until a lawn of cells appeared, halos are usually clearly visible after 24h for most strains. Differences in halo size are normally detected by eye.

Fours plates were tested, they were inoculated with different ste2p complemented BY4741Δste2p strains. The ste2p constructs used for complementation were the wild type Ste2p, the FLAG- and His$_6$-tag Ste2p^{FT-HT}, and the mutated and tagged Ste2p$^{N25,32Q-T326FT.HT}$. An untransformed strain ΔSte2p was used as negative control.

13.2. Yeast culture and overexpression

13.2.1. Culture media for *S.cerevisiae*

Two different media were used: a selective medium and a complete rich medium, whose composition is described below:

Selective complete medium for the culture of yeast cells expressing Ste2^{m}p, lacking Uracil and Leucine: Sc ØUra Øleu

	For 1 litre
Yeast Nitrogen Base Ø amino-acids	6,7 g
Drop-out supplement medium	1,4 g
Tryptophan	76 mg
Histidin	76 mg
Glucose	40 g
0,5 M sodium phosphate buffer, pH 6,0	100 ml

Selective complete medium for the culture of yeast cells expressing Aatp, lacking Uracil: Sc ØUra

	For 1 litre
Yeast Nitrogen Base Ø amino-acids	6,7 g
supplement medium Øuracil	1,92 g
Tryptophan	76 mg
Raffinose	40 g
0,5 M sodium phosphate buffer, pH 6,0	100 ml

Complete rich medium YPD (or YEPD – yeast extract peptone dextrose)

	For 1 Litre:
Yeast extract	10 g (1%)
Bacto-peptone	20 g (2%)
Dextrose	20 g (2%)

13.2.2. Culture conditions for the growth of yeast cells and protein expression

Precultures were carried out by inoculation of 10 ml of growth medium (selective or rich) with 100 µl of yeast transformant. Cells grew in preculture at 30°C for 48h until OD_{600} 8 to 9 was reached, cultures were then diluted at 0,06 OD_{600} units in 1,5 litre of the same growth medium supplemented with 2% glucose or 4% raffinose. Yeast cells grew under constant agitation (130 rpm) at 30°C for 24h until the desired OD_{600} was reached (1 to 2, 4 to 5, 6, 7, 9 or 11 to 12 the stationary phase). Expression of the protein of interest was induced at different points in time by addition of 2% galactose to the medium. In the case of the complete medium, as glucose inhibits the *GAL1*-promoter, glucose had to be removed from the medium before the addition of galactose. We therefore spun down the cells for 7 minutes at 5000xg, washed the pellet with sterile water, spun down the cells again, and repeated the protocol 3 times, and finally resuspended the pelleted cells in the induction medium. The induction was carried out for different intervals (4h, 5h, 8h or 12h). After the specified interval cells were finally harvested by centrifugation for 10 minutes at 5000xg at 4°C. The pelleted cells were washed one time with one volume of ice-cold sterile water, collected, frozen quickly in liquid nitrogen and stored at – 80°C.

For all different growth conditions, aliquots of cells were collected, and total yeast membranes were isolated and analysed.

13.3. Biochemical methods

13.3.1. Isolation of yeast total membranes

Buffers used:

Homogenisation buffer:

50 mM Tris-HCl pH7,5
1 mM EDTA
1 mM β-mercaptoethanole
10% (w/v) glycerol

Solubilisation buffer:

50 mM Tris-HCl pH7,5
400 mM NaCl
1 mM β-mercaptoethanole
20% (w/v) glycerol)

All manipulations were performed at 4°C, and all buffers contained the following protease inhibitors at these final concentrations: 1 μg/ml leupeptin, 17,4 μg/ml phenylmethylsulfonylfluoride and 1 μg/ml pepstatin A.

Cell pellets were thawed and resuspended in a ratio of 0,25 to 0,5 g (wet weight) per ml of ice-cold homogenisation buffer. Cells were then broken in a homogeniser, kept cool at 4°C (bead-beater, purchased from Roth Diagnostics GmbH), by vortexing with glass beads (Ø425-600 μm, Sigma Aldrich), in the proportion of 2,5 g of glass beads per ml of cell suspension. Glass beads were then sedimented by placing the homogeniser on ice, and the supernatant transferred to a fresh pre-cooled centrifuge tube. Glass beads were washed twice in 5 ml of ice-cold homogenisation buffer / grams of cells. Samples were then centrifuged at 1600xg for 5 minutes to pellet unbroken cells and cell debris. Supernatants were centrifuged at 200 000xg (Beckman Type 45 Ti or 60 Ti rotors) for 1h to sediment total membranes. The pellet consisting of sedimented crude membranes was resuspended in 1 volume of solubilisation buffer, in which the 400 mM NaCl permitted to strip peripheral membrane proteins.

Membranes were then harvested for 1h by a 200 000xg centrifugation. The final pellet containing the crude stripped total membranes was resuspended in solubilisation buffer, and divided in 2 ml aliquots. An estimation of the concentration was made by micro-BCA assay in the presence of 0,5% SDS using bovine serum albumin as standard. Aliquots were quickly frozen in liquid nitrogen and stored at – 80°C.

13.3.2. Quantification by micro-BCA assay

Protein concentration was determined by quantitative calorimetric determination of proteins in dilute aqueous solutions. We used the *Micro-BCA^{TM} Protein-assay* Reagent Kit purchased from Pierce (Perbio Science Deutschland GmbH), and followed the protocol implemented by Pierce, without modifications. The reagent utilises bicinchoninic acid (BCA) as the detection reagent for Cu^+, which is formed when Cu^{2+} is reduced by protein in an alkaline environment. The purple-coloured reaction product is formed by the chelation of two molecules of BCA with one cuprous ion (Cu^+). This water-soluble complex product exhibits a strong absorbance at 562 nm that is linear with increasing protein concentrations.

13.3.3. Gel electrophoresis: denaturing SDS-PAGE (Tris-Tricine "Schägger" Gels)

The separation of denaturated proteins with sodium dodecyl sulfate (SDS) was performed using the protocol as described by Schägger, H., and von Jagow, G. (Schägger, 1987). For separation of proteins in the desired range a 8% SDS-polyacrylamide gel was used.

The acrylamide stock solution was Protogel (mixture 30% Acrylamide, 0,8% Bisacrylamide) purchased from National Diagnostics (Medco Diagnostika GmbH, München, Germany).

The ammonium persulfate (APS) solution and the N,N,N´,N´,-Tetramethylethylendiamin (TEMED) catalysing the polymerisation reaction were purchased from Sigma (Munich, Germany).

Stock solutions were prepared as described in Table 9 and Table 10.

Chemicals / Buffers	Tris-HCl	SDS (w/v)	Tricine (w/v)	Glycerol (v/v)	Bromophenol blue (w/v) (Serva-blue G)	β-mercapto ethanol (v/v)	Dithiothreitol (w/v)
Anode-buffer pH 8,9	25 mM	--	--	--	--	--	--
Cathode-buffer pH 8,25	10 mM	0,01%	10 mM	--	--	--	--
Gel buffer pH 8,45	3 M	0,3%	--	--	--	--	--
Loading-buffer 6X, pH 6,8	350 mM	10%	--	30%	0,1%	12%	9,3%
TCA resuspension buffer, pH 11	100 mM	3%	--	--	--	--	3 mM

Table 9: **Composition of the buffers for Tris-Tricine SDS-PAGE**

	Separating gel	Stacking gel
Protogel	1,13 ml	0,23 ml
Gel buffer	1,34 ml	0,44 ml
Glycerol 87%	0,4 ml	--
ddH$_2$O	1,32 ml	1,12 ml
APS 10% (w/v)	28,3 µl	12 µl
TEMED	5,8 µl	2,8 µl
Final volume	4,3 ml	1,8 ml

Table 10: **Composition of stacking, and separating solutions for one Shägger gel (8%).**

All solutions were mixed in screw-capped centrifuge tubes with very gentle rocking. For solutions containing glycerol, glycerol was mixed with the gel buffer and water before addition of the acrylamide stock solution.

The separation gel polymerised for 30 minutes in the electrophoresis apparatus, with a layer of isopropanol overlaid, to fasten the polymerisation by avoiding contact with oxygen.

Then, after having rinsed with sterile H$_2$0, the stacking gel was poured and polymerised for 45 minutes. After loading of the samples on the polymerised gels, they migrated at 100 mV for around 1h30.

For sample preparation, we mixed the 6X loading buffer at a ratio sample/buffer 3/1 to maintain an excess of SDS. The samples were heated immediately after adding sample buffer for 10 min at 37°C, subsequently insoluble material was removed by centrifugation (17 000xg for 2 min) and the samples were then loaded immediately.

13.3.4. TCA precipitation

Protein precipitation is used to concentrate samples for gel analysis in a polyacrylamid-gel or to remove detergent, that can have negative influence on the migration of the protein in the SDS-PAGE.

To the sample of protein solution, an equal volume of 20% trichloroacetic acid (TCA) was added, to get a 10% final concentration. It was mixed and kept for 15 min at –20ºC and then for 15 min at 4ºC. The sample was then spun down 15 min at 14000 rpm and 4ºC. The supernatant was carefully discharged, the pellet retained and dried by inversion on tissue paper. For SDS-PAGE, the sample was resuspended in a minimal volume of TCA resuspension buffer (Table 9) and when in solution, with 6X loading buffer (Table 9). The presence of some TCA can give a yellow colour as a consequence of the acidification of the sample buffer. In this case we titrated with 1 N NaOH or 1 M TrisHCl pH 8.5 until obtaining the sample at an alkaline pH indicated by a blue colour of the sample buffer.

13.3.5. Deglycosylation

To check for glycosylation of the protein, a deglycosylation attempt was performed with the enzyme PNGase F ("N-Glycosidase F", New Englands Biolabs, Frankfurt am Main, Germany). PNGase F is an amidase from *Flavobacterium meningosepticum (purcahsed from ,* that hydrolyse the N-Glycan of a glycoprotein. The experiment was performed with 20 µg of YpMEGA/T326-*ura3d* membranes. Membranes (8,7 µl) were mixed with 1 µl of 10x denaturing buffer (0,5% SDS, 1% β-mercaptoethanol) and 0,3 µl H_2O, and incubated 10 minutes at 37°C. Then 1 µl of NP-40 (detergent Nonident P-40), 1 µl of G7 buffer (0,5 M sodium Phosphate, pH 7,5) and ± 1 µl PNGase F enzyme were added and the reaction was carried out for 1h at 37°C. A positive control was performed with bovine fetuin (purchased from Sigma) to check if the enzyme was active.

13.3.6. Concentration of the purification samples

To concentrate the samples, we used the filter unit centricon YM-50 (Millipore, Schwalbach, Germany). Centricon tubes were centrifuged at the recommended speed (1500 rpm) repeatedly for 5 to 10 minutes until the desired volume or concentration was reached. This was depending on the quantity of proteins and the intial sample volume.

13.3.7. Staining of proteins in gels

13.3.7.1. Coomassie-blue staining, modified (Weber, K. and Osborn, M., 1969)

The following solutions were used for the staining (Table 11).

Chemicals Buffers	Serva-blue G-250 (w/v)	Acetic acid (v/v)	Ethanol (v/v)	Glycerol (v/v)
Staining	0,25%	10%	5%	--
Destaining	--	10%	40%	--
Drying	--	--	10%	5%

Table 11: **Composition of the buffers for Coomassie-blue staining**

13.3.7.2. Silver-staining

The following solution were used for the staining (Table 12). The same drying protocol as for the Coomassie-blue staining was followed.

	Solutions	Incubation time
Fixation	40% ethanol, 10% acetic acid	30 min
Sensitising	30% ethanol 0,5% (v/v) glutaraldehyde 0,2% (w/v) $Na_2S_2O_3$ 0,5 M sodium acetate	30 min
Wash	H_2O	3 x 5 min
Staining	15 mM silver nitrate 0,04% (v/v) formaldehyde	20 min
Wash	H_2O	2 x 1 min
Developing	0,236 M sodium carbonate 0,02% (v/v) formaldehyde	2 to 30 min
Stop	36 mM Na_2 EDTA x 2 H_2O	10 min
Wash	H_2O	3 x 5 min
Conservation	10% ethanol, 5% glycerol	30 min

Table 12: **Composition of the buffers for silver-staining**

13.3.8. Immuno-blot analyse

As stock buffer, we used a 10X PBS (0,58 M Na_2HPO_4, 0,17 M NaH_2PO_4, 0,68 M NaCl).

The blocking reagent is the I-Block[TM] purchased from Perbio Science Deutschland GmbH.

Chemicals / Buffers	PBS	Tween-20	Blocking reagent
Blocking	1X	0,1%	0,2%
wash	1X	0,1%	--

Table 13: **Composition of the buffers for Western-blotting or dot-blotting**

13.3.8.1. Western-Blot analysis

Proteins were transferred from gel onto nitrocellulose membrane (ProtranBA 83, Schleicher & Schuell, Dassel)in a blotting tank apparatus for 1h at 100 V. A Towbin-buffer (25 mM Tris, 192 mM glycine, 0,1% SDS, 40% methanol, pH8,2-8,4) was used to pretreat the membrane, the gel and the filter paper. (Whatman, Maldstone, GB) After the transfer, the membrane was briefly rinsed with PBS 1X, and afterwards incubated in Blocking-buffer.

13.3.8.1.1. Dot-Blot analyse

A PVDF membrane (Westran®S PVDF-Membrane, Schleicher & Schuell, Dassel), pretreated with methanol, was placed onto the Dot-Blot apparatus. The samples were pipetted on the membrane. When dry, the membrane was incubated in Blocking-buffer, and the usual detection procedure was then followed.

13.3.8.1.2. Detection procedure

The membrane was incubated in 10 ml of Blocking-buffer for 45 minutes to 1h. It was afterwards incubated for 45 minutes with the primary antibody (anti-penta-His antibody, Qiagen), diluted (1:5000) in 10 ml Blocking-buffer. Two washes of 5 minutes (20 ml each wash) were then performed with the wash-buffer. The membrane was then incubated for 45 minutes with the secondary antibody (Goat anti-mouse, IGG, Qiagen), diluted in 10 ml Blocking-buffer (1:20000), to be washed afterwards three times 5 minutes in 20 ml wash buffer. Membranes were then drained before being overlaid for 5 minutes by the substrate solution (1 ml for a 6x9 cm membrane). The substrate solution used to elicit the signal by chemiluminescence was a mix Luminol/Enhancer Solution at a ratio 1/1 (supersignal West Pico chemiluminescent Substrate, Perbio Science Deutschland GmbH, Bonn, Germany). To verify the efficiency of the transfer, the polyacrylamide gel was collected after the transfer and Coomassie-blue stained to verify the absence of proteins. The membrane was then placed under a plastic transparent slide in a dark room, a film was placed on top for various times (12 seconds to 4 minutes), and the photographic film (Kodak X-OMAT-AR, Kodak AG) was processed in a automated developer (Kodak X-OMAT 1000 processor).

After scanning of the gel or the film, densitometric analysis of all gels and immuno-blots were performed with the PC-software "Scion image" (Scion corporation, Maryland, USA, release Beta 4.0.2). The distribution of the signal intensity was determined with the help of the pixel evaluation algorithm and the peak surface was calculated by surface integration.

13.4. Solubilisation

All finally chosen manipulations were performed at 4°C unless stated otherwise, and all buffers contained a protease inhibitor cocktail at final concentrations of 1 µg/ml leupeptin, 17,4 µg/ml phenylmethylsulfonylfluoride and 1 µg/ml pepstatin A.

The pellet of crude total membranes was incubated within the following different detergents:

Dodecylmaltoside (DDM)
N,N-Dimethyldodecylamine-N-oxide (LDAO)
Polyoxyethylene-9-laurylether ($C_{12}E_9$)
Triton X-100 (TX100)
N-Octyl-β-D-Glucopyranoside (OG)
N-Nonyl-β-D-Glucopyranoside (NG)
N-Dodecyl-phosphocholine (FOS12)

The incubation was carried out in solubilisation buffer, with or without 5 mM imidazole, under gentle rotation for different times (30 minutes and longer) at 4°C or RT, at a total membrane protein concentration of 5 mg/ml, with detergent at a ratio protein/detergent of 1/4, 1/2, 1/4 or 1/6 (w/w). The suspension was centrifuged at 200 000xg for 1h and 4°C to remove unsolubilised material.

A presolubilisation was performed in the case of Ste2^{m}p under the conditions previously defined (30 minutes, 4°C, ratio 1/4), chosing a detergent solubilising a high amount of total membrane proteins other than Ste2^{m}p. After the ultra-centrifugation, the pellet was incubated with detergent solubilising low amount of total membrane proteins and high amount of Ste2^{m}p. After the second ultracentrifugation, the pellets and supernatants were analysed.

13.5. Purification

13.5.1. Ste2^{m}p purification

13.5.1.1. Affinity chromotography

13.5.1.1.1. Ni^{2+}-NTA chromatography

Ni^{2+}-NTA beads (Amersham Pharmacia) were prepared by three wash steps in sterile H$_2$0, then pre-equilibrated with three wash steps with solubilisation buffer containing a concentration of DDM slightly above the CMC (0,2%).

After the solubilisation and the last centrifugation, the supernatant containing the solubilised material was incubated with a gentle rotation at 4°C overnight with the prepared Ni^{2+}-NTA beads (ratio: 100 mg of total membrane protein with 1 ml of beads). Ni^{2+}-NTA beads were loaded onto a column, and the flow through collected. Beads were washed with wash buffer, that was collected for analysis. After the washing-step, proteins were eluted with elution buffer.

Different chromatography parameters were checked for optimisation of the purification (binding to the beads, purity and homogeneity): the beads volume, the concentration of β-mercaptoethanol, the EDTA concentration, and the effect of urea. These trials were done on small scale, in a final volume of 2 ml, after a solubilisation from 10 mg of total protein within DDM.

The effect of the beads volume was tested by using volumes of 10 μl, 25 μl or 50 μl of beads.

We also tried various concentrations of β-mercaptoethanol ranging from 20 mM up to 0,75 mM EDTA.

To avoid aggregation of the protein, we checked the effect of urea by adding 8 M urea in the sample and in the separating gel.

All samples were analysed by immunoblotting.

13.5.1.1.2. Other metal-NTA chromatographies

Metal-affinity chromatography also was performed with other metal-ions: Copper (Cu^{2+}-NTA), Cobalt (Co^{2+}-NTA) or Zinc (Zn$^+$-NTA). We used the same purification conditions for these matrices as for the Ni^{2+}-NTA purification.

13.5.1.1.3. FLAG-affinity chromatography

FLAG agarose was prepared in batch: 1 ml of resin (Sigma Aldrich) was washed 3 times in 0,1 M glycine-HCl pH 3,5 by centrifugation (4 minutes at 1000xg). The resin was then resuspended in 7 ml of 50 mM Tris-HCl pH 7,5, 400 mM NaCl, 20% glycerol and 20 mM imidazole. Beads were afterwards pelleted and resuspended in 12 ml of the same buffer and pooled with the eluate from the affinity purification. The incubation was carried out overnight at 4°C with rotation.

After the resin was packed, the flow through was collected, and the resin washed with the same buffer but supplemented with 125 mM imidazole, and the protein eluted with this buffer supplemented with 100 µg/ml of FLAG peptide (Sigma Aldrich). The column was stripped with 3 ml of 0,1 M glycine-HCl pH 3,5.

13.5.1.2. Anion-exchange chromatography

As Ste2^{m}p has a pI of 8,93, we chose an anion-exchange chromatography. The eluates from the first purification were loaded onto a sepharose cation-exchange resin (CM Sepharose^{TM} fast flow, Amersham Biosciences). The same protocol as for the affinity-chromatography was applied.

In a batch procedure, 100 mg of total membranes were solubilised with 2% DDM. Then, a Ni^{2+}-NTA purification was performed and the eluate was concentrated to 3,5 ml. The concentrate was divided in 5 samples of 700 µl each (theoretically containing solubilised Ste2^{m}p from 20 mg of total membranes) which were again concentrated in order to resuspend the samples in a final volume of 500 µl of the desired buffers: 20 mM phosphate buffer pH6,5, 20 mM phosphate buffer pH7, 20 mM HEPES buffer pH7,5, 20 mM HEPES buffer pH8, or 20 mM bicine buffer pH8,5. All buffers contained 20 mM NaCl. Each sample was incubated with 20 µl of resin for 10 minutes. The suspensions were then gently centrifuged to pellet the resin. The supernatants were collected and analysed on a Western-blot. The comparison of the amount of Ste2^{m}p in the supernatants to the one in the Ni^{2+}-NTA eluate allowed an evaluation of the binding quality. The same procedure was performed by testing 100 µl resin.

To test the effect of the NaCl concentration, a Ni^{2+}-NTA purification was performed after a solubilisation of 200 mg of total membranes with 2% DDM,. We exchanged the buffer of the final eluate to 20 mM HEPES buffer pH 7,5 (containing 20 mM NaCl), before concentrating it to 4,5 ml. These 4,5 ml were then divided in 9 samples of 500 µl each (containing theoritically solubilised Ste2^{m}p from ~20 mg of total membranes). Each sample was concentrated and resuspended in 500 µl of the same buffer, but containing in addition different NaCl concentrations (50, 100, 150, 200, 250, 300, 350, 400, or 450 mM). All samples were then incubated 10 minutes in the 100 µl of resin volume. After the incubation, the suspensions were then gently centrifuged to pellet the resin, the supernatants were collected and analysed on a Western-blot. The comparison of the amount of Ste2^{m}p in the supernatants to the one in the Ni^{2+}-NTA eluate allowed an evaluation of the NaCl concentration suitable for the protein elution.

13.5.1.3. Size-exclusion chromatography (gel-filtration)

Eluates from the metal-affinity chromatography, concentrated and filtered, were analysed on a sephadex S200 column (pharmacia biotech), in Tris-HCl buffer pH 7,5. The flow was 40 µl/min. The loaded samples had a volume of 50 µl. Fractions of 80 µl were collected, and analysed on Coomassie-blue stained SDS gel and immunoblot. Fractions corresponding to a peak observed on the chromatogram were pooled and concentrated.

13.5.1.4. Final buffers used for the different chromatographies

Chromatography	Resin	Steps	Column Volumes (CV)	Chemicals					pH
				Tris (mM)	HEPES (mM)	NaCl (mM)	Glycerol (%)	Imidazole (mM)	
Ni^{2+}-affinity	Ni^{2+}-NTA	wash	20	50	--	400	20	50	7,5
		elution	15	20	--	150	20	500	7,5
Other metal ions-affinity	Cu^{2+}, Co^{2+}, Zn^+- NTA	wash	30	50	--	400	20	0	7,5
		elution	15	20	--	150	5	500	7,5
Flag-affinity	Flag-agarose	wash	20	50	--	400	20	125	7,5
		elution	8	50	--	400	20	125	7,5
ion-exchange	Cation	wash	15	--	20	150	5	100	7,5
		elution	10	--	20	300	5	100	7,5
Size-exclusion	Sephadex	wash	2	50	--	300	10	100	7,5

Table 14: **Summary of the different finaly chosen buffers used for the different chromatographies for Ste2^{m}p**

All buffers contained 1 mM β-mercaptethanol and 500 mM α-factor.

Chromatography	Resin	Optimised parameters					
		Resin volume	pH	β-mercapto-ethanol	EDTA	NaCl	Urea
Metal-affinity	Ni^{2+}-NTA	X	--	X	X	X	X
ion-exchange	Cation	X	X	--	--	X	--

Table 15: **Optimised parameters for each chromatography**

13.5.2. Aatp purification

13.5.2.1. Heat treatment

Solubilisation was performed with each detergent, and the soluble fractions containing solubilised Aatp were submitted to heat treatment at different temperatures (65, 80 or 95°C) for 5 minutes or at 90°C for different times (5, 10 and 15 minutes), then cooled on ice for 10 minutes and centrifuged afterwards at 200 000xg for 1h at 4°C. Pellets were discarded, supernatants analysed on silver-stained SDS gel and immunoblot.

In the case of the solubilisation within DM and DDM, a time-course of the stability of Aatp after heat treatment for different times was performed. Aatp was solubilised in the presence of DM or DDM and the solubilised samples were incubated at 90°C for different times: 1, 3, 5, 7 or 10 minutes.

13.5.2.2. Metal-affinity chromatography with Ni^{2+}- NTA beads, and heat treatment.

Ni^{2+}-NTA beads were prepared by three wash steps in sterile H_2O, then pre-equilibrated with three wash steps with solubilisation buffer containing a concentration of DDM slightly above the CMC (0,2%).

This step was performed after a solubilisation of 100 mg of proteins in the presence of DDM. The supernatant containing the solubilised protein was incubated overnight at 4°C with 1 ml of Ni^{2+}-NTA beads. The beads were then packed in a column, the flow-through was collected.

Beads were then washed with the wash buffer which was collected for analysis. After the washing-step, proteins were eluted with the elution buffer.

13.5.2.3. Size-exclusion chromatography.

Eluates from the metal-affinity chromatography, concentrated and filtered, were analysed on a sephadex S200 column (Sephadex, Amersham Biosciences). The Na_2HPO_4 buffer was exchanged during this step into Tris-HCl buffer. The flow was 40 µl/min. The samples had a volume of 50 µl. Fractions of 80 µl were collected. The analysis of all samples on a Coomassie-stained SDS gel and immunoblot permitted to correlate the peak observed on the chromatogram with the presence of a band which migrated on the supposed size and corresponding to Aatp. The purest fractions were pooled and concentrated, and analysed by Mass-Spectrometry. The final buffers used for the different chromatographies are presented Table 16.

Chromatography	Steps	Column Volumes (CV)	Chemicals					pH
			Tris (mM)	NaH_2PO_4 (mM)	NaCl (mM)	Glycerol (%)	Imidazole (mM)	
Ni^{2+}-affinity	wash	4	--	50	400	20	10	8
	elution	16	--	50	400	20	500	8
Size-exclusion chromatography	elution		50	--	400	20	500	7,5

Table 16: **Composition of the final buffers for the chromatographies for Aatp**

13.6. Radioactive assays

13.6.1. Media and solutions for radioactive assays

YM1 medium

	Per 1 litre	
Yeast Extract	5	g
Bacto-peptone	10	g
Yeast Nitrogen Base w/o amino acids	6,7	g
Succinic acid	10	g
Sodium hydroxide	6	g
Glucose	10	g

Sodium Azide: NaN_3 (10 mM final concentration)

Solubility in H_2O is 41.7% at $17^{o}C$ (Merck index) i.e. > 1 M

Potassium Fluoride dihydrate: KF (10 mM final concentration)

Solubility in H_2O is 349.3 g/100 ml at $18^{o}C$ (Merck index) i.e. > 1 M

***p*-tosyl-L-arginine methyl ester**: TAME (10 mM final concentration)

Solubility in H_2O is > 100 mM

YM1+i medium

The required amounts of NaN_3, KF and are weighted and dissolved directly in the appropriate volume of YM1 buffer. NaN_3 and KF are poisons of both oxidative and glycolytic energy metabolism that prevent cell growth and inhibit energy-dependent processes such as endocytosis that may affect binding, TAME inhibits proteolysis of α-factor

Polyethyleneimine (PEI)

PEI coats filters with a negative charge, which encourages the binding of proteins. It is used to help trap solubilised receptors and receptor containing membranes on the filter when separating the bound from unbound radioligand. We used GF/F filters (25 mm, Whatman, VWR international GmbH) instead of usual GF/B filters as some solubilised receptors have been reported to pass through GF/B filters.

α-factors

[^{3}H] α-factor (m.w. 1670)

Trp-His-Trp-Leu-Gln-Leu-Lys-Pro-Gly-Gln-Pro-Met-Tyr.

1 mCi/ml; 56Ci/mmol $\Rightarrow$ 1 µCi = 17.86 pmol = 17.86 µM

$\Rightarrow$ 2.2 x 10^6 dpm = 17.86 pmol

$\Rightarrow$ 123180 dpm = 1 pmol

[L-Ala^9]α-factor and [D-Ala^9]α-factor

Trp-His-Trp-Leu-Gln-Leu-Lys-Pro-<u>Ala</u>-Gln-Pro-Met-Tyr.

The mutated codon Ala^9 is underlined (peptide synthetised by the peptide synthese service of the Max-Planck-Institute of Biochemistry)

13.6.2. Quantitation of α-factor receptor expression levels in yeast total membranes

Both media YM1+i (wash buffer) and 0,3% PEI were cooled to 4°C. At least half an hour before use, GF/F filters were soaked in ice-cold 0,3% (v/v) PEI (in YM1+i) at 4°C.

The following labeling buffers were prepared in minisorp tubes (that have low protein binding): YM1+i with 300 nM final of [^{3}H]α-factor, and YM1+i with the same concentration of [^{3}H]α-factor and 300 µM final of non-radioactive α-factor (100xK$_D$ or 100xhighest concentration, which ever is greatest) to determine non-specific binding.

[^{3}H]α-factor binding was assessed by using 2 µg of stripped membranes. Membranes were thawed on ice, and diluted in ice-cold YM1+i so to reach a concentration of 0,13 mg/ml (2 µg of membranes in 15 µl). Specific binding was calculated at one concentration of [^{3}H]α-factor (300 nM final) and by subtracting unspecific binding in the presence of non-radioactive α-factor from total binding.

From the aliquots of diluted membranes, 15 µl were pipetted into 5 ml Minisorp tubes (Nalge Nunc international GmbH, Wiesbaden, Germany) at RT, and 15 µl of labeling buffer was added and mixed. After 5 min of incubation, 3x5 µl aliquots were collected to determine total [^{3}H]α-factor concentration. The incubation was carried out for further 30 min at RT, and was then terminated by the addition of 500 µl of ice-cold YM1+i, and immediate filtered on presoaked GF/F filters. Filters were then placed in scintillation vials (20 ml Polyvials®, Zinsser analytic GmbH, Frankfurt, Germany) containing 10 ml of scintillation fluid (Rotiszint® eco plus, Roth GmbH). Samples were left overnight at RT before counting in a scintillation counter (liquid Scintillation Analyser, Tri-carb 2100 TR, Packard). The dpm quantity was then divided by the specific activity to give the amount of pmol of receptor in the membranes.

13.6.3. Functionality binding-assay

Both media YM1+i (wash buffer) and 0,3% PEI were cooled to 4°C. At least half an hour before use, GF/F filters were soaked in ice-cold 0,3% (v/v) PEI (in YM1+i) at 4°C.

The following labeling buffers were prepared in Minisorp tubes (that have low protein binding reference: YM1+i with 300 nM final of [^{3}H]α-factor, and YM1+i with the same concentration of [^{3}H]α-factor and 300 µM final of non-radioactive α-factor (100xK_d or 100xhighest concentration, which ever is greatest) to determine non-specific binding.

[^{3}H]α-factor binding was assessed by using 2 µg of stripped membranes. The membranes were thawed on ice, and diluted in ice-cold YM1+i so to reach a concentration of 0,13 mg/ml (2 µg of membranes for 15 µl). Specific binding was calculated by testing different concentrations of [^{3}H]α-factor, 25, 50,100, 300, 600 nM final, and by substracting the unspecific binding from total binding in the presence of non-radioactive α-factor.

From the aliquots of diluted membranes, 25 µl were pipetted into Minisorp tubes at RT, and 25 µl of labeling buffer were added and mixed.

After 5 min of incubation, 3x5 µl aliquots were collected to determine total [^{3}H]α-factor concentration. The incubation was carried out for further 30 min at RT, and was then terminated by the addition of 500 µl of ice-cold YM1+i and immediate filtered on presoaked GF/F filters. Filters were then placed in scintillation tubes containing 10 ml of scintillation fluid. Samples were left overnight at RT before counting in a scintillation counter. The dpm quantity was then divided by the specific activity to give the amount of pmol of receptor in the membranes.

13.6.4. Inhibition-assay

Two atomically identical (but stereochemical distinct) α-factor stereoisomers, [L-Ala^9]α-factor and [D-Ala^9]α-factor were chosen because of their identical atomic compositions (and thus identical hydrophobicities).

The media YM1+i (wash buffer) and 0,3% PEI were prepared first and cooled to 4°C before use. At least half an hour before use, GF/F filters were soaked in ice-cold 0,3% (v/v) PEI (in YM1+i) at 4°C.

The following labeling buffers were prepared in Minisorp tubes (that have low protein binding): YM1+i with different concentrations of these competitors: 0, 3, 10, 30, 100, 300, 1000 and 3000 nM for the [D-Ala^9]α-factor, and 0, 0,03, 0,1, 0,3, 1, 3, 10 and 30 nM for the [L-Ala^9]α-factor. The non-specific binding was determined with non-radioactive α-factor at a 30 µM final concentration. The [^{3}H]α-factor solution had a fixed concentration of 600 nM.

Membranes were then thawed on ice, and diluted in ice-cold YM1+i to reach a 0,13 mg/ml concentration (10 µg of membranes for 15 µl).

From each individual test solution (also for the cold peptide solution), 150 µl were added to 20 µl of the diluted [^{3}H]α-factor solution.

For each prepared solutions, 50 µl were pipetted in triplicate into fresh minisorp tubes. To start the binding reaction, 50 ml of the diluted membranes were added to each tube and incubated for 1h at RT. The reaction was then terminated by the addition of 500 µl of ice-cold YM1+i and immediately filtered on presoaked GF/F filters. Filters were then placed in scintillation tubes containing 10 ml of scintillation fluid. Samples were left overnight at RT before counting in a scintillation counter.

To determine the total [^{3}H]α-factor concentration, 3x5 µl aliquots were collected.

13.7. Crystallisation

13.7.1. Additional preparation for the crystallisation

After the two-step purification performed as described above, the final eluate from the size-exclusion chromatography was incubated with Biobeads (Biorad), at a ratio of 200 mg of beads for 1 ml of solution, at 4°C under agitation. Aliquots of 30 µl were collected at different times (15, 30, 45 minutes, 1h, 1h30, 2h, 2h30) and analysed on 8% SDS-polyacrylamide gel.

The final pure protein sample was concentrated (2,5 mg/ml) and filtered and used for the 3D- and the 2D-crystallisation trials.

13.7.2. 2D-crystallisation method

Pure protein were sent to Dr. Patrick Bron (UMR-CNRS 6026 "Interactions cellulaires et moléculaires, Rennes, France) for 2D-crystallisation trials. The observations were done with the electronic microscope Technai Sphera 200 kV LAB6, after colouration of the samples by 2% uranyl acetate.

13.7.2.1. Monolayer Nickel-Lipid

The trials were performed according to the protocol of Levy and coworkers (Levy *et al.*, 1999). The Ni^{2+}-lipid monolayer was coated on the buffer surface in a Teflon well. Two different monolayers were used: one composed of 100% Ni^{2+}-lipid (DOGS-NTA) and one composed of 50% / 50% lipids nickel/DOPC (DOGS-NTA/DOPC or DOGS-NTA/DOPG). This mixture was concentrated to 0,5 mg/ml, in a chloroform/methanol solution. A volume of 0,5 ml was spread on the buffer surface, and left for at least 4h.

The detergent-solubilised protein, at a final concentration of 1 mg/ml in the last purification buffer, was mixed with classical lipid mixture, composed of EPC/EPA of *E.coli*, or PEG. The final ratio lipid/protein, that has to be comprised between 0,2 and 1, was in this case of 0,5. After the monolayer was homogeneously spread on the air-buffer interface, between 5 to 8 µg (5 to 8 µl) of the protein/lipid solution were pipetted under the monolayer for incubation, through the injection hole. Detergent was added before inorder to remain above the CMC (concentration above 10 times the CMC).

After a 2h incubation, one can verify under the optical microscope the state of the monolayer. Different buffers with different ions were used, at a 20mM concentration: $CaCl_2$, $MgCl_2$ et $MgSO_4$. DOTM was also tried, 5 µl at 0.5%.

The rigidity of the monolayer was estimated with the photonic microscope. The rigidity is directly correlated with the amount of proteins that are bound to the monolayer. Biobeads were then added (~ 5mg) under slight agitation, to remove the excess of detergents. After a varying period (1 to 3 days for example), the monolayer was transferred on an carbon grid, coloured with 2% uranyl acetate and observed on an electronic microscope. Sixteen crystallisation conditions were screened in total, with or without ions.

13.7.2.2. Reconstitution in proteoliposomes

Some reconstitution trials were also performed (classical method) with a mixture of lipids from *E.coli*. The two lipid/protein ratios tried were 0,2 and 0,8 (w/w), with or without 20 mM Mg^{2+}, in a final volume of 50 µl, in the presence of DDM.

The incubation was carried out overnight, before a sequential addition of 2 times 5 mg of Biobeads under slight agitation.

After one day, the mixture was transferred to another tube to stop the absorption on Biobeads, and the incubation went on for a second day. As the observation revealed no successful reconstitution, to favour the proteoliposomes, three cycles of freezing/thawing (liquid nitrogen/ice) were performed, and samples were then left on the bench at RT one day before an additionnal observation.

The detergent-solubilised protein was mixed with classical lipid mixture, composed of EPC/EPA of *E.coli*, or PEG (polyethylen glycol).

The two lipid/protein ratios tried were 0,2 and 0,8 (w/w), with or without 20 mM Mg^{2+}, in a final volume of 50 µl, with DDM.

13.7.3. 3D-crystallisation method

13.7.3.1. Manual trials (hanging-drop method)

We used the silicon plates (Q-plates, 24 reservoirs) and the crystallisation screens from Hampton Research (Aliso Viejo, CA, USA): MembFac, Index, Crystal Screen 1 and Crystal Screen 2. For each condition, we used 0,5 ml for the reservoir, and we pipetted on a 22 mm silicon glassplate 0,8 µl of protein sample, to which we added 0,5 µl from the reservoir. The glassplate was hung over the reservoir and the covered silicon plates were stored at 18°C. All drops were observed under the optical microscope Olympius SZX12.

13.7.3.2. Automated trials

Automated assays were performed by Crelux GmbH, Martinsried, Germany. A total of 600 different conditions were screened, with the sitting-drop method. A volume of 0,1 µl of protein sample was used for each conditions. Covered plates were stored at 18°C. All drops were observed under the optical microscope Olympius SZX12.

13.8. Characterisation

13.8.1. N-terminal sequencing

To confirm the sequence of the purified protein, 30 µl of the purified eluate were analysed by the N-terminal sequencing service of the Max-Planck-Institute of Biochemistry (department of Prof. Lottspeich). This analysis was performed by N-terminal Edman-sequencing. The sequence of the amino acids could be determined by the gradual digestion of the N-terminal part at each amino acid (selectively cleaves the N-terminal peptide bond).

13.8.2. MALDI-TOF analysis

Purified samples on SDS-PAGE were analysed by peptide mass fingerprint in the mass-spectrometry analysis service of the Max-Planck-Institute of Biochemistry (group of Frank Siedler, department of Prof. Oesterhelt).

References

Abel, M.G., Lee, B.K., Naider, F. and Becker, J.M. (1998a) Mutations affecting ligand specificity of the G-protein-coupled receptor for the Saccharomyces cerevisiae tridecapeptide pheromone. *Biochim Biophys Acta*. **1448**: 12-26.

Abel, M.G., Zhang, Y.L., Lu, H.F., Naider, F. and Becker, J.M. (1998b) Structure-function analysis of the Saccharomyces cerevisiae tridecapeptide pheromone using alanine-scanned analogs. *J Pept Res*. **52**: 95-106.

Andersen, B. and Stevens, R.C. (1998) The human D1A dopamine receptor: heterologous expression in Saccharomyces cerevisiae and purification of the functional receptor. *Protein Expr Purif*. **13**: 111-119.

Arnott, M.A., Michael, R.A., Thompson, C.R., Hough, D.W. and Danson, M.J. (2000) Thermostability and thermoactivity of citrate synthases from the thermophilic and hyperthermophilic archaea, Thermoplasma acidophilum and Pyrococcus furiosus. *J Mol Biol*. **304**: 657-668.

Asturias, F.J. and Kornberg, R.D. (1999) Protein crystallization on lipid layers and structure determination of the RNA polymerase II transcription initiation complex. *J Biol Chem*. **274**: 6813-6816.

Bhargava, J., Shashikant, C.S., Carr, J.L., Juan, H., Bentley, K.L. and Ruddle, F.H. (1999) Direct cloning of genomic DNA by recombinogenic targeting method using a yeast-bacterial shuttle vector, pClasper. *Genomics*. **62**: 285-288.

Bill, R.M. (2001) Yeast--a panacea for the structure-function analysis of membrane proteins? *Curr Genet*. **40**: 157-171.

Blumer, K.J. and Thorner, J. (1990) Beta and gamma subunits of a yeast guanine nucleotide-binding protein are not essential for membrane association of the alpha subunit but are required for receptor coupling. *Proc Natl Acad Sci U S A*. **87**: 4363-4367.

Blumer, K.J., Reneke, J.E. and Thorner, J. (1988) The STE2 gene product is the ligand-binding component of the alpha-factor receptor of Saccharomyces cerevisiae. *J Biol Chem*. **263**: 10836-10842.

Bockaert, J. and Pin, J.P. (1998) [Use of a G-protein-coupled receptor to communicate. An evolutionary success]. *C R Acad Sci III*. **321**: 529-551.

Bockaert, J. and Pin, J.P. (1999) Molecular tinkering of G protein-coupled receptors: an evolutionary success. *Embo J*. **18**: 1723-1729.

Bohm, G. and Jaenicke, R. (1994) Relevance of sequence statistics for the properties of extremophilic proteins. *Int J Pept Protein Res*. **43**: 97-106.

Brisson, A., Olofsson, A., Ringler, P., Schmutz, M. and Stoylova, S. (1994) Two-dimensional crystallization of proteins on planar lipid films and structure determination by electron crystallography. *Biol Cell*. **80**: 221-228.

Brisson, A., Bergsma-Schutter, W., Oling, F., Lambert, O., Reviakine, I. (1999) Two-dimensional crystallization of proteins on lipid monolayers at the air–water interface and transfer to an electron microscopy grid. *Journal of Crystal Growth* **196**: 456–470.

Britton, K.L., Yip, K.S., Sedelnikova, S.E., Stillman, T.J., Adams, M.W., Ma, K.*, et al* (1999) Structure determination of the glutamate dehydrogenase from the hyperthermophile Thermococcus litoralis and its comparison with that from Pyrococcus furiosus. *J Mol Biol*. **293**: 1121-1132.

Bult, C.J., White, O., Olsen, G.J., Zhou, L., Fleischmann, R.D., Sutton, G.G.*, et al* (1996) Complete genome sequence of the methanogenic archaeon, Methanococcus jannaschii. *Science*. **273**: 1058-1073.

Caffrey, M. (2003) Membrane protein crystallization. *J Struct Biol*. **142**: 108-132.

Caponigro, G., Abedi, M. and Kamb, A. (2003) Functional analysis of expressed peptides that bind yeast STE proteins. *J Biotechnol*. **103**: 213-225.

Chan, M.K., Mukund, S., Kletzin, A., Adams, M.W. and Rees, D.C. (1995) Structure of a hyperthermophilic tungstopterin enzyme, aldehyde ferredoxin oxidoreductase. *Science*. **267**: 1463-1469.

Chapot, M.P., Eshdat, Y., Marullo, S., Guillet, J.G., Charbit, A., Strosberg, A.D. and Delavier-Klutchko, C. (1990) Localization and characterization of three different beta-adrenergic receptors expressed in Escherichia coli. *Eur J Biochem*. **187**: 137-144.

Chen, Q. and Konopka, J.B. (1996) Regulation of the G-protein-coupled alpha-factor pheromone receptor by phosphorylation. *Mol Cell Biol*. **16**: 247-257.

Columbus, L., Lipfert, J., Klock, H., Millett, I., Doniach, S. and Lesley, S.A. (2006) Expression, purification, and characterization of Thermotoga maritima membrane proteins for structure determination. *Protein Sci*. **15**: 961-975.

Courty, S., Lebeau, L., Martel, L., Lenné, P.-F., Balavoine, F., Dischert, W.*, et al* (2002) Two-Dimensional Crystallization of a Histidine-Tagged Protein on Monolayers of Fluidity-Enhanced Ni2+-Chelating Lipids. *Langmuir* **18**: 9502-9512.

David, N.E., Gee, M., Andersen, B., Naider, F., Thorner, J. and Stevens, R.C. (1997) Expression and purification of the Saccharomyces cerevisiae alpha-factor receptor (Ste2p), a 7-transmembrane-segment G protein-coupled receptor. *J Biol Chem*. **272**: 15553-15561.

de Jong, L.A., Grunewald, S., Franke, J.P., Uges, D.R. and Bischoff, R. (2004) Purification and characterization of the recombinant human dopamine D2S receptor from Pichia pastoris. *Protein Expr Purif*. **33**: 176-184.

Dhami, G.K., Anborgh, P.H., Dale, L.B., Sterne-Marr, R. and Ferguson, S.S. (2002) Phosphorylation-independent regulation of metabotropic glutamate receptor signaling by G protein-coupled receptor kinase 2. *J Biol Chem*. **277**: 25266-25272.

Dohlman, H.G. and Thorner, J.W. (2001) Regulation of G protein-initiated signal transduction in yeast: paradigms and principles. *Annu Rev Biochem*. **70**: 703-754.

Dosil, M., Schandel, K.A., Gupta, E., Jenness, D.D. and Konopka, J.B. (2000) The C terminus of the Saccharomyces cerevisiae alpha-factor receptor contributes to the formation of preactivation complexes with its cognate G protein. *Mol Cell Biol*. **20**: 5321-5329.

Duran-Avelar, M.J., Ongay-Larios, L., Zentella-Dehesa, A. and Coria, R. (2001) The carboxy-terminal tail of the Ste2 receptor is involved in activation of the G protein in the Saccharomyces cerevisiae alpha-pheromone response pathway. *FEMS Microbiol Lett*. **197**: 65-71.

Eilers, M., Hornak, V., Smith, S.O. and Konopka, J.B. (2005) Comparison of class A and D G protein-coupled receptors: common features in structure and activation. *Biochemistry*. **44**: 8959-8975.

Engelman, D.M., Chen, Y., Chin, C.N., Curran, A.R., Dixon, A.M., Dupuy, A.D.*, et al* (2003) Membrane protein folding: beyond the two stage model. *FEBS Lett*. **555**: 122-125.

Erickson, J.R., Wu, J.J., Goddard, J.G., Tigyi, G., Kawanishi, K., Tomei, L.D. and Kiefer, M.C. (1998) Edg-2/Vzg-1 couples to the yeast pheromone response pathway selectively in response to lysophosphatidic acid. *J Biol Chem*. **273**: 1506-1510.

Ferreira, K.N., Iverson, T.M., Maghlaoui, K., Barber, J. and Iwata, S. (2004) Architecture of the photosynthetic oxygen-evolving center. *Science*. **303**: 1831-1838.

Galvez, T. and Pin, J.P. (2003) [How do G-protein-coupled receptors work? The case of metabotropic glutamate and GABA receptors]. *Med Sci (Paris)*. **19**: 559-565.

Garavito, R.M. and Ferguson-Miller, S. (2001) Detergents as tools in membrane biochemistry. *J Biol Chem*. **276**: 32403-32406.

Gimpl, G., Klein, U., Reilander, H. and Fahrenholz, F. (1995) Expression of the human oxytocin receptor in baculovirus-infected insect cells: high-affinity binding is induced by a cholesterol-cyclodextrin complex. *Biochemistry*. **34**: 13794-13801.

Griffith, D.A., Delipala, C., Leadsham, J., Jarvis, S.M. and Oesterhelt, D. (2003) A novel yeast expression system for the overproduction of quality-controlled membrane proteins. *FEBS Lett*. **553**: 45-50.

Grisshammer, R. and Tate, C.G. (1995) Overexpression of integral membrane proteins for structural studies. *Q Rev Biophys*. **28**: 315-422.

Gross, M. and Jaenicke, R. (1994) Proteins under pressure. The influence of high hydrostatic pressure on structure, function and assembly of proteins and protein complexes. *Eur J Biochem*. **221**: 617-630.

Gudermann, T., Schoneberg, T. and Schultz, G. (1997) Functional and structural complexity of signal transduction via G-protein-coupled receptors. *Annu Rev Neurosci*. **20**: 399-427.

Gudermann, T., Grosse, R. and Schultz, G. (2000) Contribution of receptor/G protein signaling to cell growth and transformation. *Naunyn Schmiedebergs Arch Pharmacol*. **361**: 345-362.

Hasegawa, J., Loh, H.H. and Lee, N.M. (1987) Lipid requirement for mu opioid receptor binding. *J Neurochem*. **49**: 1007-1012.

Hasler, L., Heymann, J.B., Engel, A., Kistler, J. and Walz, T. (1998) 2D crystallization of membrane proteins: rationales and examples. *J Struct Biol*. **121**: 162-171.

Hofmann, K.a.S., W. (1993) A database of membrane spanning proteins segments. *Biol. Chem. Hoppe-Seyler*. **374**: 166.

Hunte, C., Koepke, J., Lange, C., Rossmanith, T. and Michel, H. (2000) Structure at 2.3 A resolution of the cytochrome bc(1) complex from the yeast Saccharomyces cerevisiae co-crystallized with an antibody Fv fragment. *Structure*. **8**: 669-684.

Imperiali, B. and Rickert, K.W. (1995) Conformational implications of asparagine-linked glycosylation. *Proc Natl Acad Sci U S A*. **92**: 97-101.

Imperiali, B. and O'Connor, S.E. (1999) Effect of N-linked glycosylation on glycopeptide and glycoprotein structure. *Curr Opin Chem Biol*. **3**: 643-649.

Jackson, M.E., Pratt, J.M., Stoker, N.G. and Holland, I.B. (1985) An inner membrane protein N-terminal signal sequence is able to promote efficient localisation of an outer membrane protein in Escherichia coli. *Embo J*. **4**: 2377-2383.

Jaenicke, R. (1996) How do proteins acquire their three-dimensional structure and stability? *Naturwissenschaften*. **83**: 544-554.

Jaenicke, R. and Bohm, G. (1998) The stability of proteins in extreme environments. *Curr Opin Struct Biol*. **8**: 738-748.

Jaenicke, R., Schurig, H., Beaucamp, N. and Ostendorp, R. (1996) Structure and stability of hyperstable proteins: glycolytic enzymes from hyperthermophilic bacterium Thermotoga maritima. *Adv Protein Chem*. **48**: 181-269.

Jiang, Y., Lee, A., Chen, J., Cadene, M., Chait, B.T. and MacKinnon, R. (2002a) Crystal structure and mechanism of a calcium-gated potassium channel. *Nature*. **417**: 515-522.

Jiang, Y., Lee, A., Chen, J., Cadene, M., Chait, B.T. and MacKinnon, R. (2002b) The open pore conformation of potassium channels. *Nature*. **417**: 523-526.

Jidenko, M., Nielsen, R.C., Sorensen, T.L., Moller, J.V., le Maire, M., Nissen, P. and Jaxel, C. (2005) Crystallization of a mammalian membrane protein overexpressed in Saccharomyces cerevisiae. *Proc Natl Acad Sci U S A*. **102**: 11687-11691.

Jones, W.J., Leigh, J.A., Mayer, F., Woese, C.R. and Wolfe, R.S. (1983) Methanococcus jannaschii sp. nov., an extremely thermophilic methanogen from a submarine hydrothermal vent. *Arch. Microbiol.* **136**: 254–261.

Kajkowski, E.M., Price, L.A., Pausch, M.H., Young, K.H. and Ozenberger, B.A. (1997) Investigation of growth hormone releasing hormone receptor structure and activity using yeast expression technologies. *J Recept Signal Transduct Res*. **17**: 293-303.

Kamiya, N. and Shen, J.R. (2003) Crystal structure of oxygen-evolving photosystem II from Thermosynechococcus vulcanus at 3.7-A resolution. *Proc Natl Acad Sci U S A*. **100**: 98-103.

Katada, S., Tanaka, M. and Touhara, K. (2004) Structural determinants for membrane trafficking and G protein selectivity of a mouse olfactory receptor. *J Neurochem*. **90**: 1453-1463.

Kelly, C.A., Nishiyama, M., Ohnishi, Y., Beppu, T. and Birktoft, J.J. (1993) Determinants of protein thermostability observed in the 1.9-A crystal structure of malate dehydrogenase from the thermophilic bacterium Thermus flavus. *Biochemistry*. **32**: 3913-3922.

King, K., Dohlman, H.G., Thorner, J., Caron, M.G. and Lefkowitz, R.J. (1990) Control of yeast mating signal transduction by a mammalian beta 2-adrenergic receptor and Gs alpha subunit. *Science*. **250**: 121-123.

Konopka, J.B., Jenness, D.D. and Hartwell, L.H. (1988) The C-terminus of the S. cerevisiae alpha-pheromone receptor mediates an adaptive response to pheromone. *Cell*. **54**: 609-620.

Kornberg, R.D.a.D., S.A. (1991) Two-dimensional crystals of proteins on lipid layers. *curr. Opin. Struct. Biol.* **1**: 642-646.

Kuhn, P., Wilson, K., Patch, M.G. and Stevens, R.C. (2002) The genesis of high-throughput structure-based drug discovery using protein crystallography. *Curr Opin Chem Biol.* **6**: 704-710.

Lacapere, J.J., Stokes, D.L., Mosser, G., Ranck, J.L., Leblanc, G. and Rigaud, J.L. (1997) Two-dimensional crystal formation from solubilized membrane proteins using Bio-Beads to remove detergent. *Ann N Y Acad Sci.* **834**: 9-18.

Ladds, G., Goddard, A. and Davey, J. (2005) Functional analysis of heterologous GPCR signalling pathways in yeast. *Trends Biotechnol.* **23**: 367-373.

Ladds, G., Davis, K., Hillhouse, E.W. and Davey, J. (2003) Modified yeast cells to investigate the coupling of G protein-coupled receptors to specific G proteins. *Mol Microbiol.* **47**: 781-792.

Lagane, B., Gaibelet, G., Meilhoc, E., Masson, J.M., Cezanne, L. and Lopez, A. (2000) Role of sterols in modulating the human mu-opioid receptor function in Saccharomyces cerevisiae. *J Biol Chem.* **275**: 33197-33200.

Lanfermeijer, F.C., Venema, K. and Palmgren, M.G. (1997) Purification of heterologously expressed plant plasma membrane H(+)-ATPase by Ni(2+)-affinity chromatography. *Ann N Y Acad Sci.* **834**: 139-141.

Lanfermeijer, F.C., Venema, K. and Palmgren, M.G. (1998) Purification of a histidine-tagged plant plasma membrane H+-ATPase expressed in yeast. *Protein Expr Purif.* **12**: 29-37.

le Maire, M., Moller, J.V. and Champeil, P. (1987) Binding of a nonionic detergent to membranes: flip-flop rate and location on the bilayer. *Biochemistry.* **26**: 4803-4810.

le Maire, M., Champeil, P. and Moller, J.V. (2000) Interaction of membrane proteins and lipids with solubilizing detergents. *Biochim Biophys Acta.* **1508**: 86-111.

Lebeau, L., Lach, F., Venien-Bryan, C., Renault, A., Dietrich, J., Jahn, T.*, et al* (2001) Two-dimensional crystallization of a membrane protein on a detergent-resistant lipid monolayer. *J Mol Biol.* **308**: 639-647.

Leberer, E., Thomas, D.Y. and Whiteway, M. (1997) Pheromone signalling and polarized morphogenesis in yeast. *Curr Opin Genet Dev.* **7**: 59-66.

Lee, S.H. and Altenberg, G.A. (2003) Expression of functional multidrug-resistance protein 1 in Saccharomyces cerevisiae: effects of N- and C-terminal affinity tags. *Biochem Biophys Res Commun.* **306**: 644-649.

Leuther, K.K., Bushnell, D.A. and Kornberg, R.D. (1996) Two-dimensional crystallography of TFIIB- and IIE-RNA polymerase II complexes: implications for start site selection and initiation complex formation. *Cell.* **85**: 773-779.

Levy, D., Chami, M. and Rigaud, J.L. (2001) Two-dimensional crystallization of membrane proteins: the lipid layer strategy. *FEBS Lett.* **504**: 187-193.

Levy, D., Mosser, G., Lambert, O., Moeck, G.S., Bald, D. and Rigaud, J.L. (1999) Two-dimensional crystallization on lipid layer: A successful approach for membrane proteins. *J Struct Biol.* **127**: 44-52.

Lin-Cereghino, J. and Cregg, J.M. (2000) Heterologous protein expression in the methylotrophic yeast Pichia pastoris. *FEMS Microbiology Reviews.* **24**: 45-66.

Lin, J.C., Parrish, W., Eilers, M., Smith, S.O. and Konopka, J.B. (2003) Aromatic residues at the extracellular ends of transmembrane domains 5 and 6 promote ligand activation of the G protein-coupled alpha-factor receptor. *Biochemistry*. **42**: 293-301.

Liu, S., Henry, L.K., Lee, B.K., Wang, S.H., Arshava, B., Becker, J.M. and Naider, F. (2000) Position 13 analogs of the tridecapeptide mating pheromone from Saccharomyces cerevisiae: design of an iodinatable ligand for receptor binding. *J Pept Res*. **56**: 24-34.

Loison, G., Vidal, A., Findeli, A., Roitsch, C., Balloul, J.M. and Lemoine, Y. (1989) High level of expression of a protective antigen of schistosomes in Saccharomyces cerevisiae. *Yeast*. **5**: 497-507.

Loll, P.J. (2003) Membrane protein structural biology: the high throughput challenge. *J Struct Biol*. **142**: 144-153.

López-Marqués, R.L., Perez-Castineira, J.R., Buch-Pedersen, M.J., Marco, S., Rigaud, J.L., Palmgren, M.G. and Serrano, A. (2005) Large-scale purification of the proton pumping pyrophosphatase from Thermotoga maritima: a "Hot-Solve" method for isolation of recombinant thermophilic membrane proteins. *Biochim Biophys Acta*. **1716**: 69-76.

McPherson, A. (2004) Introduction to protein crystallization. *Methods*. **34**: 254-265.

Mentesana, P.E. and Konopka, J.B. (2001) Mutational analysis of the role of N-glycosylation in alpha-factor receptor function. *Biochemistry*. **40**: 9685-9694.

Mohraz, M. (1999) Reconstitution of detergent-solubilized Na,K-ATPase and formation of two-dimensional crystals. *J Struct Biol*. **125**: 76-85.

Mombelli, E., Shehi, E., Fusi, P. and Tortora, P. (2002) Exploring hyperthermophilic proteins under pressure: theoretical aspects and experimental findings. *Biochim Biophys Acta*. **1595**: 392-396.

Morsomme, P., Chami, M., Marco, S., Nader, J., Ketchum, K.A., Goffeau, A. and Rigaud, J.L. (2002) Characterization of a hyperthermophilic P-type ATPase from Methanococcus jannaschii expressed in yeast. *J Biol Chem*. **277**: 29608-29616.

Mosser, G. (2001) Two-dimensional crystallogenesis of transmembrane proteins. *Micron*. **32**: 517-540.

Mukherjee, S. and Guptasarma, P. (2005) Direct proteolysis-based purification of an overexpressed hyperthermophile protein from Escherichia coli lysate: a novel exploitation of the link between structural stability and proteolytic resistance. *Protein Expr Purif*. **40**: 71-76.

Nagi, A.D. and Regan, L. (1997) An inverse correlation between loop length and stability in a four-helix-bundle protein. *Fold Des*. **2**: 67-75.

Naider, F. and Becker, J.M. (2004) The alpha-factor mating pheromone of Saccharomyces cerevisiae: a model for studying the interaction of peptide hormones and G protein-coupled receptors. *Peptides*. **25**: 1441-1463.

Nekrasova, E., Sosinskaya, A., Natochin, M., Lancet, D. and Gat, U. (1996) Overexpression, solubilization and purification of rat and human olfactory receptors. *Eur J Biochem*. **238**: 28-37.

Nogi, T., Kobayashi, M., Nozawa, T. and Miki, K. (2000) Crystallization and preliminary crystallographic analysis of the high-potential iron-sulfur protein from Thermochromatium tepidum. *Acta Crystallogr D Biol Crystallogr*. **56**: 656-658.

Noskov, V.N., Kouprina, N., Leem, S.H., Ouspenski, I., Barrett, J.C. and Larionov, V. (2003) A general cloning system to selectively isolate any eukaryotic or prokaryotic genomic region in yeast. *BMC Genomics.* **4**: 16.

Nunez, M.T. and Glass, J. (1982) Reconstitution of the transferrin receptor in lipid vesicles. Effect of cholesterol on the binding of transferrin. *Biochemistry.* **21**: 4139-4143.

O'Connor, S.E. and Imperiali, B. (1996) Modulation of protein structure and function by asparagine-linked glycosylation. *Chem Biol.* **3**: 803-812.

Okkels, J.S. (1996) A URA3-promoter deletion in a pYES vector increases the expression level of a fungal lipase in Saccharomyces cerevisiae. *Ann N Y Acad Sci.* **782**: 202-207.

Opekarova, M. and Tanner, W. (2003) Specific lipid requirements of membrane proteins--a putative bottleneck in heterologous expression. *Biochim Biophys Acta.* **1610**: 11-22.

Overton, M.C. and Blumer, K.J. (2002) The extracellular N-terminal domain and transmembrane domains 1 and 2 mediate oligomerization of a yeast G protein-coupled receptor. *J Biol Chem.* **277**: 41463-41472.

Palczewski, K. (2006) G protein-coupled receptor rhodopsin. *Annu Rev Biochem.* **75**: 743-767.

Palczewski, K., Kumasaka, T., Hori, T., Behnke, C.A., Motoshima, H., Fox, B.A.*, et al* (2000) Crystal structure of rhodopsin: A G protein-coupled receptor. *Science.* **289**: 739-745.

Parekh, R.N. and Wittrup, K.D. (1997) Expression level tuning for optimal heterologous protein secretion in Saccharomyces cerevisiae. *Biotechnol Prog.* **13**: 117-122.

Parekh, R.N., Shaw, M.R. and Wittrup, K.D. (1996) An integrating vector for tunable, high copy, stable integration into the dispersed Ty delta sites of Saccharomyces cerevisiae. *Biotechnol Prog.* **12**: 16-21.

Parrish, W., Eilers, M., Ying, W. and Konopka, J.B. (2002) The cytoplasmic end of transmembrane domain 3 regulates the activity of the Saccharomyces cerevisiae G-protein-coupled alpha-factor receptor. *Genetics.* **160**: 429-443.

Pausch, M.H. (1997) G-protein-coupled receptors in Saccharomyces cerevisiae: high-throughput screening assays for drug discovery. *Trends Biotechnol.* **15**: 487-494.

Payette, P., Gossard, F., Whiteway, M. and Dennis, M. (1990) Expression and pharmacological characterization of the human M1 muscarinic receptor in Saccharomyces cerevisiae. *FEBS Lett.* **266**: 21-25.

Perez-Castineira, J.R., Lopez-Marques, R.L., Losada, M. and Serrano, A. (2001) A thermostable K(+)-stimulated vacuolar-type pyrophosphatase from the hyperthermophilic bacterium Thermotoga maritima. *FEBS Lett.* **496**: 6-11.

Perl, D., Schmidt, F.X. (2002) Some like it hot: The molecular determinants of protein thermostability [Review]. [Review] *Chembiochem.* **3**: 39-44.

Platt, A. and Reece, R.J. (1998) The yeast galactose genetic switch is mediated by the formation of a Gal4p-Gal80p-Gal3p complex. *Embo J.* **17**: 4086-4091.

Porath, J. and Olin, B. (1983) Immobilized metal ion affinity adsorption and immobilized metal ion affinity chromatography of biomaterials. Serum protein affinities for gel-immobilized iron and nickel ions. *Biochemistry.* **22**: 1621-1630.

Porath, J., Carlsson, J., Olsson, I. and Belfrage, G. (1975) Metal chelate affinity chromatography, a new approach to protein fractionation. *Nature*. **258**: 598-599.

Posas, F., Takekawa, M. and Saito, H. (1998) Signal transduction by MAP kinase cascades in budding yeast. *Curr Opin Microbiol*. **1**: 175-182.

Price, L.A., Kajkowski, E.M., Hadcock, J.R., Ozenberger, B.A. and Pausch, M.H. (1995) Functional coupling of a mammalian somatostatin receptor to the yeast pheromone response pathway. *Mol Cell Biol*. **15**: 6188-6195.

Raths, S.K., Naider, F. and Becker, J.M. (1988) Peptide analogues compete with the binding of alpha-factor to its receptor in Saccharomyces cerevisiae. *J Biol Chem*. **263**: 17333-17341.

Reilander, H. and Weiss, H.M. (1998) Production of G-protein-coupled receptors in yeast. *Curr Opin Biotechnol*. **9**: 510-517.

Reneke, J.E., Blumer, K.J., Courchesne, W.E. and Thorner, J. (1988) The carboxy-terminal segment of the yeast alpha-factor receptor is a regulatory domain. *Cell*. **55**: 221-234.

Rice, D.W., Yip, K.S., Stillman, T.J., Britton, K.L., Fuentes, A., Connerton, I., *et al* (1996) Insights into the molecular basis of thermal stability from the structure determination of Pyrococcus furiosus glutamate dehydrogenase. *FEMS Microbiol Rev*. **18**: 105-117.

Rigaud, J., Chami, M., Lambert, O., Levy, D. and Ranck, J. (2000) Use of detergents in two-dimensional crystallization of membrane proteins. *Biochim Biophys Acta*. **1508**: 112-128.

Rigaud, J.L. (2002) Membrane proteins: functional and structural studies using reconstituted proteoliposomes and 2-D crystals. *Braz J Med Biol Res*. **35**: 753-766.

Rigaud, J.L., Mosser, G., Lacapere, J.J., Olofsson, A., Levy, D. and Ranck, J.L. (1997) Bio-Beads: an efficient strategy for two-dimensional crystallization of membrane proteins. *J Struct Biol*. **118**: 226-235.

Romanos, M.A., Scorer, C.A. and Clare, J.J. (1992) Foreign gene expression in yeast: a review. *Yeast*. **8**: 423-488.

Rosenbusch, J.P. (1990) The critical role of detergents in the crystallization of membrane proteins. *J Struct Biol*. **104**: 134-138.

Rosenbusch, J.P. (2001) Stability of membrane proteins: relevance for the selection of appropriate methods for high-resolution structure determinations. *J Struct Biol*. **136**: 144-157.

Rosenbusch, J.P., Lustig, A., Grabo, M., Zulauf, M. and Regenass, M. (2001) Approaches to determining membrane protein structures to high resolution: do selections of subpopulations occur? *Micron*. **32**: 75-90.

Rosenow, M.A., Magee, C.L., Williams, J.C. and Allen, J.P. (2002) The influence of detergents on the solubility of membrane proteins. *Acta Crystallogr D Biol Crystallogr*. **58**: 2076-2081.

Sachs, J.N. and Engelman, D.M. (2006) Introduction to the membrane protein reviews: the interplay of structure, dynamics, and environment in membrane protein function. *Annu Rev Biochem*. **75**: 707-712.

Sambrook, J., Fritsch, E.F. and Maniatis, T. (1989) Molecular cloning: a laboratory manual, 2nd edition. *Cold Spring Harbor laboratory*.

Sarramegna, V., Talmont, F., Demange, P. and Milon, A. (2003) Heterologous expression of G-protein-coupled receptors: comparison of expression systems fron the standpoint of large-scale production and purification. *Cell Mol Life Sci*. **60**: 1529-1546.

Sarramegna, V., Muller, I., Milon, A. and Talmont, F. (2006) Recombinant G protein-coupled receptors from expression to renaturation: a challenge towards structure. *Cell Mol Life Sci*. **63**: 1149-1164.

Sautel, M. and Milligan, G. (2000) Molecular manipulation of G-protein-coupled receptors: a new avenue into drug discovery. *Curr Med Chem*. **7**: 889-896.

Schägger, H.a.v.J., G. (1987) Tricine-sodium dodecylsulfate-polyacrylamide gel electrophoresis for the separation of proteins in the range from 1 to 100 kDa. *Anal. Biochem.* **166**: 369-379.

Schneider, D., Liu, Y., Gerstein, M. and Engelman, D.M. (2002) Thermostability of membrane protein helix-helix interaction elucidated by statistical analysis. *FEBS Lett.* **532**: 231-236.

Schoneberg, T., Schultz, G. and Gudermann, T. (1999) Structural basis of G protein-coupled receptor function. *Mol Cell Endocrinol.* **151**: 181-193.

Schoneberg, T., Schulz, A. and Gudermann, T. (2002) The structural basis of G-protein-coupled receptor function and dysfunction in human diseases. *Rev Physiol Biochem Pharmacol.* **144**: 143-227.

Schuck, S., Honsho, M., Ekroos, K., Shevchenko, A. and Simons, K. (2003) Resistance of cell membranes to different detergents. *Proc Natl Acad Sci U S A*. **100**: 5795-5800.

Shi, C., Shin, Y.O., Hanson, J., Cass, B., Loewen, M.C. and Durocher, Y. (2005) Purification and characterization of a recombinant G-protein-coupled receptor, Saccharomyces cerevisiae Ste2p, transiently expressed in HEK293 EBNA1 cells. *Biochemistry.* **44**: 15705-15714.

Shiraki, K., Nishikori, S., Fujiwara, S., Hashimoto, H., Kai, Y., Takagi, M. and Imanaka, T. (2001) Comparative analyses of the conformational stability of a hyperthermophilic protein and its mesophilic counterpart. *Eur J Biochem.* **268**: 4144-4150.

Sil, A.K., Xin, P. and Hopper, J.E. (2000) Vectors allowing amplified expression of the Saccharomyces cerevisiae Gal3p-Gal80p-Gal4p transcription switch: applications to galactose-regulated high-level production of proteins. *Protein Expr Purif.* **18**: 202-212.

Sil, A.K., Alam, S., Xin, P., Ma, L., Morgan, M., Lebo, C.M.*, et al* (1999) The Gal3p-Gal80p-Gal4p transcription switch of yeast: Gal3p destabilizes the Gal80p-Gal4p complex in response to galactose and ATP. *Mol Cell Biol.* **19**: 7828-7840.

Sizmann, D., Kuusinen, H., Keranen, S., Lomasney, J., Caron, M.G., Lefkowitz, R.J. and Keinanen, K. (1996) Production of adrenergic receptors in yeast. *Receptors Channels.* **4**: 197-203.

Soulimane, T., Than, M.E., Dewor, M., Huber, R. and Buse, G. (2000a) Primary structure of a novel subunit in ba3-cytochrome oxidase from Thermus thermophilus. *Protein Sci.* **9**: 2068-2073.

Soulimane, T., Buse, G., Bourenkov, G.P., Bartunik, H.D., Huber, R. and Than, M.E. (2000b) Structure and mechanism of the aberrant ba(3)-cytochrome c oxidase from thermus thermophilus. *Embo J.* **19**: 1766-1776.

Spassov, V.Z., Karshikoff, A.D. and Ladenstein, R. (1995) The optimization of protein-solvent interactions: thermostability and the role of hydrophobic and electrostatic interactions. *Protein Sci.* **4**: 1516-1527.

Spiegel, A.M. (1996) Defects in G protein-coupled signal transduction in human disease. *Annu Rev Physiol.* **58**: 143-170.

Spiegel, A.M. (2000) G protein defects in signal transduction. *Horm Res.* **53 Suppl 3**: 17-22.

Stevens, R.C. (2000a) Design of high-throughput methods of protein production for structural biology. *Structure.* **8**: R177-185.

Stevens, R.C. (2000b) High-throughput protein crystallization. *Curr Opin Struct Biol.* **10**: 558-563.

Strader, C.D., Sigal, I.S. and Dixon, R.A. (1989) Genetic approaches to the determination of structure-function relationships of G protein-coupled receptors. *Trends Pharmacol Sci.* **Suppl**: 26-30.

Strader, C.D., Fong, T.M., Tota, M.R., Underwood, D. and Dixon, R.A. (1994) Structure and function of G protein-coupled receptors. *Annu Rev Biochem.* **63**: 101-132.

Szilagyi, A. and Zavodszky, P. (1995) Structural basis for the extreme thermostability of D-glyceraldehyde-3-phosphate dehydrogenase from Thermotoga maritima: analysis based on homology modelling. *Protein Eng.* **8**: 779-789.

Thompson, M.J. and Eisenberg, D. (1999) Transproteomic evidence of a loop-deletion mechanism for enhancing protein thermostability. *J Mol Biol.* **290**: 595-604.

Ton, V.K. and Rao, R. (2004) Functional expression of heterologous proteins in yeast: insights into Ca2+ signaling and Ca2+-transporting ATPases. *Am J Physiol Cell Physiol.* **287**: C580-589.

Vallier, L.G., Segall, J.E. and Snyder, M. (2002) The alpha-factor receptor C-terminus is important for mating projection formation and orientation in Saccharomyces cerevisiae. *Cell Motil Cytoskeleton.* **53**: 251-266.

Van den Berg, B., Clemons, W.M., Jr., Collinson, I., Modis, Y., Hartmann, E., Harrison, S.C. and Rapoport, T.A. (2004) X-ray structure of a protein-conducting channel. *Nature.* **427**: 36-44.

Versele, M., Lemaire, K. and Thevelein, J.M. (2001) Sex and sugar in yeast: two distinct GPCR systems. *EMBO Rep.* **2**: 574-579.

Vetriani, C., Maeder, D.L., Tolliday, N., Yip, K.S., Stillman, T.J., Britton, K.L.*, et al* (1998) Protein thermostability above 100 degreesC: a key role for ionic interactions. *Proc Natl Acad Sci U S A.* **95**: 12300-12305.

Vieille, C. and Zeikus, G.J. (2001) Hyperthermophilic enzymes: sources, uses, and molecular mechanisms for thermostability. *Microbiol Mol Biol Rev.* **65**: 1-43.

Vogt, G. and Argos, P. (1997) Protein thermal stability: hydrogen bonds or internal packing? *Fold Des.* **2**: S40-46.

Vogt, G., Woell, S. and Argos, P. (1997) Protein thermal stability, hydrogen bonds, and ion pairs. *J Mol Biol.* **269**: 631-643.

von Zastrow, M. (2002) Regulation of G protein-coupled receptor by phosphorylation and endocytosis. *Neuropsychopharmacology: The Fifth Generation of Progress.*: 59-70.

Wallin, E. and von Heijne, G. (1998) Genome-wide analysis of integral membrane proteins from eubacterial, archaean, and eukaryotic organisms. *Protein Sci.* **7**: 1029-1038.

Walz, T. and Grigorieff, N. (1998) Electron Crystallography of Two-Dimensional Crystals of Membrane Proteins. *J Struct Biol.* **121**: 142-161.

Wang, X., He, X., Yang, S., An, X., Chang, W. and Liang, D. (2003) Structural basis for thermostability of beta-glycosidase from the thermophilic eubacterium Thermus nonproteolyticus HG102. *J Bacteriol.* **185**: 4248-4255.

Watson, S. and Arkinstall, S. (1994) The G-Protein linked Receptor Facts Book. 1–291.

Werten, P.J., Remigy, H.W., de Groot, B.L., Fotiadis, D., Philippsen, A., Stahlberg, H.*, et al* (2002) Progress in the analysis of membrane protein structure and function. *FEBS Lett.* **529**: 65-72.

Wiener, M.C. (2004) A pedestrian guide to membrane protein crystallization. *Methods.* **34**: 364-372.

Wiener, M.C.a.S., C.F. (2001) The development of membrane protein crystallization screens based upon detergent solution properties. *Journal of Crystal Growth* **232** 426–431.

Xue, C.B., Eriotou-Bargiota, E., Miller, D., Becker, J.M. and Naider, F. (1989) A covalently constrained congener of the Saccharomyces cerevisiae tridecapeptide mating pheromone is an agonist. *J Biol Chem.* **264**: 19161-19168.

Xue, C.B., McKinney, A., Lu, H.F., Jiang, Y., Becker, J.M. and Naider, F. (1996) Probing the functional conformation of the tridecapeptide mating pheromone of Saccharomyces cerevisiae through study of disulfide-constrained analogs. *Int J Pept Protein Res.* **47**: 131-141.

Yernool, D., Boudker, O., Jin, Y. and Gouaux, E. (2004) Structure of a glutamate transporter homologue from Pyrococcus horikoshii. *Nature.* **431**: 811-818.

Yin, D., Gavi, S., Shumay, E., Duell, K., Konopka, J.B., Malbon, C.C. and Wang, H.Y. (2005) Successful expression of a functional yeast G-protein-coupled receptor (Ste2) in mammalian cells. *Biochem Biophys Res Commun.* **329**: 281-287.

Yip, K.S., Stillman, T.J., Britton, K.L., Artymiuk, P.J., Baker, P.J., Sedelnikova, S.E.*, et al* (1995) The structure of Pyrococcus furiosus glutamate dehydrogenase reveals a key role for ion-pair networks in maintaining enzyme stability at extreme temperatures. *Structure.* **3**: 1147-1158.

Yip, T.T., Nakagawa, Y. and Porath, J. (1989) Evaluation of the interaction of peptides with Cu(II), Ni(II), and Zn(II) by high-performance immobilized metal ion affinity chromatography. *Anal Biochem.* **183**: 159-171.

Young, J.D., Casey, J.R. and Reithmeier, R.A. (2002) Meeting report: membrane proteins in health and disease. *Biochem Cell Biol.* **80**: v-xi.

Abbreviations

°C	degree Celsius	RNA	Ribonucleic acid
A	Ampere	RT	Room Temperature
Å	Angström	sec	Seconds
ATP	Adenosine-5´-Triphosphate	SEC	Size-Exclusion Chromatography
Amp^R	Ampicilline resistance gene	TCA	Tricholoroacetic acid
APS	Ammonium Persulfate	TEMED	N,N,N´,N´-Tetramethyl-ethylendiamine
B_{max}	Maximum Binding capacity	Tris	Tris-(Hydroxymethyl)-amminomethane
bp	Base paire	u	unit
BSA	Bovine Serum Albumine	v/v	Volume per Volume
Can^R or kan^R	Canamycin resistance gene	w/v	Weight per Volume
Ci	Curie	w/w	Weight per Weight
cm	centimetre	Ø	without
CMC	Critical micelle concentratrion		
Da	Dalton		
DMSO	Dimethylsulfoxid		
DNA	Deoxyribonucleic Acid		
dNTP	Deoxyribonucleotid-triphosphate		
dpm	Disintegration per minute		
DTT	Dithiothreitol		
EDTA	Ethylenediaminetetraacetic acid		
e.g.	exampli gratia		
Fig.	Figure		
g	Gram		
GDP	Guanidin-Diphosphate		
GPCR	g-Protein Coupled Receptor		
GTP	Guanidin-Triphosphate		
h	Hour		
i.e.	id est		
K_d	Dissociation constant		
kV	kilovolt		
l	litre		
µCi	microcurie		
µF	microfarad		
µl	microlitre		
µM	micromolar		
m	meter		
M	Molar		
mg	milligram		
min	minute(s)		
ml	millilitre		
MW	Molecular weight		
Neo^R	Neomycin resistance gene		
nm	nanometre		
nM	nanomolar		
NTA	Nitrilotriacetic acid		
N-Glycosylation	Asparagine-glycosylation		
Ω	Ohm		
OD_x	Optical density at x nm		
PAGE	Polyacrylamide Gel Electrophoresis		
PBS	Phosphate Buffered Saline		
PCR	Polymerase Chain Reaction		
PEG	Polyethylen Glycol		
pH	reverse logarythmic representation of relative H^+ concentration		
pmol	picomole		
PVDF	Polyvinyliden Fluoride		

Aknowledgements

I am very grateful to Prof. Dr. Dieter Oesterhelt for supervising and accompanying this PhD project, his generous support and scientific freedom, and to have offered me the opportunity to work in a motivating and stimulating atmosphere. I thank him as well for his fairness and his understanding about scientific or non-scientific questions.

I am especially grateful to Dr. Birgit Wiltschi to have considerably helped me during the writing of this thesis, and made it possible to print it out. I thank her very much for her support, for the numerous constructive discussions and all what she taught me during the last year of my PhD. I thank her for her conviviality which made the atmosphere of our office very nice.

I thank Dr. Douglas D. Griffith for introducing me to the project and his supervision at the bench the 2 first years of my PhD.

I am indebted to Dr. Patrick Bron for introducing me to the research and converting me in particular to the field of membrane proteins. I thank him for his friendship, his advices and his help since seven years, for all questions and important choices I had to take concerning research and scientific directions. Thanks also for the 2D-crystallisation trials he performed on my PhD project.

I am thankful to Dr. Jörg Tittor to have listened to me and adviced me when I was worrying or asking something about the work or another field. I thank him for his friendship and his enthousiasm to organise nice bike-tours, jogging training and parties in the lab, contributing to the nice global atmosphere.

I thank Eleanor Haack for her bureaucratic and understanding unbureaucratic help, always with the smile.

I thank Peter Reichelt for his great help for the experimental cloning part, to have proofread some part of this thesis, and for the nice conversations and nice atmosphere in our lab, together with Katrin Krzak and Dr. Douglas D. Griffith.

I thank Christian Pohl and Markus Haindl to have friendly proofread the first drafts of this dissertation.

For the technical part, I thank Dr. Martin Grininger and Petra Wollmann for their help in crystallisation, Reinhardt Mentele for the N-terminal sequencing (department of Prof. Lottspeich), Dr. Karin Rodewald for the sequencing, Dr. Michalis Aivaliotis and Sigrid Bauer for the Mass-spectrometric analysis.

I thank also all my former and present colleagues for their friendship and the nice working atmosphere, that helped me to integrate in Germany, learn german and keep very nice memories from this unique experience. Thanks to the jogging group, with which it was really nice to train.

I am especially very grateful to my friends Dr. Laure Guenin, Dr. Anja Hanisch and Frédéric Grange, who followed and shared my feelings during all these PhD years. I thank them to have always been here for me for the nice and the difficult moments.
I thank as well all my friends for their friendship and help, and in particular Dr. Steffi Offermann, Andreas Unterschütz, Christian Pohl, Markus Haindl, Dr. Marlon Hinner, Dr. Xenia Brinkmann, Stephan Eibel, Claudia Hubert, Magdalena Czemplik, Sandra Lepthien and Tina Wolschner, to have contributed to make this experience in Germany wonderful and unique.

And finally I want to thank my parents and my brother. I thank them to have encouraged me all along these universitary studies. I thank them for what they brought me, for their unconditional support and their belief in me. I dedicate them this work. Merci à vous.

Anna Le Bris

Personal data

Date of Birth	06 Januar 1977
Place of Birth	Quimper (Frankreich)
Nationality	French

Education

10.2002-03.2007   **PhD in Biochemistry**

Max-Planck-Institute of Biochemistry, Martinsried

Department of Membrane Biochemistry

Thesis   **Overexpression and purification of membrane proteins in yeast:**

The GPCR α-factor receptor and a methanococcal transporter

Supervised by Prof. Dr. Dieter Oesterhelt

09.2001-09.2002   **Master (Diploma) in Biochemistry, Cell and Molecular Biology**

University of Dijon (Bourgogne), France

Thesis   **Study of the proteins of chemoreception in the coakroach**

Blattella germanica

Supervised by Dr. Rémy Brossut.

09.2000-07.2001   **Maitrise (4th year) in Biochemistry**

University of Rennes, France

09.1998-07.2000   **Licence (3rd year, Bachelor) in Biochemistry**

University of Rennes, France

09.1997-07.1998   **DEUG (2nd year) in general Biology**

University of Angers, France

09.1995-07.1997   **Entrance examination of medical studies**

University of Angers, France

07.1995   **Scientific A-level (Baccalauréat)**

With the specialisations: Biology, Chemistry, Physics and Mathematics